ไซยาไนด์ฟลูออเรสเซนต์เซ็นเซอร์จากอนุพันธ์ไดฟีนิลแอเซทิลีน

นายเอกชัย คำศรี

วิทยานิพนธ์นี้เป็นส่วนหนึ่งของการศึกษาตามหลักสูตรปริญญาวิทยาศาสตรมหาบัณฑิต
สาขาวิชาเคมี ภาควิชาเคมี
คณะวิทยาศาสตร์ จุฬาลงกรณ์มหาวิทยาลัย
ปีการศึกษา 2554

CYANIDE FLUORESCENT SENSORS FROM DIPHENYLACETYLENE DERIVATIVES

Mr. Akachai Khumsri

A Thesis Submitted in Partial Fulfillment of the Requirements

for the Degree of Master of Science Program in Chemistry

Department of Chemistry

Faculty of Science

Chulalongkorn University

Academic Year 2011

Thesis Title	CYANIDE FLUORESCENT SENSORS FROM DIPHENYLACETYLENE DERIVATIVES
By	Mr. Akachai Khumsri
Field of Study	Chemistry
Thesis Advisor	Associate Professor Mongkol Sukwattanasinitt, Ph.D.
Thesis Co-advisor	Gamolwan Tumcharern, Ph.D.

Accepted by the Faculty of Science, Chulalongkorn University in Partial Fulfillment of the Requirements for the Master's Degree

…….. Dean of the Faculty of Science
(Professor Supot Hannongbua, Dr.rer.nat.)

THESIS COMMITTEE

…….. Chairman
(Assistant Professor Warinthorn Chavasiri, Ph.D.)

……..……. Thesis Advisor
(Associate Professor Mongkol Sukwattanasinitt, Ph.D.)

……..……. Thesis Co-advisor
(Gamolwan Tumcharern, Ph.D.)

…….. Examiner
(Assistant Professor Paitoon Rashatasakhon, Ph.D.)

…….. External Examiner
(Jitapa Sumranjit, Ph.D.)

เอกชัย คำศรี : ไซยาไนด์ฟลูออเรสเซนต์เซ็นเซอร์จากอนุพันธ์ไดฟีนิลแอเซทิลีน. (CYANIDE FLUORESCENT SENSORS FROM DIPHENYLACETYLENE DERIVATIVES) อ.ที่ปรึกษาวิทยานิพนธ์หลัก : รศ.ดร.มงคล สุขวัฒนาสินิทธ์, อ.ที่ปรึกษาวิทยานิพนธ์ร่วม : ดร.กมลวรรณ ธรรมเจริญ, 81 หน้า.

สารเรืองแสงใหม่ทั้งสี่ตัวที่ประกอบไปด้วยหมู่ไดฟีนิลลีนแอเซทิลีนเป็นหน่วยเรืองแสง และมีหมู่ซาลิไซลัลดีไฮด์สำหรับเป็นหมู่ตรวจวัดไอออนของไซยาไนด์ ถูกสังเคราะห์ได้โดยใช้ปฏิกิริยาคู่ควบโซโนกาชิระเป็นปฏิกิริยาหลักในการสังเคราะห์ ซึ่งสารเรืองแสงที่สังเคราะห์ขึ้นมาใหม่สามารถทำการตรวจวัดไอออนของไซยาไนด์ได้อย่างจำเพาะเจาะจงในตัวทำละลายผสมน้ำกับ DMSO และในน้ำที่มีสารลดแรงตึงผิว ไตรตอนเอ็กซ์-100 เป็นส่วนผสม โดยการออกแบบโครงสร้างสารอาศัยการลดกระบวนการ internal charge transfer (ICT) ในการวิเคราะห์ ภายใต้สภาวะที่มีไซยาไนด์ไอออนหมู่ฮัลดีไฮด์จะเปลี่ยนไปเป็นหมู่ไซยาโนไฮดริน ทำให้เกิดการระงับกระบวนการเกิดเรโซแนนซ์ของอิเล็กตรอนไปยังหมู่อัลดีไฮด์ มีผลทำให้เกิดการยับยังกระบวนการ ICT ของสารเรืองแสง F3 ที่ประกอบด้วยหมู่ซาลิซาลิกหนึ่งหมู่ และมีหมู่ไดฟีนิลลีนแอเซทิลีนสองหมู่ ให้สัญญาณการตรวจวิเคราะห์ที่สูงกว่าสารเรืองแสงตัวอื่นที่สังเคราะห์ ซึ่งสามารถยืนยันได้ด้วยค่าประสิทธิ์ภาพการเรืองแสง ก่อนเติมและหลังเติมไซยาไนด์ โดยในงานวิจัยนี้สามารถทำการตรวจวัดความเข้มข้นของไอออนของไซยาไนด์ได้ที่ระดับความเข้มข้นตั้งแต่ 1.6 μM (42 ppb) ซึ่งสามารถตรวจวัดหาความเข้มข้นของไอออนของไซยาไนด์ได้น้อยกว่าความเข้มข้นของไอออนของไซยาไนด์ที่องค์การอนามัยโลก (WHO) กำหนดไว้ในน้ำดื่มไม่ควรเกิน 2.7 μM และสำหรับทดสอบโดยใช้กระดาษพบว่า สามารถตรวจวัดปริมาณไซยาไนด์ได้ในระดับ 5 นาโนโมลโดยการสังเกตด้วยตาเปล่า

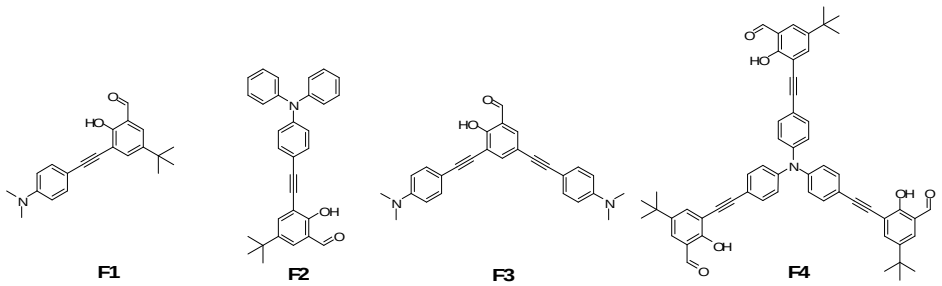

ภาควิชา เคมี ลายมือชื่อนิสิต .....

สาขาวิชา เคมี ลายมือชื่อ อ.ที่ปรึกษาวิทยานิพนธ์หลัก .....

ปีการศึกษา 2554 ลายมือชื่อ อ.ที่ปรึกษาวิทยานิพนธ์ร่วม .....

5272637223: MAJOR CHEMISTRY
KEYWORDS: CYANIDE / FLUORESCENCE SENSOR

AKACHAI KHUMSRI: CYANIDE FLUORESCENT SENSORS FROM DIPHENYLACETYLENE. ADVISOR: ASSOC. PROF. MONGKOL SUKWATTASINITT, Ph.D. CO-ADVISOR: GAMOLWAN TUMCHARERN, Ph.D., 81 pp.

A novel series cyanide fluorescence sensors (**F1**-**F4**) containing phenylene-ethynylene as fluorogenic center and salicylaldehyde as CN^- receptor were successfully synthesized by using Sonogashira coupling reaction as a key synthetic step. The sensors exhibited selective fluorescence turn-on responses in contact with cyanide anion in aqueous DMSO or aqueous media containing Triton X-100 non ionic surfactant. The fluorescence turn-on signal is associated with the reduction of the quenching effect by internal charge transfer (ICT) process within the sensing molecules. Upon the addition of cyanide anion, the resonance electron withdrawing aldehyde group is converted into the corresponding cyanohydrin which is no longer capable of withdrawing the electrons by the resonance effect. **F3**, which contain one salisadehyde group and two phenylene-ethynylenes, gives the highest cyanide sensitivity among four compounds synthesized. The fluorescence quantum yields determined before and after the cyanide addition confirm that the fluorescence quenching by the ICT process in **F3** is reduced the most. The detection limit of this cyanide sensor is 1.6 μM (42 ppb) in the aqueous media which is below the concentration limited by WHO in drinking water of 2.7 μM. The paper-based solid state sensors fabricated from **F3** allow naked eye detection of cyanide anion down to 5 nanomole.

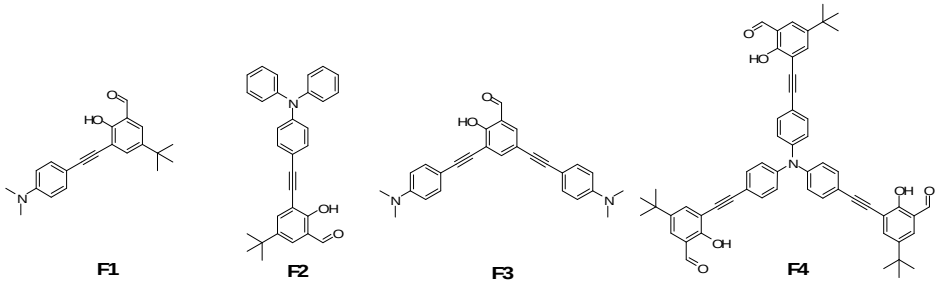

Department : Chemistry Student's Signature .....
Field of Study : Chemistry Advisor's Signature .....
Academic Year : 2011 Co-advisor's Signature .....

ACKNOWLEDGEMENTS

I wish to express my deep gratitude to my advisor, Associate Professor Dr. Mongkol Sukwattanasinitt, my co-advisor Dr. Gamolwan Tumcharern for their generous advice, invaluable guidance and encouragement throughout the course of this research.

I would like to gratefully acknowledge the committee, Assistant Professor Dr. Warinthorn Chavasiri, Assistant Professor Dr. Paitoon Rashatasakhon and Dr. Jitapa Sumranjit for their comments, guidance and extending cooperation over my presentation. I would like to thank Dr. Anawat Ajavakom, Assistant Professor Dr. Sumrit Wacharasindhu and Dr. Nakorn Niamnont for their attention and suggestions during our research group meeting.

I would like to express my gratitude to Organic Synthesis Research Unit (OSRU), Department of Chemistry, Faculty of Science, Chulalongkorn University for providing the chemicals and facilities throughout the course of study.

A deep affectionate gratitude is acknowledged to my beloved family for their understanding, encouragement and support throughout the education course. I especially thank Warathip Siripornnoppakhun, Thichamporn Eaidkong, Sasikarn Ampornpun, Eakkaphon Rattanangkool and Kunnigar Vongnam for their suggestions and guidance. I would like to thank all of my friends for their friendship, especially Nattaporn Kimpitak, Daranee Homraruen, Kanokthorn Boonkitpatarakul, Wannapa Yuanboonlim and Jade'tapong Klahan for their help during the course of my graduate research. Moreover, I would like to thank Jaume Bartés Creus, Thanarath Pisuchpen their suggestions and encouragement. I would like to thank all my friends in our research group for their great friendships and suggestion.

I would like to thanks Center of Excellence on Petrochemical and Materials Technology, ADB under the Petroleum & Petrochemical Technology Consortium and Thailand Graduate Institute of Science and Technology. These scholarships can help my student life.

Finally, I would like to express my thankfulness to my beloved parents who always stand by my side during both of my pleasant and hard time.

CONTENTS

CHAPTER Page

LIST OF TABLES

LIST OF FIGURES

LIST OF SCHEMES

LIST OF ABBREVIATIONS

A	acceptor
Ar	aromatic
calcd	calculated
^{13}C NMR	carbon-13 nuclear magnetic resonance
$CDCl_3$	deuterated chloroform
D	donor
d	doublet (NMR)
dd	doublet of doublet (NMR)
ESIMS	electrospray ionization mass spectrometry
equiv	equivalent (s)
FT-IR	fourier transform infrared spectroscopy
g	gram (s)
^{1}H NMR	proton nuclear magnetic resonance
Hz	Hertz
HRMS	high resolution mass spectrum
h	hour (s)
ICT	internal charge transfer
IR	infrared
J	coupling constant
mg	milligram (s)
mL	milliliter (s)
mmol	millimole (s)
m/z	mass per charge
m	multiplet (NMR)
mp	melting point
M.W.	molecular weight
M	molar
MHz	megahertz
rt	room temperature
s	singlet (NMR)

THF	tetrahydrofuran
UV	ultraviolet
δ	chemical shift
°C	degree Celsius
µL	microliter (s)
µM	micromolar (s)
Φ	quantum yield
% yield	percentage yield

CHAPTER I

INTRODUCTION

1.1 Overview

Cyanide is very toxic to human even at low contamination can cause death because it can strongly inhibit the process of cellular respiration when entering into human blood system by interacting with a heme unit in the active site of cytochrome aa_3[1]. It however remains wildly used (1.5 million tons per year) and its poisoning may occur in particular industry such as in metal trades, mining, electroplating, jewellery manufacturing, and X-ray film recovery [2]. In nature, cassava, cyanogenic algae, bacteria and fungi can produce and release cyanide compounds that sometime causes food and water contamination [3]. Water-soluble potassium and sodium cyanide salts have been known to be ones of the most lethal chemical reagents and even used as poisoning materials [4-5]. The maximum concentration of cyanide allowed in drinking water by the WHO manual is 2.7 μM [6]. Detection of cyanide ion under biologically relevant aqueous solution is thus vital for safety management and forensic investigation.

1.2 Fluorescence spectra

The fluorescence spectrum provides information for analysis. The fluorescence processes that occur between the absorption and emission of light are usually described by the Jablonski diagram, which [7-8] are used in a variety of forms, to illustrate various molecular processes that can occur in excited states. A simplified Jablonski diagram shown in **Figure 1.1** when photons is absorbed by a molecule, the electronic state of the molecule changes from the ground state to one of many vibrational levels in one of the excited electronic states. The excited electronic state is usually the first excited singlet state, **S1**. Once the molecule is in this excited state, relaxation can occur via several processes. Fluorescence is one of these

processes and results in the emission of photon. The length of time between absorption and emission is usually relatively, often in the order of 10^{-9} to 10^{-8} seconds.

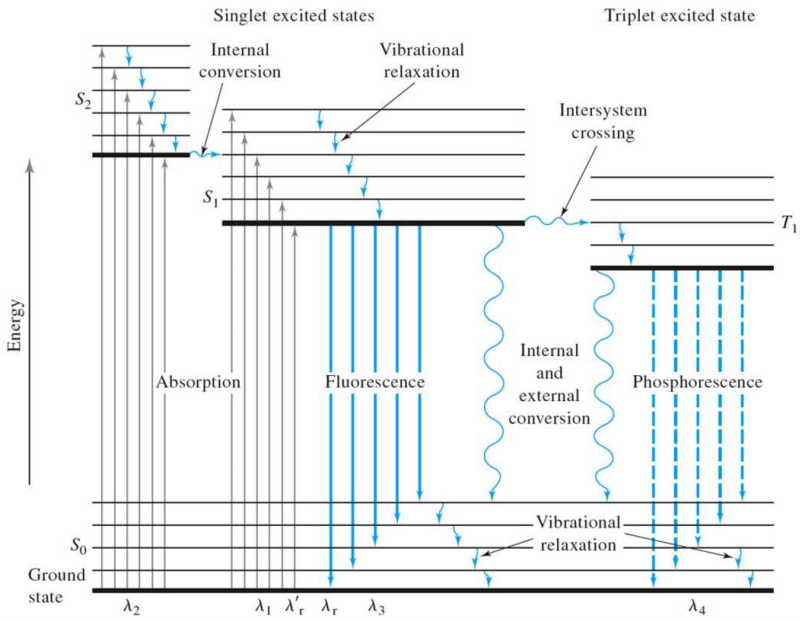

Figure 1.1 Jablonski Energy Diagram explaining fluorescence processes.

1.3 Locally excited and internal charge transfer states.

Fluorescence process is begins with a molecule at a ground state (S0) absorb photon and excited to higher energy level; as a consequence, the molecule is changed to be at the excited to state S1 or higher which has the same geometry as the molecule at the ground state following the Frank-Condon principle (**Figure 1.2**). After the excitation, molecule usually release energy as non-radiative decay called internal conversion to the most stable geometry state of S1 known as locally excited (LE) state. Then the remaining photon energy is emitted as an emission or radiative decay to take the molecule back to the ground state. However, in some cases, molecule in the LE state may undergo other pathway to release the energy without emission (non-radiative decay). For example, a substance with structure composed of both good electron donating and withdrawing groups by electron delocalization process can

delocalize electron pair within the molecule which is called internal charge transfer (ICT) process to convert to the ICT excited state (**Figure 1.3**). This ICT state has lower energy with different geometry from the LE state. ICT excited state then relex to the original ground state that has the same geometry as ICT excited state. This relaxation may either give light within or outside the visible light spectrum [9-17]. Due to multi-step process, ICT emission generally has lower fluorescence quantum yield somparing with LE state. The ICT state usually gives longer wavelength and is usually stabilized by polar solvent (**Figure 1.4**) due to ICT excited state stabilization [18-19].

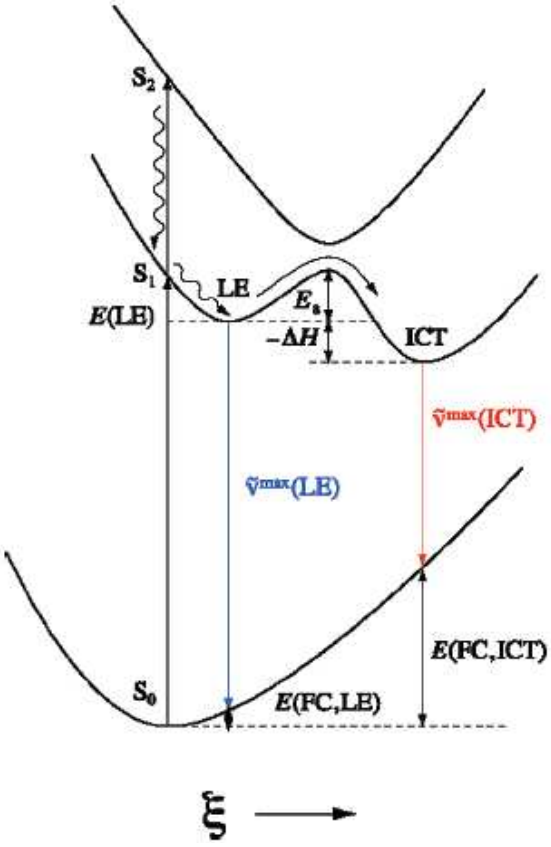

Figure 1.2 Potential energy surfaces of the ground state (S0) is excited to and S1 or S2 and then relaxed to LE, and ICT (FC = Franck-Condon).

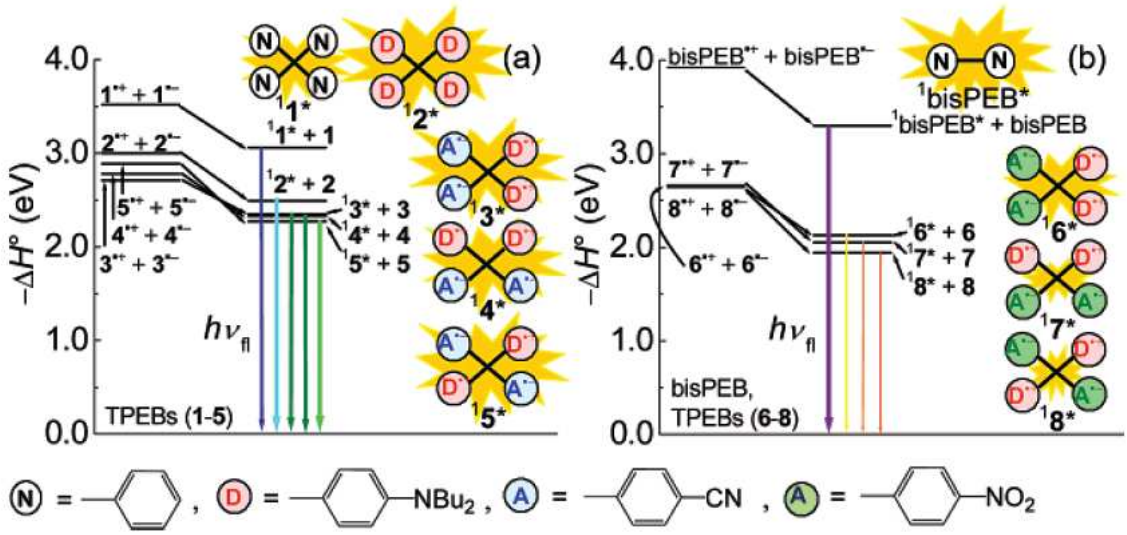

Figure 1.3 Energy level diagram for radiolysis induced chemiluminescence of TPEBs (**1**-**5** (a) and **6**-**8** (b)) and bisPEB (b). **N**, **D**, and **A** denote neutral-, electron donor-, and electron acceptor type molecules, respectively. $\mathbf{D}^{\cdot+}$ and $\mathbf{A}^{\cdot-}$ denote **D** radical cation and **A** radical anion, respectively.

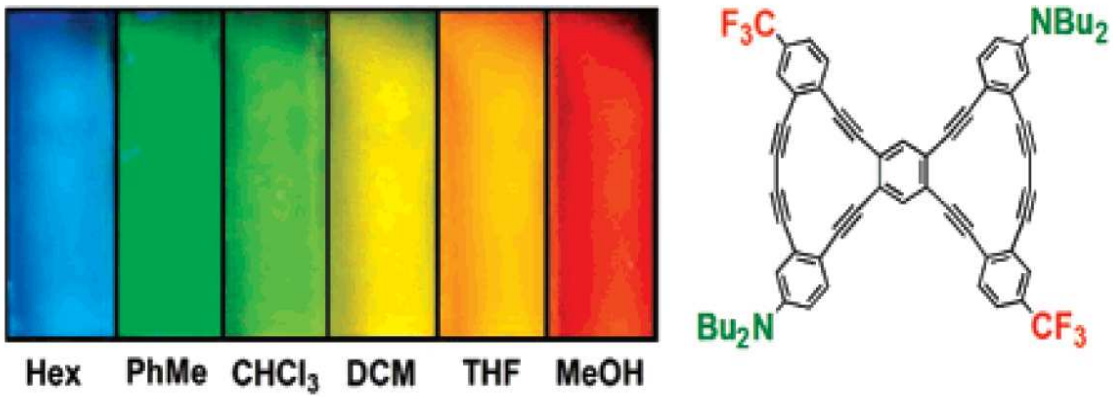

Figure 1.4 Photographic images of bis-(dehydrobenzoannuleno)benzene (DBA) chromophores in organic solvents under black light.

1.4 Structure of fluorescent Compounds

Attention in chemical and biological sensing systems relies upon rapid and high selectivity. The methods have been progressively improved using redox [20], chromogenic [21], or fluorogenic [22] changes as the detection signals. Conjugated polymers (CPs) have emerged as one of the most important classes of transducing materials. They transform a chemical signal to easily measurable electrical or optical events. Fluorescence based methodologies have attracted much interest due to their intrinsic sensitivity and selectivity [23]. Considerable efforts have been devoted to the design of fluorescent compounds to be used as transducers. CPs with delocalized π-electron systems have attracted an overpowering interest due to their versatile optical and electrical properties [24]. **Figure 1.5** shows structures of a variety of CPs commonly investigated, including polythiophene (1) [25], polypyrrole (2) [26], polyfluorene (3) [27], poly(*para*-phenylenevinylene) (4) [28], and poly(*para*-phenyleneethynylene) (5) [29]. The delocalized electronic structure of CPs enables them to exhibit efficient absorption and strong emission, and produce amplified signal changes upon interacting with various analytes.

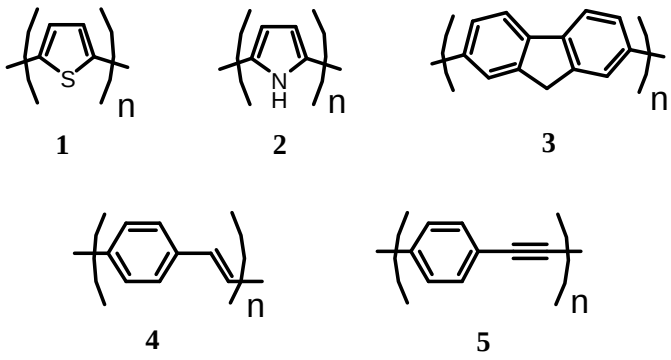

Figure 1.5 Molecular structures of some common conjugated polymers (CPs).

1.5 Fluorescent sensors based on phenylene-ethynylene derivatives

Phenyleneethynylene is an important class of π-conjugated molecules currently applied as fluorescent transducers in various optical sensing systems. Critical features spurring interest in and usefulness of this class of compounds include their structural rigidity allowing more predictable geometry, high fluorescence quantum efficiency and efficient syntheses. During the past decade, a number of crucial developments of both small and polymeric phenyleneethynylene conjugated systems have been witnessed, mostly containing para-phenyleneethynylene moieties, into more sensitive and selective sensors for wider applications. Palladium-catalyzed cross-coupling polymerization offers the benefits of mild reaction conditions, wide functional group, and solvent compatibility for preparation of many para-phenyleneethynylenes [30-31].

1.6 Cyanide fluorescent sensors based on nucleophilic attack on hydrogen-bonded carbonyl groups

In 2005, Lee et al. [32] have synthesized a chemodosimeter having a salicylaldehyde moiety as a binding unit and a coumarin skeleton as a sensing unit. A coumarin-based fluorescent chemodosimeter has been developed for selective detection of cyanide ion over other anions in water at physiological pH. This significantly enhanced fluorescence intensity was probably caused by the addition of cyanide converts the aldehyde group into tetrahedral cyanohydrin which in turn destroys its electron withdrawing ability and thus reduces the ICT process.

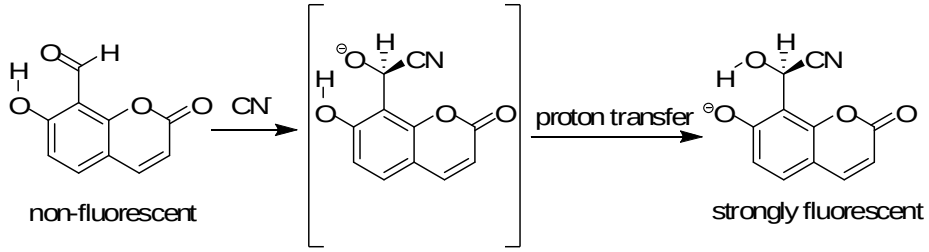

Figure 1.6 The mechanism of cyanide ion monitoring of cumarin derivatives.

In 2009, Jo et al. [33] have reported **3** containing diphenylacetylene derivatives in which the π-conjugated backbone was functionalized with an aldehyde group to render the molecule nonfluorescent. The N-H---O hydrogen bond across the 2,2′- functionalized diphenylacetylene turn motif activates the carbonyl group toward nucleophilic attack, and structure conversion of this internal quencher site by reaction with cyanide ion obtains a rapid enhancement. Binding of an ammonium group to the hydrogen bond donor part significantly increased both the response kinetics and the intensity of the fluorescence signal. The structurally optimized molecular **3** responds absolutely to μM-level cyanide in water at physiological pH with no interference from other anions.

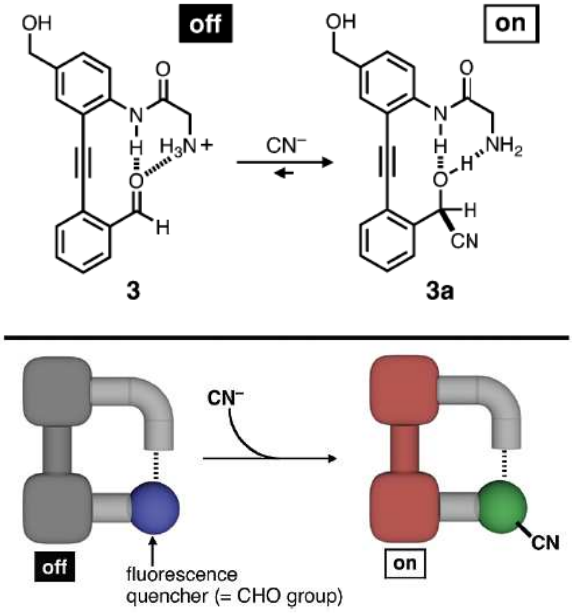

Figure 1.7 Detection of cyanide by **3** through the formation of fluorescent cyanohydrin adduct **3a**.

In 2011, Khatua et al. [34] have designed and synthesized two new ruthenium complexes for detecting cyanide based on the famous formation of cyanohydrins. Upon the addition of 2.0 equiv of cyanide, Both $1[PF_6]_2$ and $2[PF_6]_2$ was enhanced 55-fold within 15 s along with a diagnostic blue shift of the emission by more than 100 nm in acetronitrile. The color change from red to yellow and orange luminescence can be observed by the naked.

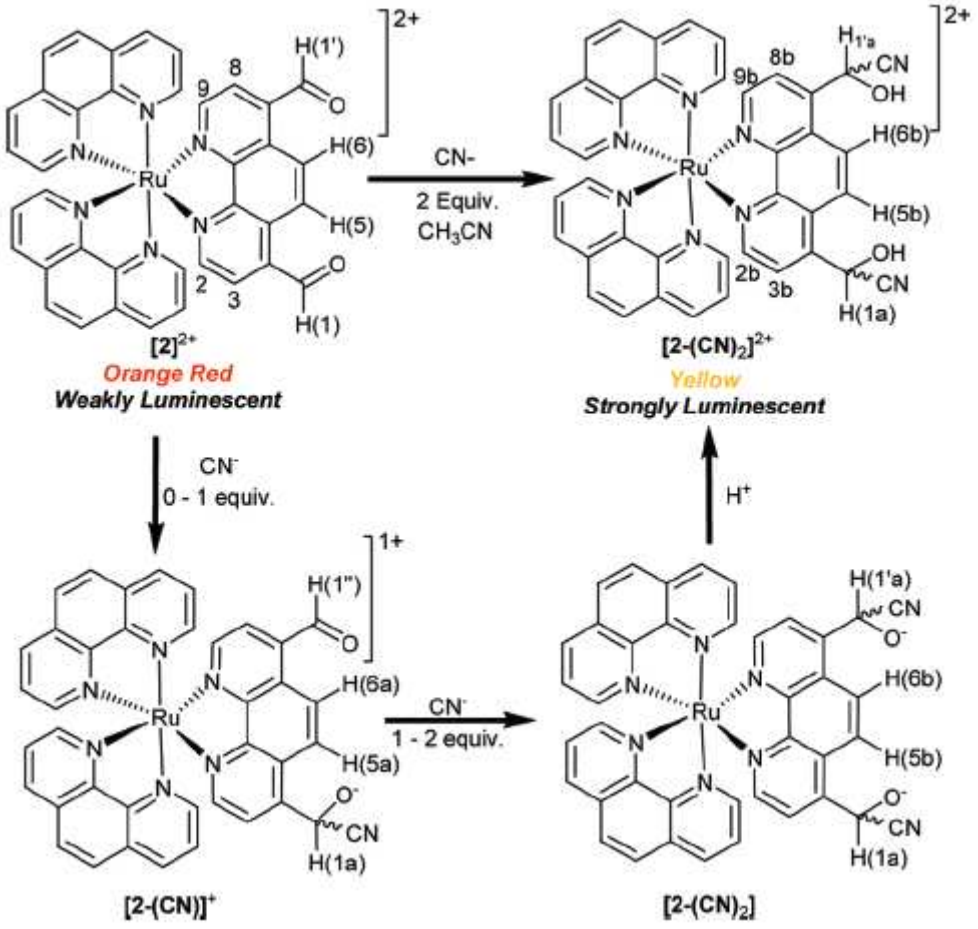

Figure 1.8 Cyanide detection by Probe $2[PF_6]_2$ Based on cyanohydrins formation

1.7 Cyanide fluorescent sensors based on borane derivatives

In 2005, Badugu et al. [35] have developed and synthesized three water-soluble fluorescent probes to determine cyanide sensing up to physiologically lethal levels. The fluorescence sensor is based on the ability of boronic acid to complex cyanide and its change from being electron deficient ($R\text{-}B(OH)_2$) in the absence of cyanide at physiological pH to being electron rich ($R\text{-}B\text{-}(CN)_3$) upon cyanide complexation (**Figure 1.9**). Ensuing cyanide binding extenuate the internal charge transfer within the probes, a change in the electronic properties within the probes, consequent in enhanced fluorescence signals as a function of increased solution cyanide concentration.

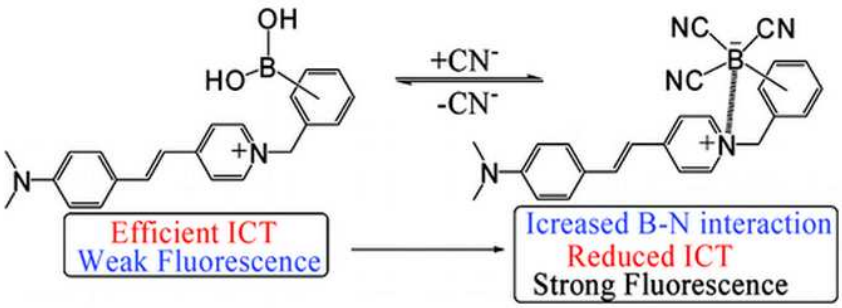

Figure 1.9 Complexation of fluorescent probes with aqueous free cyanide

In 2011, Jamkratoke et al. [36] have designed and synthesized three fluorescence sensors containing naphthoquinoneimidazole and boronic acid using an acceptor-donor-acceptor (A-D-A system) **3a**, **3b**, and **3c** (**Figure 1.0**) that have been developed with high selectivity for cyanide as turn-on cyanide probes in the CTAB micellar system. These A-D-A probes offer considerable promises as cyanide selective fluorescence probes was switched on upon substitution of cyanide on sensors in the CTAB micelle with a large response emission band at 460 nm and a large blue shift (ca. 100 nm). In this approach, CTAB can incorporate 3b and 3c to provide powerful probes for detecting a very low concentration of CN^- in water.

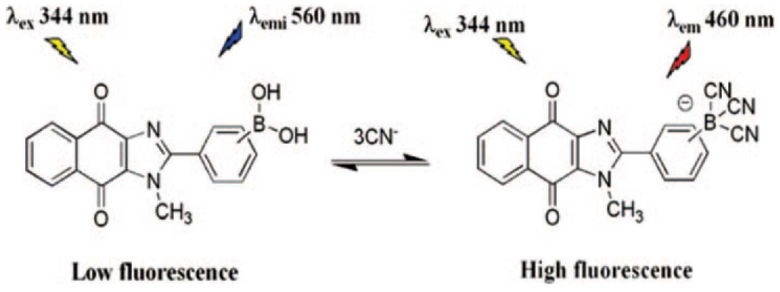

Figure 1.10 Reaction mechanism of **3a**, **3b**, and **3c**.

1.8 Cyanide Fluorescent sensors based on heterocyclic ring systems

In 2006, Yang et al. [37] have designed and synthesized new fluorescence sensors, that selective chemosensor has been developed to detect cyanide in water at micromolar concentrations. The acridinium salt used in this sensor system is prepared in a single step from an acridine orange base. Detection is based on the acridinium ion (**Figure 1.11**), nucleophilic addition of cyanide ion to the 9-position of the acridinium ion. This process induces a great reduce in fluorescence intensity and a noticeable color change. The sensitivity and selectivity of the system in aqueous media for cyanide ion over other anions is surprisingly high. In addition, the sensitivity of both the fluorescence- and colorimetric-based assays is below 2.7 µM, the concentration is acceptable to limit allowed of CN- to be presented in water by World Health Organization (WHO) suggested by the World Health Organization (WHO) as the maximum allowable to be present in drinking water.

Figure 1.11 Reaction mechanism of receptor **2** for the CN^- sensing.

1.9 Cyanide Fluorescent sensors based on indolium

In 2011, Kim et al. [38] have reported **1** containing a conjugated indole-coumarin skeleton (**Figure 1.12**) has been prepared and displayed considerable dual changes in both absorption (blue-shift) and emission (turn-on) bands exclusively for potassium cyanide sensors. It is obviously thoughtful that in **1** an ICT takes place from the N atom in coumarin to the positive charged indole group. However, The ICT was disrupted by CNreaction with **1** simply because the nucleophilic addition of the cyanide anion toward the –C=N⊕– of **1**. Thus, the reaction weakens to give an apparent color change of **1** from deep blue to pale yellow that upon the addition of CN^-, The ICT blocking in **1**-CN is due to the conjugation breaking between coumarin and indole groups, which can be a main reason for the fluorescence enhancement of **1**-CN is mainly due to the blocking of conjugation-based ICT process.

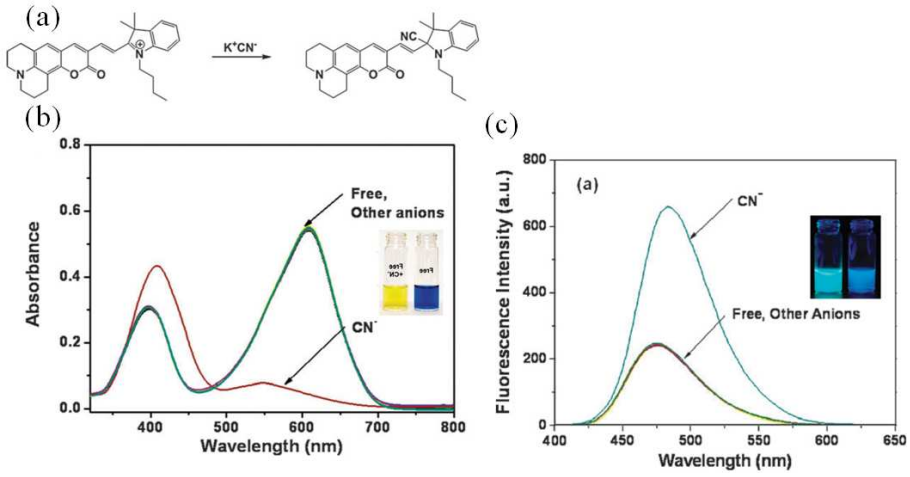

Figure 1.12 (a) Reaction mechanism of 1 for the CN^- addition. (b) Absorption spectra of 1 (20.0 mM) and fluorescence spectra (b) of 1 (5.0 mM) withaddition of K^+ salts of F^-, Cl^-, Br^-, I^-, $CH_3CO_2^-$, HSO_4^-, HPO_4^{2-}, HCO_3^-, NO_3^-, ClO_4^-, CN^-, and SCN^- (10 equiv, respectively) in H_2O–CH_3CN (5 : 95, v/v).

In 2011, Shiraishi et al. [39] have developed a novel and highly sensitive fluorescence sensor based on coumarin–spiropyran fluorescent probes (**2**) for the determination of cyanide. The receptor **2**, a coumarin–spiropyran conjugate (**Figure**

1.13), is nonfluorescent, but shows a blue fluorescence via a nucleophilic interaction with cyanide ion under UV irradiation. The detection limit determined based on the S/B criteria is 0.5 μM and enables accurate determination of the lowest level of cyanide ion in a buffered water/MeCN mixture (8/2 v/v; pH 9.3).

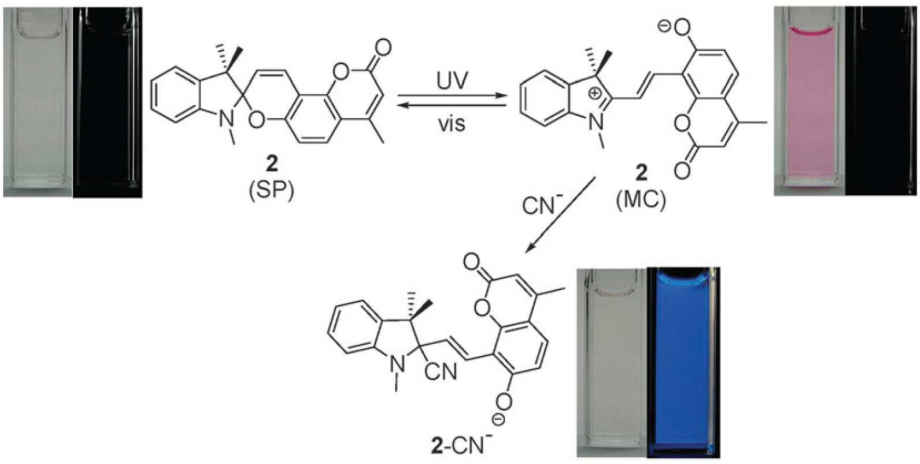

Figure 1.13 Reaction mechanism of receptor 2 for the CN^- sensing.

1.10 Objective of this research

This research aims to synthesize new fluorophores containing salicylaldehyde group as a sensor unit. All compounds contain phenylene-ethynylene repeating unit. For the assessment of ICT process effect on fluorophores, the study of photophysical properties of these fluorophores and fluoresence enhancement ratio (I/I_0) are conducted and used for the applications for analysis of cyanide ion in aqueous system.

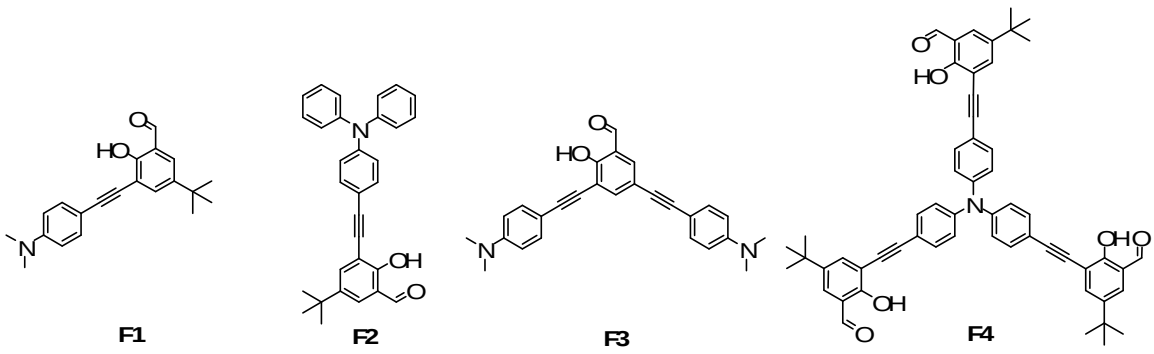

Figure 1.14 Structures of target molecules.

CHAPTER II

EXPERIMENTAL

2.1 Chemicals and materials

N,*N*-dimethylaniline, trimethylsilylacetylene, triphenylphosphine, bis(triphenylphosphine)palladium(II)dichloride ($PdCl_2(PPh_3)_2$), sodium thiosulfate, benzyltrimethylammonium chloride, potassium hydroxide, potassium carbonate, calcium carbonate, and were purchased from Fluka. Triphenylamine, iodine monochloride, copper (I) iodide, 1, 8-diazabicyclo [5.4.0] undec-7-ene (DBU), 18-Crown-6, 1,4-Diiodobenzene, 2-hydroxybenzaldehyde and quinine sulfate were purchased from Aldrich. All other reagents were non-selectively purchased from Sigma-Aldrich, Fluka or Merck and used without further purification. For most reactions, solvents such as dichloromethane and acetonitrile were reagent grade stored over molecular sieves. In anhydrous reactions, solvents such as THF and toluene were dried and distilled before use according to the standard procedures. All column chromatography was operated using Merck silica gel 60 (70-230 mesh). Thin layer chromatography (TLC) was performed on silica gel plates (Merck F245). Solvents used for extraction and chromatography such as dichloromethane, hexane, ethyl acetate and methanol were commercial grade and distilled before use while diethyl ether and chloroform were reagent grade. Milli-Q water was used in all experiments unless specified otherwise. The most reactions were carried out under positive pressure of N_2 filled in rubber balloons.

2.2 Analytical instruments

The melting points of all products were acquired from a melting point apparatus (Electrothermal 9100, Fisher Scientific, USA). Elemental (C, H, N) analyses were performed on a PE 2400 series II analyzer (Perkin-Elmer, USA). Mass spectra were recorded on a Microflex MALDI-TOF mass spectrometer (Bruker Daltonics) using doubly recrystallized α-cyano-4-hydroxy cinnamic acid (CCA) as a matrix. The HRMS spectra were measured on an electrospray ionization mass spectrometer (microTOF, Bruker Daltonics). Fourier transform infrared spectra were acquired on Nicolet 6700 FT-IR spectrometer equipped with a mercury-cadmium

telluride (MCT) detector (Nicolet, USA). ^{1}H-NMR and ^{13}C-NMR spectra were acquired from sample solution in $CDCl_3$, acetone-d_6, CD_3CN, CD_3OD and DMSO-d_6 on Varian Mercury NMR spectrometer (Varian, USA) at 400 MHz and100 MHz, respectively. The UV-visible absorption spectra were obtained from a Varian Cary 50 UV-Vis spectrophotometer (Varian, USA) and the fluorescence emission spectra were recorded on a Varian Cary Eclipse spectrofluorometer (Varian, USA).

2.3 Synthesis of fluorophores F1-F3

2.3.1 Preparation of 5-*tert*-butyl-2-hydroxybenzaldehyde.

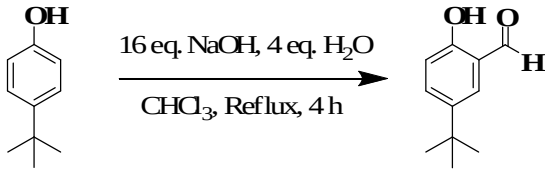

16 %

4-*t*ert-Butylphenol (10.00 g, 66.57 mmol), NaOH (21.25 g, 0.53 mol) and DI water (2.4 g, 0.132 mol) were mixed in trichloromethane (150 mL) by stirring with a magnetic bar in a round-bottom flask. The mixture was refluxed for 1 h and then NaOH (10.62 g, 0.265 mol) and DI water (1.2 g, 0.066 mol) were again added. After 1 more hour, NaOH (10.62 g, 0.265 mol) and DI water (1.2 g, 0.066 mol) were added for the third time. The stirring was continued at reflux temperature overnight before the mixture was allowed to cool to room temperature. The organic layer was separated and the aqueous phase was extracted with dichloromethane (2 × 50 mL) and the combined organic was dried over anhydrous $MgSO_4$. The solvent was evaporated and the residue was dissolved in a minimal amount of dichloromethane. The solution was eluted through a silica gel column by gradient solvents starting from pure hexane to dichloromethane/hexane (1/3 v/v) to afford the desired product after solvent removal as a brown viscous liquid (1.90 g, 16% yield). ^{1}H NMR ($CDCl_3$, 400 MHz): δ (ppm) 10.88 (s, 1H), 9.89 (s, 1H), 7.58 (d, *J* = 8.8 Hz, 1H), 7.51 (s, 1H), 6.93 (d, *J* = 8.8 Hz, 1H), 1.32 (s, 9H); ^{13}C NMR ($CDCl_3$, 100 MHz): δ (ppm) 196.4, 159.2, 142.4, 134.3, 129.4, 119.7, 116.9, 33.7, 30.9.

2.3.2 Preparation of 5-tert-butyl-2-hydroxy-3-iodobenzaldehyde.

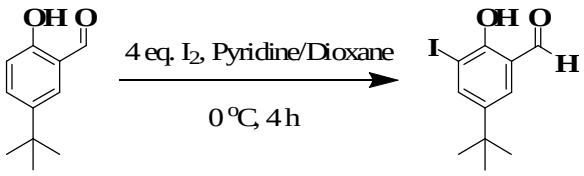

99 %

Iodine (11.40 g, 44.89 mmol), was dissolved in dioxane (10 mL) and pyridine (10 mL) by stirring with a magnetic bar in a round-bottom flask at 0 ºC for 15 min. The solution was added with 5-*tert*-butyl-2-hydroxybenzaldehyde (2.00 g, 11.22 mmol) and the mixture was stirred at reflux for 4 h. The solvent was evaporated and $Na_2S_2O_3$ solution (20% w/v) was then added to the dark viscous residual oil until it turned light yellow. The mixture was extracted with dichloromethane (3 × 50 mL). The combined organic phase was washed with water (2 × 100 mL) and dried over anhydrous $MgSO_4$. The solution was evaporated by rotary evaporator to afford the desired product as a brown solid (3.31 g, 97% yield). ^{1}H NMR ($CDCl_3$, 400 MHz): δ (ppm) 11.6 (s, 1H), 9.8 (s, 1H), 7.5 (s, 1H), 1.3 (s, 1H); ^{13}C NMR ($CDCl_3$, 100 MHz): δ (ppm) 195.5, 158.0, 144.7, 143.6, 130.3, 119.7, 85.2, 33.9, 31.0.

2.3.3 Preparation of N,N-dimethyl-4-((trimethylsilyl)ethynyl)aniline.

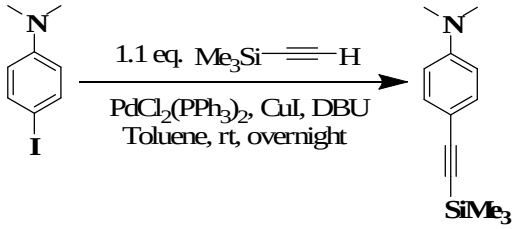

88 %

4-iodo-*N*,*N*-dimethylaniline (2.51 g, 10 mmol), $PdCl_2(PPh_3)_2$ (0.35 g, 0.5 mmol) and CuI (0.08 g, 0.5 mmol) was dissolved in toluene (10 mL) by stirring with a magnetic bar in a round-bottom flask. 1,8-Diazabicycloundec-7-ene (DBU, 1.67 g, 11

mmol mL) was added and followed by trimethylsilylacetylene (1.08 g, 11 mmol). The reaction mixture was stirred at room temperature for 4 h and then filtered. The solid precipitate was washed with toluene (3 × 15 mL) and the filtrate was evaporated. The residue was dissolved in a minimal amount of dichloromethane and eluted through a silica gel column by gradient solvents starting from pure hexane to dichloromethane/hexane (1/3) as an eluent to afford the desired product after solvent removal as light yellow solid (2.17 g, 90% yield). mp: 88-89°C; ^{1}H NMR ($CDCl_3$, 400 MHz): δ (ppm) 7.11(d, *J* = 7.2 Hz, 2H), 6.35 (d, *J* = 7.2 Hz, 2H), 2.72 (s, 6H), 0.01 (s, 9H); ^{13}C NMR ($CDCl_3$, 100 MHz): δ (ppm) 149.9, 132.9, 111.3, 109.6, 106.3, 90.9, 39.9, 0.01.

2.3.4 Preparation of 4-ethynyl-*N, N*-dimethylaniline.

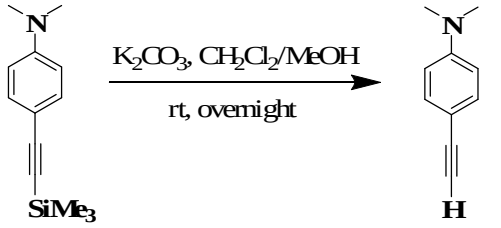

93 %

N,*N*-Dimethyl-4-((trimethylsilyl)ethynyl)aniline (1.00 g, 4.6 mmol) and K_2CO_3 (0.059 g, 0.43 mmol) were dissolved in dichloromethane (15 mL) and methanol (15 mL) by stirring with a magnetic bar in a round-bottom flask. The reaction mixture was stirred at room temperature for 24 h. Next addition of water, the organic layer was separated and the aqueous phase was extracted with dichloromethane (2 × 50 mL) and was then dried over anhydrous MgSO4. The filtrate was evaporated and the residue was eluted through a silica gel column by gradient solvents starting from pure hexane to dichloromethane/hexane (1/3) as an eluent to afford 4-ethynyl-*N*,*N*-dimethylaniline as a brown-yellow solid (0.60 g, 91 % yield). mp: 67-69°C. ^{1}H NMR ($CDCl_3$, 400 MHz): δ (ppm) 7.37 (d, *J* = 8.8 Hz, 2H), 6.62 (d, *J* = 8.8 Hz, 2H), 2.97 (s, 7H); ^{13}C NMR (CDCl3, 100 MHz): δ (ppm) 150.4, 133.2, 111.7, 108.7, 84.9, 74.9, 40.

2.3.5 Preparation of F1.

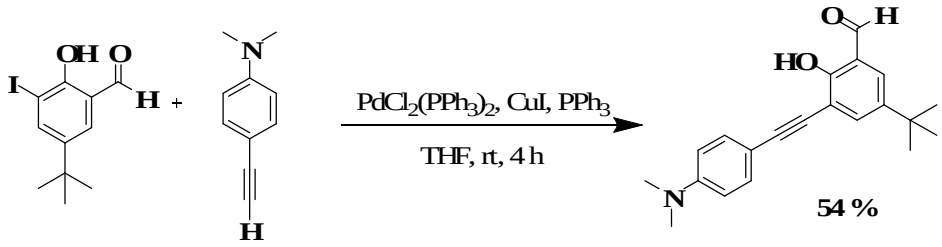

5-*t*ert-Butyl-2-hydroxy-3-iodobenzaldehyde (1.14 g, 3.76 mmol), $PdCl_2(PPh_3)_2$ (132 mg, 0.19 mmol), CuI (36 mg, 0.19 mmol), PPh_3(51 mg, 0.19 mmol) and 4-ethynyl-N,N-dimethylaniline (0.66 g, 4.51 mmol) were dissolved in tetrahydrofuran (10 ml) and triethylamine (10 mL) by stirring with a magnetic bar in a round-bottom flask. The reaction mixture was stirred at room temperature for 24 h. The mixture was filtered and the filtrate was evaporated. The residue was eluted through a silica gel column by gradient solvents starting from pure hexane to dichloromethane/hexane (3/1) as an eluent to afford F1 as a yellow solid (0.83 g, 54 % yield). ^{1}H NMR ($CDCl_3$, 400 MHz) δ (ppm) 10.60 (s, 1H), 7.79-7.77 (m, 4H), 6.82 (s, 1H), 6.78 (d, *J* = 8.8 Hz, 2H), 3.04 (s, 6H), 1.41 (s, 9 H).; ^{13}C NMR ($CDCl_3$, 100 MHz) δ (ppm) 188.6, 158.5, 152.8, 150.7, 146.1, 131.3, 126.3, 123.0, 120.5, 119.8, 112.0, 99.9, 97.4, 40.2, 34.7, 31.6.; MALDI-TOF m/z Calcd for $C_{21}H_{23}NO_2$, 321.173 Found: 320.457.

2.3.6 Preparation of 4-iodo-N,N-diphenylaniline.

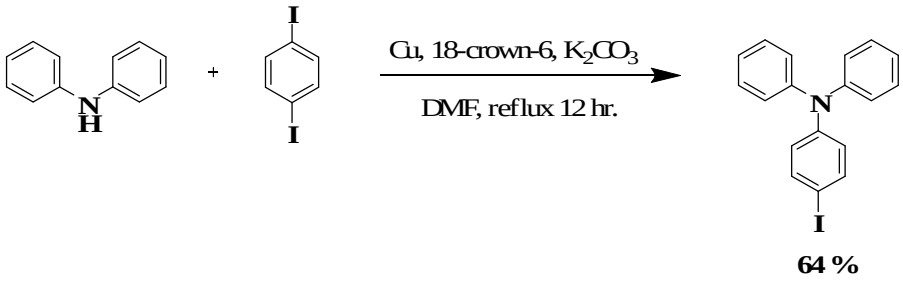

Diphenylamine (1.00 g, 5.91 mmol), 1,4-diiodobenzene (5.84 g, 17.7 mmol), Cu (400 mg, 6.31 mmol), K_2CO_3 (980 mg, 7.09 mmol) and 1,4,7,10,13,16-

hexaoxacyclooctadecane (18-Crown-6, 42mg, 0.160 mmol) were dissolved in dimethylformamide (10 ml) by stirring with a magnetic bar in a round-bottom flask. The reaction mixture was stirred and refluxed for 12 h. Next addition of water, the organic layer was separated and the aqueous phase was extracted with dichloromethane (2 × 50 mL) and was then dried over anhydrous $MgSO_4$. The mixture was filtered and the filtrate was evaporated. The solid precipitate was washed with dichloromethane (3 × 15 mL) and the filtrate was evaporated. The residue was eluted through a silica gel column by gradient solvents starting from pure hexane to dichloromethane/hexane (1/2) as an eluent to the desired product after solvent removal as a white solid (1.30 g, 60% yield). ^{1}H NMR ($CDCl_3$, 400 MHz): δ (ppm) 7.50 (d, *J* = 8.8 Hz, 2H), 7.26 (t, *J* = 2.7 Hz, 4H), 7.10-7.02 (m, 6H) [40].

2.3.7 Preparation of 4-(trimethylsilyl)ethynyl-N,N-diphenylaniline.

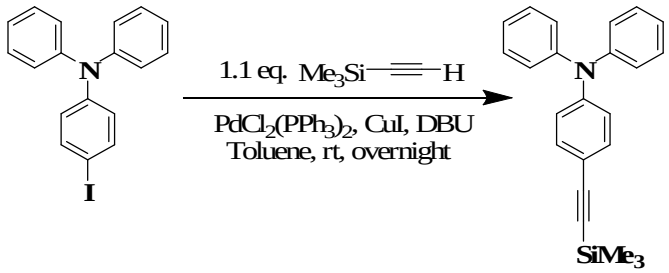

87 %

4-Iodo-*N*,*N*-diphenylaniline (0.71 g, 1.914 mmol), $PdCl_2(PPh_3)_2$ (70 mg, 0.096 mmol) and CuI (19 mg, 0.06 mmol) was dissolved in toluene (10 mL) by stirring with a magnetic bar in a round-bottom flask. 1,8-Diazabicycloundec-7-ene (DBU, 0.32 g, 2.105 mmol) was added and followed by trimethylsilyl acetylene (0.206 g, 2.11 mmol). The reaction mixture was stirred at room temperature for 4 h and then filtered. The solid precipitate was washed with toluene (3 × 15 mL) and the filtrate was evaporated. The residue was dissolved in a minimal amount of dichloromethane and eluted through a silica gel column by hexane to afford the desired product after solvent removal as light yellow oil (0.57 g, 87% yield). ^{1}H NMR ($CDCl_3$, 400 MHz): δ (ppm) 7.32-7.24 (m, 6H), 7.09-7.03 (m, 6H), 6.95 (d, *J* = 8.8 Hz, 2H), 6.81 (d, *J* =

8.4 Hz, 2H), 0.24 (s, 9H); ^{13}C NMR ($CDCl_3$, 100 MHz: δ (ppm) 148.1, 147.2, 132.9, 129.4, 124.9, 123.5, 122.2, 116.0, 105.4, 93.1, 1.0.

2.3.8 Preparation of 4-ethynyl-N,N-diphenylaniline.

91 %

4-(Trimethylsilyl)ethynyl-*N*,*N*-diphenylaniline (0.50 g, 1.46 mmol) and K_2CO_3 (1.73 g, 1.46 mmol) were dissolved in dichloromethane (15 mL) and methanol (15 mL) by stirring with a magnetic bar in a round-bottom flask at room temperature for 4 h. Next addition of water, the organic layer was separated and the aqueous phase was extracted with dichloromethane (2 × 50 mL) and was then dried over anhydrous $MgSO_4$. The solvent was evaporated and the residue was dissolved in a minimal amount of toluene and eluted through a silica gel column by gradient solvents starting from pure hexane to dichloromethane/hexane (1/4) to afford the desired product after solvent removal as a blown solid (0.36 g, 91 % yield). ^{1}H NMR ($CDCl_3$, 400 MHz): δ (ppm) 7.32 (d, *J* = 8.8 Hz, 2H), 7.28-7.24 (m, 4H), 7.10-7.03 (m, 6H), 6.97 (d, *J* = 8.8 Hz, 2H), 3.01 (s, 1H); ^{13}C NMR ($CDCl_3$, 100 MHz): δ (ppm) 148.5, 147.3, 133.2, 129.6, 125.2, 123.8, 122.2, 115.0, 110.9, 84.1.

2.3.9 Preparation of F2

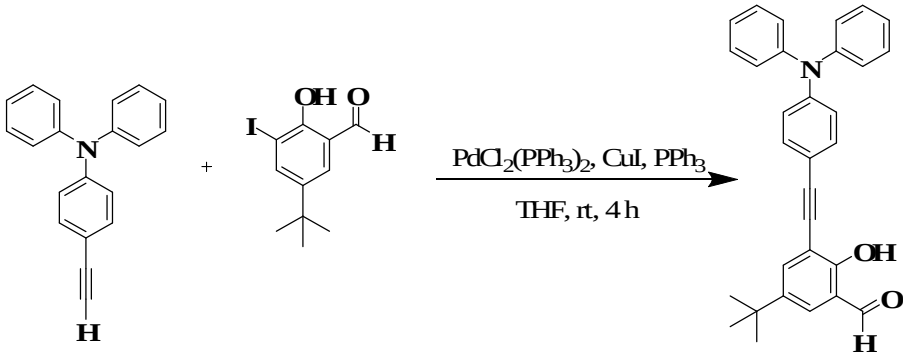

66 %

5-tert-butyl-2-hydroxy-3-iodobenzaldehyde (0.37 g, 1.22 mmol), $PdCl_2(PPh_3)_2$ (36 mg, 0.056 mmol), CuI (11 mg, 0.056 mmol) and PPh_3 (15 mg, 0.056 mmol) were dissolved in tetrahydrofuran (10 mL) by stirring with a magnetic bar in a round-bottom flask. Triethylamine (10 mL) was added and followed by 4-ethynyl-N,N-diphenylaniline (0.36 g, 1.11 mmol). The reaction mixture was stirred at room temperature for 4 h and then filtered. The solid precipitate was washed with dichloromethane (3 × 15 mL) and the filtrate was evaporated. The residue was dissolved in a minimal amount of dichloromethane and eluted through a silica gel column by gradient solvents starting from pure hexane to dichloromethane/hexane (3/1 v/v) to afford the desired product after solvent removal as a yellow solid (0.33 g, 66 % yield). ^{1}H NMR ($CDCl_3$, 400 MHz) δ (ppm) 10.70 (s, 1H), 7.94 (d, *J* = 4.8 Hz, 2H), 7.86 (d, *J* = 8.8 Hz, 2H), 7.43-7.18 (m, 12H), 1.53(s, 9H); ^{13}C NMR ($CDCl_3$, 100 MHz) δ (ppm) 188.0, 157.2, 152.4, 148.2, 146.7, 146.0, 130.6, 129.0, 125.7, 124.5, 123.2, 123.0, 122.7, 122.2, 121.1, 119.6, 99.0, 34.4, 31.3.; MALDI-TOF m/z Calcd for $C_{31}H_{27}NO_2$, 445.204 Found: 445.540.

2.3.10 Preparation of 2-hydroxy-3,5-diiodobenzaldehyde.

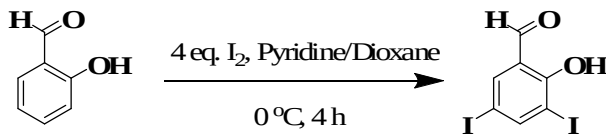

76 %

Iodine (24.90 g, 98.03 mmol), was dissolved in dioxane (20 mL) and pyridine (20 mL) by stirring with a magnetic bar in a round-bottom flask at 0 ºC for 15 min. The solution was added with 2-hydroxybenzaldehyde (3.00 g, 24.55 mmol) and the mixture was stirred at reflux for 4 h. The solvent was evaporated and $Na_2S_2O_3$ solution (20% w/v) was then added to the dark viscous residual oil until it turned light yellow. The mixture was extracted with dichloromethane (3 × 50 mL). The combined organic phase was washed with water (2 × 100 mL) and dried over anhydrous $MgSO_4$. The solution was evaporated by rotary evaporator to afford the desired product as a purple solid (6.99 g, 76%); ^{1}H NMR ($CDCl_3$, 400 MHz): δ (ppm) 11.70 (s, 1H), 9.68 (s, 1H), 8.21 (s, 1H), 7.81 (s, 1H); ^{13}C NMR ($CDCl_3$, 100 MHz): δ (ppm) 194.2, 159.6, 152.5, 141.6, 121.4, 86.7, 80.7.

2.3.11 Preparation of F3.

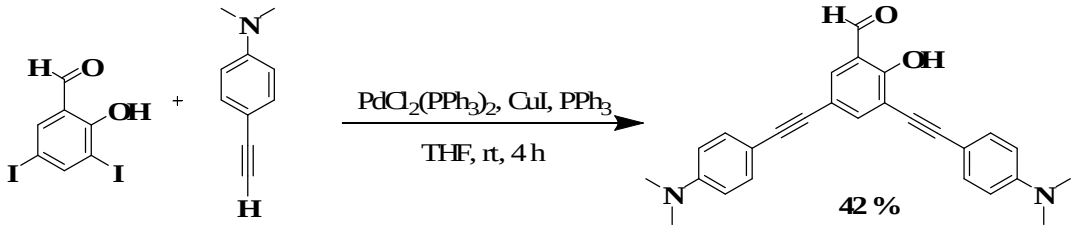

2-Hydroxy-3,5-diiodobenzaldehyde (0.93 g, 3.07 mmol), $PdCl_2(PPh_3)_2$ (132 mg, 0.19 mmol), CuI (36 mg, 0.19 mmol) and PPh_3(51 mg, 0.19 mmol) were dissolved in tetrahydrofuran (10 ml) by stirring with a magnetic bar in a round-bottom flask. Triethylamine (10 mL) was added and followed by 4-ethynyl-N,N-dimethylaniline (0.49 g, 3.38 mmol). The reaction mixture was stirred at room temperature for 4 h and then filtered. The solid precipitate was washed with dichloromethane (3 × 15 mL) and the filtrate was evaporated. The residue was dissolved in a minimal amount of dichloromethane and eluted through a silica gel column by gradient solvents starting from pure hexane to dichloromethane/hexane (3/1 v/v) to afford the desired product after solvent removal as a yellow solid (0.41 g, 42 % yield). ^{1}H NMR ($CDCl_3$, 400 MHz) δ (ppm) 10.51 (s, 1H), 7.83(s, 1H), 7.82(s, 1H), 7.75(d, *J* = 8.8 Hz, 2H), 7.40 (d, *J* = 8.6 Hz, 2H), 6.79 (s, 1H), 6.75 (d, *J* = 8.6 Hz, 2H), 6.65 (d, *J* = 8.2 Hz, 2H), 3.02 (s, 1H), 2.98 (s, 6H); ^{13}C NMR ($CDCl_3$, 100

MHz) δ (ppm) 187.8, 132.5, 131.7, 130.1, 128.2, 126.7, 126.4, 126.2, 120.2, 119.1, 111.9, 111.7, 96.9, 40.0, 29.5.; MALDI-TOF m/z Calcd for $C_{27}H_{24}N_2O_2$, 408.184 Found: 408.783.

2.3.12 Preparation of 4, 4′, 4′′-triiodotriphenylamine.

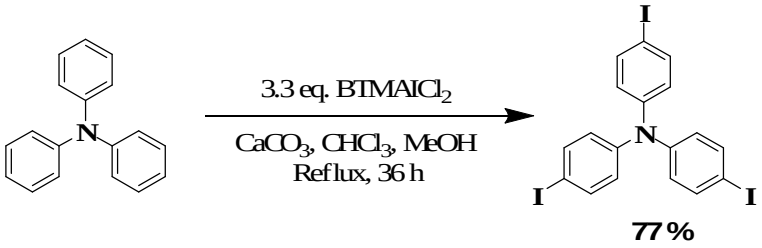

Triphenylamine (5.00 g, 20 mmol) in chloroform (100 mL) and methanol (50 mL) was added with $BTMAICl_2$ (23.41 g, 67 mmol) and $CaCO_3$ (12.00 g, 120 mmol). The reaction mixture was allowed to reflux for 72 h and 20% $Na_2S_2O_3$ solution was then added to the mixture until the mixture became light yellow. The mixture was filtered and the filtrate was extracted with dichloromethane (3 × 50 mL). The combined organic phase was washed with water (2 × 100 mL) and dried over anhydrous $MgSO_4$. The solution was concentrated and the residue was reprecipitated in methanol from dichloromethane solution. Triiodotriphenylamine was obtained (9.78 g, 77%) as a white solid: mp; 182-184^oC; ^1H NMR ($CDCl_3$, 400 MHz): δ (ppm) 7.53 (d, *J* = 7.5 Hz, 6H), 6.80 (d, *J* = 7.5 Hz, 6H); ^{13}C NMR ($CDCl_3$, 100 MHz): δ (ppm) 146.6, 138.5, 126.1, 88.7; MALDI-TOF m/z Calcd. for $C_{18}H_{12}I_3N$, 622.810 Found: 622.561.

2.3.13 Preparation of 4, 4’, 4’’-trimethylsilylethynylphenylamine.

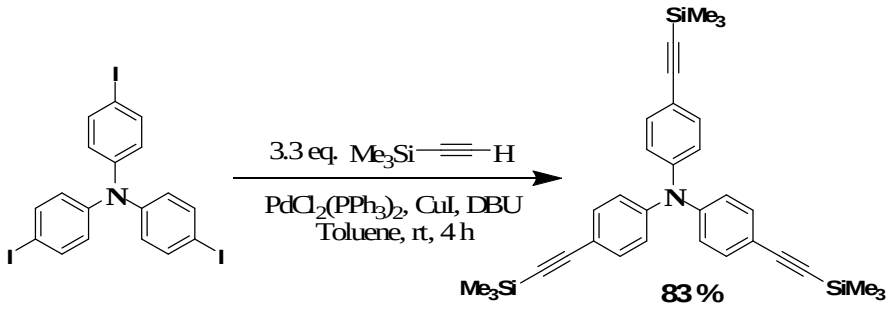

Triiodotriphenylamine (2.00 g, 3.2 mmol), $PdCl_2(PPh_3)_2$ (0.11 g, 0.16 mmol) and CuI (30 mg, 0.16 mmol) was dissolved in toluene (10 mL) by stirring with a magnetic bar in a round-bottom flask. 1,8-Diazabicycloundec-7-ene (DBU, 2 mL) was added and followed by trimethylsilyl acetylene (1.09 g, 11.2 mmol).[8] The reaction mixture was stirred at room temperature for 4 h and then filtered. The solid precipitate was washed with toluene (3 × 15 mL) and the filtrate was evaporated. The residue was dissolved in a minimal amount of dichloromethane and eluted through a silica gel column by hexane to afford the desired product after solvent removal as light yellow oil (0.57 g, 83% yield). ^{1}H NMR ($CDCl_3$, 400 MHz): δ (ppm) 7.34 (d, *J* = 8.4 Hz, 6H), 6.96 (d, *J* = 8.4 Hz, 6H), 0.24 (s, 27H); ^{13}C NMR ($CDCl_3$, 100 MHz): δ (ppm) 146.7, 133.1, 123.8, 117.7, 104.8, 93.9, 0.1.

2.3.14 Preparation of 4, 4', 4''-triethynylphenylamine.

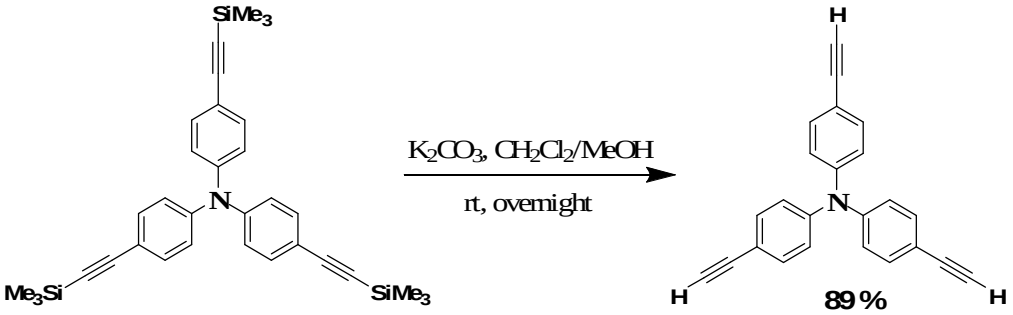

4,4′,4′′-Trimethylsilylethynylphenylamine (2.00 g, 3.7 mmol) and K_2CO_3 (0.508 g, 0.43 mmol) was dissolved in dichloromethane (15 mL) and methanol (15 mL) by stirring with a magnetic bar in a round-bottom flask. The reaction mixture was stirred at room temperature for 24 h. The organic layer was separated and the aqueous phase was extracted with dichloromethane (2 × 50 mL) and was then dried over anhydrous $MgSO_4$. The solvent was evaporated and the residue was dissolved in a minimal amount of dichloromethane and eluted through a silica gel column by gradient solvents starting from pure hexane to dichloromethane/hexane (1/4 v/v) to afford the desired product after solvent removal as a blown solid (1.06 g, 89% yield). ^{1}H NMR ($CDCl_3$, 400 MHz): δ (ppm) 7.38 (d, *J* = 8.4 Hz, 6H), 7.01 (d, *J* = 8.4 Hz,

6H), 3.06 (s, 3H); ^{13}C NMR ($CDCl_3$, 100 MHz): δ (ppm) 147.0, 133.3, 123.9, 116.8, 83.4, 77.0.

2.3.15 Preparation of F4.

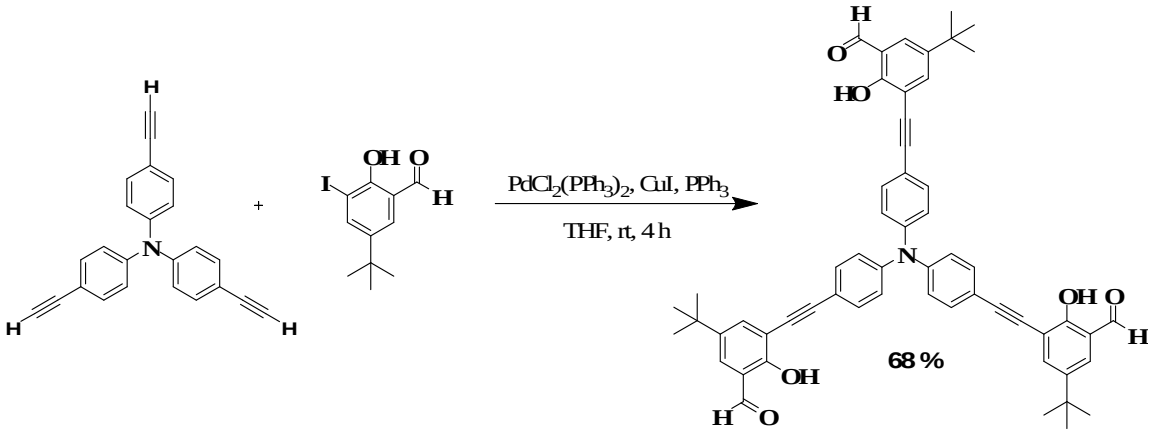

5-*t*ert-Butyl-2-hydroxy-3-iodobenzaldehyde (1.17 g, 3.84 mmol), $PdCl_2(PPh_3)_2$ (95 mg, 0.144 mmol), CuI (27 mg, 0.144 mmol) and PPh_3 (38 mg, 0.144 mmol) were dissolved in tetrahydrofuran (10 mL) by stirring with a magnetic bar in a round-bottom flask. Triethylamine (10 mL) was added and followed by 4,4′,4′′-triethynylphenylamine (0.60 g, 0.96 mmol). The reaction mixture was stirred at room temperature for 4 h and then filtered. The solid precipitate was washed with dichloromethane (3 × 15 mL) and the filtrate was evaporated. The residue was dissolved in a minimal amount of dichloromethane and eluted through a silica gel column by gradient solvents starting from pure hexane to dichloromethane/hexane (3/1 v/v) to afford the desired product after solvent removal as a yellow solid (0.28 g, 68% yield). ^{1}H NMR (Acetone-D_6, 400 MHz): δ (ppm) 10.4 (s, 3H), 7.88 (d, *J* = 8.8 Hz, 6H), 7.87 (s, 3H), 7.81 (s, 3H), 7.20 (d, *J* = 8.8 Hz, 6H), 7.18 (s, 1 H), 1.36 (s, 27H); ^{13}C NMR (Acetone-D_6, 100 MHz): δ (ppm) 189.9, 158.9, 154.0, 149.2, 133.0, 128.2, 126.8, 126.2, 125.4, 124.3, 122.3, 102.3, 36.4, 32.9; MALDI-TOF m/z Calcd for $C_{51}H_{57}NO_6$, 845.372 Found: 845.455 [M^+].

2.4 Photophysical property study

The stock solutions of 500 µM fluorophores in DMSO or 1 % DMSO in 10 mM HEPES buffer pH 7.4 were prepared.

2.4.1 UV-Visible spectroscopy

The UV-Visible absorption spectra of the stock solutions of fluorophores were recorded from 250 nm to 600 nm at ambient temperature.

2.4.2 Fluorescence spectroscopy

The stock solutions of 500 µM fluorophores were diluted to 1 and 5 µM, respectively, with their respective solvents. The emission spectra of fluorophores were recorded from 370 nm to 700 nm at ambient temperature using an excitation wavelength at 360 to 400 nm, respectively.

2.4.3 Fluorescence quantum yields

The fluorescence quantum yield of fluorophores were performed in DMSO and HEPES buffer (10 mM) pH 7.4 by using quinine sulphate ($\Phi F = 0.54$) in 0.1 M H_2SO_4 as a reference [41]. The UV-Visible absorption spectra of five analytical samples and five reference samples at varied concentrations were recorded. The maximum absorbance of all samples should never exceed 0.1. The fluorescence emission spectra of the same solutions using appropriate excitation wavelengths selected were recorded based on the absorption maximum wavelength (λmax) of each compound. Graphs of integrated fluorescence intensities were plotted against the absorbance at the respective excitation wavelengths. Each plot should be a straight line with 1 interception and gradient *m* [42].

In addition, the fluorescence quantum yield (ΦF) was obtained from plotting of integrated fluorescence intensity *vs* absorbance represented into the following equation:

$$\Phi_X = \Phi_{ST}\left(\frac{Grad_X}{Grad_{ST}}\right)\left(\frac{\eta_X^2}{\eta_{ST}^2}\right)$$

The subscripts Φ_{ST} denote the fluorescence quantum yield of a standard reference which used quinine sulfate in 0.1 M H_2SO_4 (Φ = 0.54) and Φ_X is the fluorescence quantum yield of sample and η is the refractive index of the solvent.

2.5 Fluorescent sensor study

2.5.1 Anion sensor

The excitation wavelength was 378 nm, 373 nm, 382 nm and 395 nm for F1, F2, F3 and F4 and the emission was recorded from 383-700 nm. Sodium anion solutions were prepared in Milli-Q water. Concentrations of all stock sodium anion solutions were adjusted to 150 mM and were added with the desired volumes (10 μL) to the fluorophore solutions. The final volumes of the mixtures were adjusted to 1 mL to afford the final concentration of 5 μM for the fluorophores and 1,500 μM for anion.

2.5.2 Surfactants study

The excitation wavelength was 373 nm and the emission was recorded from 383-700 nm. Surfactants solutions were prepared in Milli-Q water. Concentrations of all stock sodium anion solutions were adjusted to 50 mM and were added with the desired volumes (2000 μL) to the fluorophore solutions. The final volumes of the mixtures were adjusted to 1 mL to afford the final concentration of 5 μM for the fluorophores and 10 μM for surfactants.

CHAPTER III

RESULTS AND DISCUSSION

3.1 Cyanide fluorescence sensors from F1, F2 and F3

In this contribution, we investigated fluorophores **F1-F3** (**Figure 3.1**) containing the salicylaldehyde probe conjugated with phenylene-ethynylene fluorogenic units. In our design to enhance the CN^- sensitivity of the probe, different electron donating amino groups were incorporated at the other end of the phenylene-ethynylene conjugated system to promote the initial ICT process of the salicylaldehyde probe. One of these fluorophore gives shows excellence sensitivity that it can be use in aqueous HEPES buffer system.

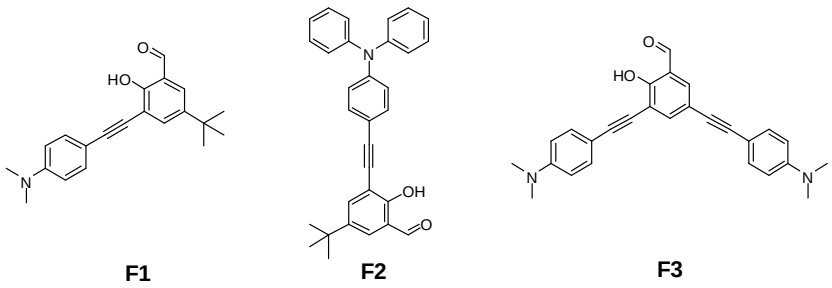

Figure 3.1 Fluorophore molecules **F1**, **F2**, and **F3**.

3.1.1 Synthesis and characterization of F1, F2 and F3

The fluorophores (**F1-F3**) were synthesized according to Scheme 3.1 using Sonogashira coupling as the key reaction. The synthesis was started with the Sonogashira coupling of 4-iodo-dimethylaniline with ethynyltrimethylsilane using DBU in toluene and followed by desilylation to afford 4-ethynyl-*N*,*N*-dimethylaniline. The reactive core of **F2**, 4-ethynyl-*N*,*N*-diphenylaniline was prepared from substitution reaction of diphenylamine with 1,4-diiodobenzene followed by the Sonogashira coupling with ethynyltrimethylsilane using DBU in toluene and proceeded by desilylation. The subsequent coupling of the resulting 5-tert-butyl-3-iodosalicylaldehyde with 4-ethynyl-*N*,*N*-dimethylaniline and with 4-

ethynyltriphenylamine gave **F1** and **F2** respectively. For **F3**, salicylaldehyde was fist double iodinated to give diiodosalicylaldehyde. The subsequent coupling with 2.2 equivalents of 4-ethynyl-*N*,*N*-dimethylaniline yielded the desired **F3**.

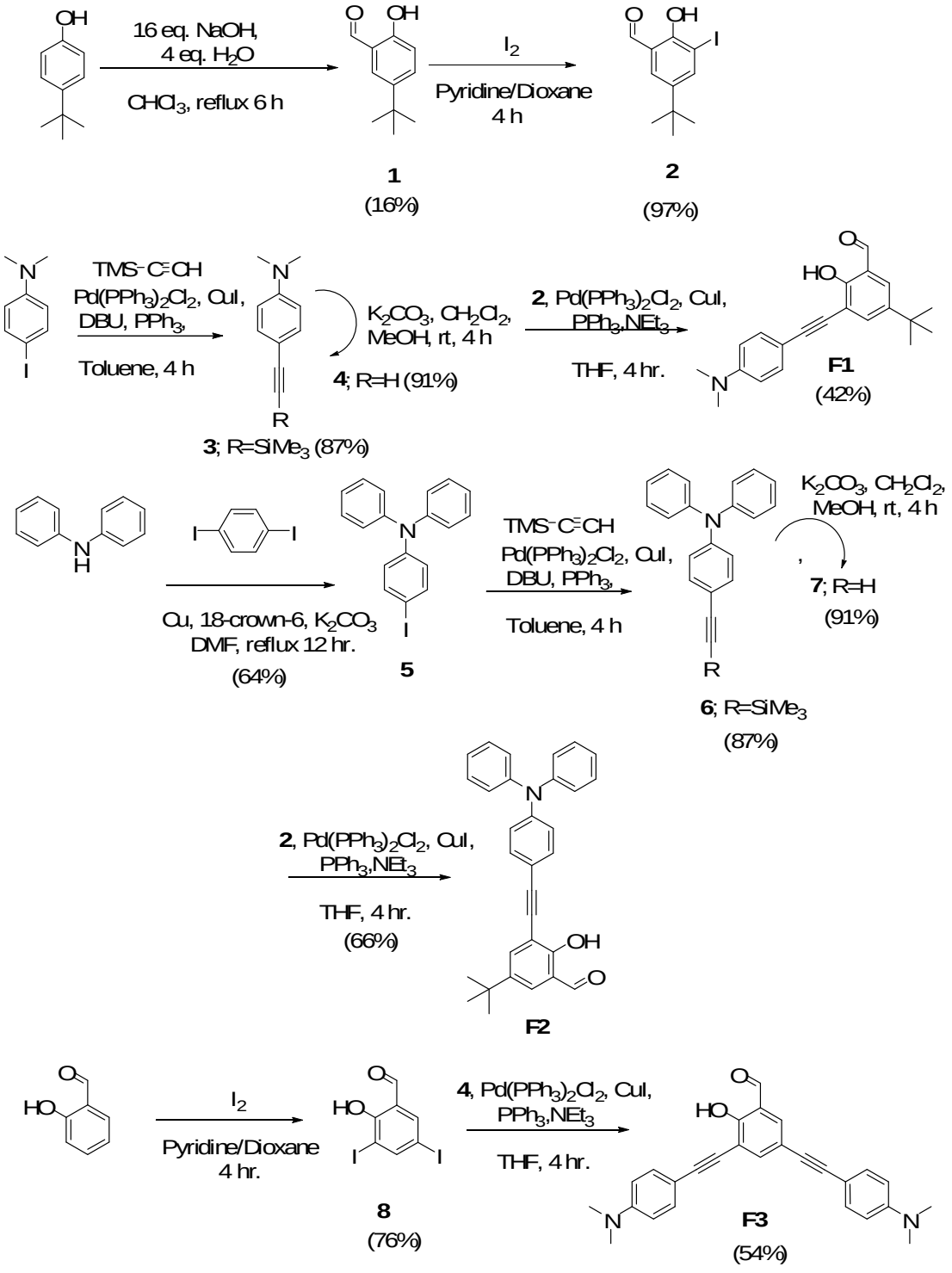

Scheme 3.1 Synthetic route of fluorophore **F1**, **F2**, and **F3**.

The ^{1}H-NMR spectra of compound **2**, **4**, and **F1** are shown in **Figure 3.2** All signals can be assigned to all protons in each corresponding structure. Initially, compound **2** showed two singlet signals at 11.6, 9.8, 8.0, 7.6 and 1.3 ppm corresponding to its aldehyde, hydroxy, aromatic and alkyl protons, respectively. Then, compound **2** coupling with **4** by using Sonogashira reaction, the methyl amine product showed signals of the methyl amine protons as a singlet at 3.0 ppm and singlet signals at and 10.6 as a aldehyde proton from compound **2** .

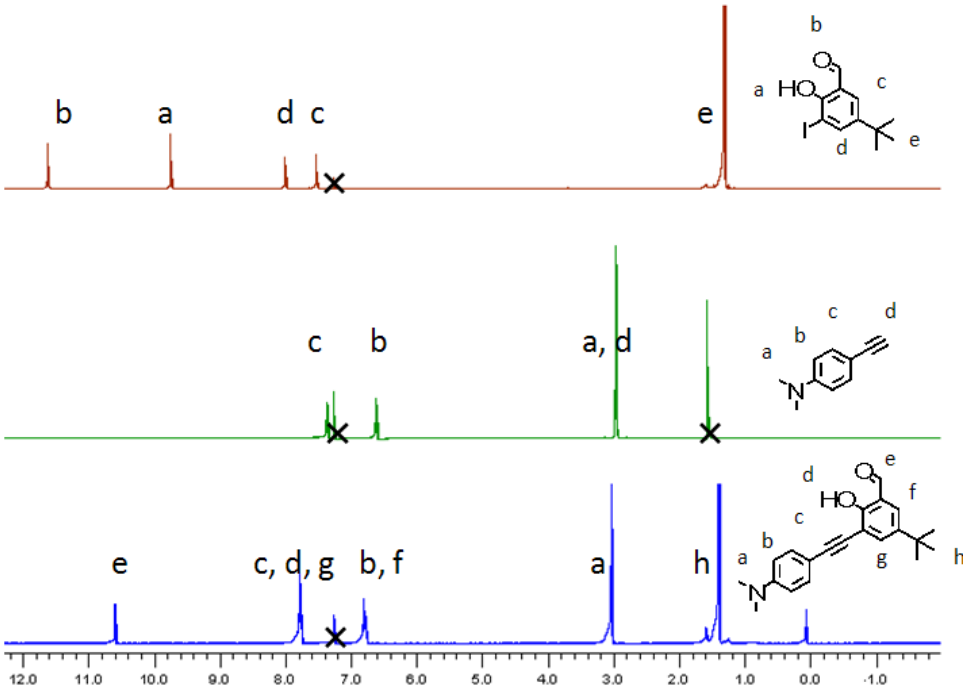

Figure 3.2 ^{1}H-NMR (400 MHz) spectra of starting material compounds of **2**, **4** and **F1** in $CDCl_3$.

Compound **5** showed signals of aromatic protons as two triplet at 7.3 and 7.0 ppm and three doublet signals at 7.5, 7.1 and 6.8 ppm. Then, compound **5** coupling with ethynyltrimethylsilane by using Sonogashira reaction, the trimethylsilane product showed signals of the methylsilane protons as a singlet at 0.2 ppm. The desilylation of compound **6** gave compound **7.** The spectrum showed that the singlet signal of the trimethylsilane protons at 0.2 ppm totally disappeared upon the desilylation. Upon incorporation of compound **2**, **F2** showed new signals of the

aldehyde proton as a singlet at 10.7 ppm and one singlet signals of alkyl protons at 1.5 ppm (**Figure 3.3**).

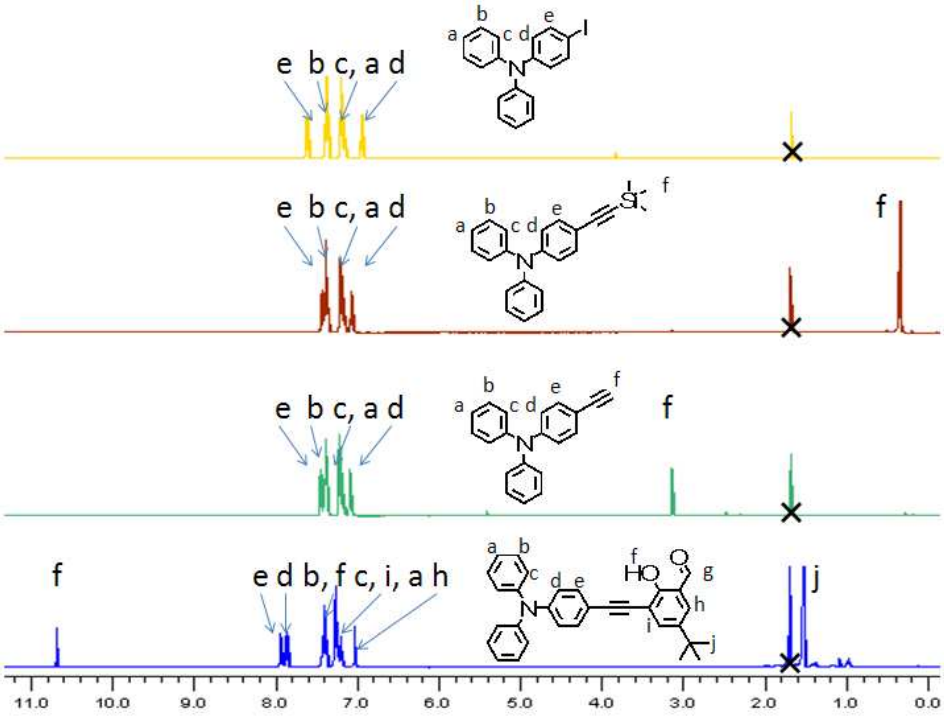

Figure 3.3 ^{1}H-NMR (400 MHz) spectra of starting material compounds of **5**, **6**, **7** and **F2** in $CDCl_3$.

The ^{1}H-NMR spectra of compound **8**, **4**, and **F3** are shown in **Figure 3.4**. The compound **8** showed four singlet signals at 11.7, 9.7, 8.2 and 7.8 ppm corresponding to its aldehyde, hydroxy, and two aromatic protons, respectively. Then, compound **8** coupling with compound **4** by using Sonogashira reaction, the methyl amine product showed two signals of the methyl amine protons as a singlet at 3.0 ppm (3.00 and 3.04 ppm) and the spectrum showed that the singlet signal of the aldehyde proton at 10.5 ppm totally appeared upon incorporation of compound **8**.

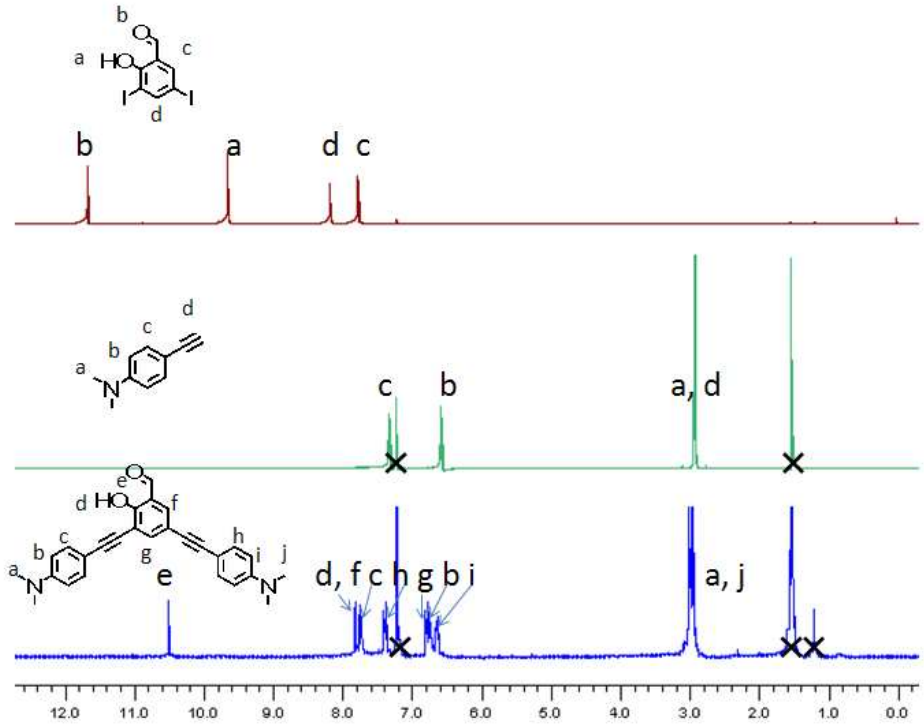

Figure 3.4 ^{1}H-NMR (400 MHz) spectra of starting material compounds of **8**, **4** and **F3** in $CDCl_3$.

3.1.2 Photophysical property study of F1, F2 and F3

The electronic absorption and emission spectroscopy of **F1**-**F3** were studied in an aqueous DMSO solvent and their photophysical properties are compiled in **Table 3.1**. The fluorophores exhibited two major absorption maxima (300-335 and 380-385 nm; **Figure 3.5**) associated with two π-π* electron transitions (S0→S2 and S0→S1) of the π-conjugated phenylene-ethynylene system[43]. Each fluorophore showed a single maximum emission wavelength around 415-444 nm (**Figure 3.5**). The greater Stroke shift of **F2** and **F3** implied the greater involvement of the ICT process in the excited states of these fluorophores. To evaluate **F1**-**F3** as the cyanide sensors, the emission spectrum of each fluorophore solution before and after the addition of sodium cyanide was recorded.

Table 3.1 Photophysical properties of **F1-F3** in 90%DMSO/10 mM HEPES buffer pH 7.4

Compound	λ_{ab} (nm)	log ε	λ_{em} (nm)
F1	320, 380	4.35, 4.24	415
F2	300, 383	4.40, 4.52	440
F3	335, 385	4.91, 3.49	444

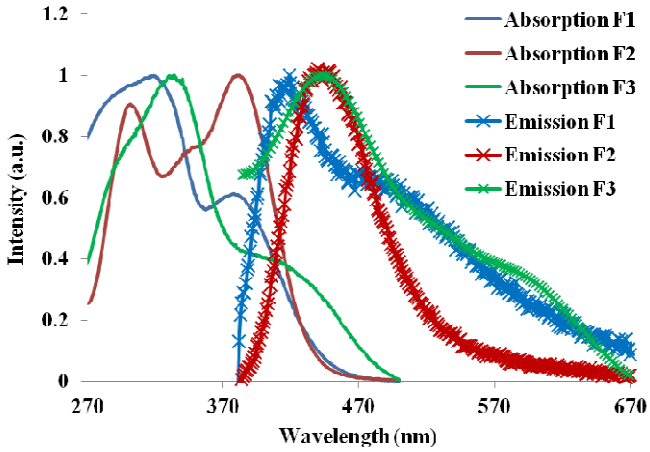

Figure 3.5 Electronic absorption spectra and emission spactra of **F1**, **F2**, and **F3** (5 µM) in 90%DMSO/10 mM HEPES buffer pH 7.4

The presence of cyanide ion substantially enhanced the emission signal of the fluorophores (**Figure 3.6**). The results clearly demonstrate that **F1-F3** are promising as the fluorescence turn-on cyanide sensors. The effects of solvent on the sensitivity of the fluorophores were studied by varying the content of DMSO in the buffer solution from 10-90%. **Figure 3.7** shows that the optimum media for **F1**, **F2** and **F3** should contain 80%, 70%, and 90% DMSO, respectively. In their optimum medium, **F3** provided the highest sensitivity with fluoresence enhancement ratio (I/I_0) of 114.

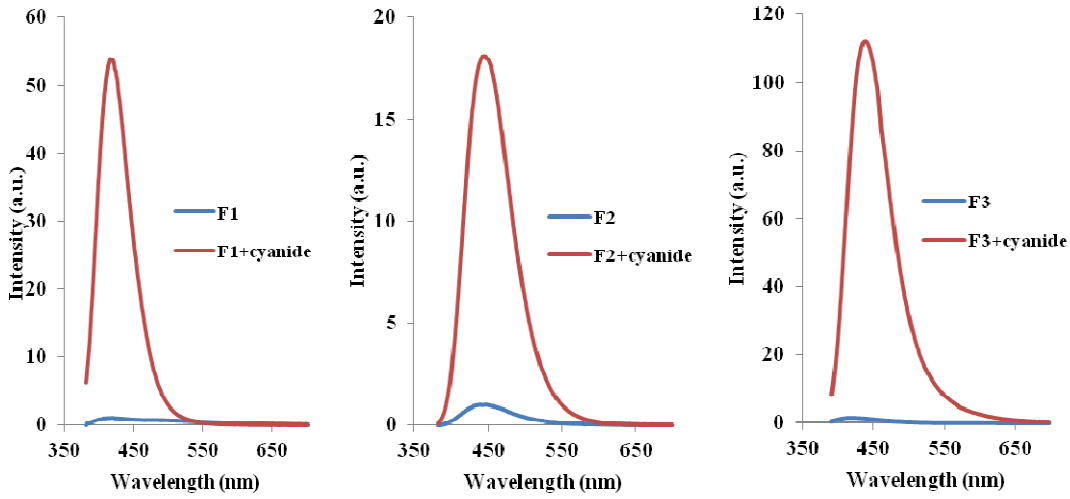

Figure 3.6 Emission spectra of the solutions of **F1**, **F2** , and **F3** (5µM) upon the addition of sodium cyanide (1.5 mM) in 90%DMSO/10 mM HEPES buffer pH 7.4.

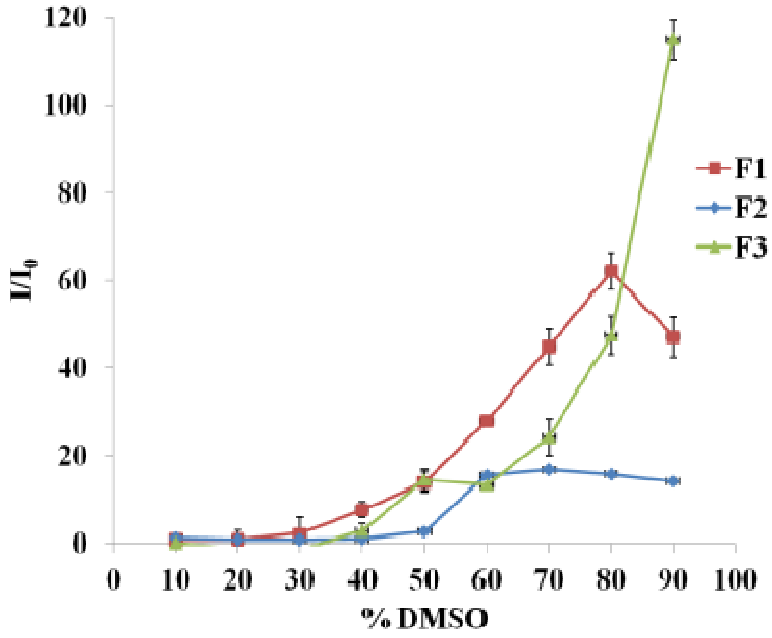

Figure 3.7 Fluorescence enhancement (I/I_0) of **F1**, **F2**, and **F3** (5µM) upon the addition of sodium cyanide (1.5 mM) in 10 mM HEPES buffer pH 7.4 mixed with DMSO (10-90% v/v).

The drastic drop of the sensitivity observed in media with high water contents may be attributed to the poor water solubility of these fluorophores. To determine if the sensitivity was associated with the ICT process, the fluorescence quantum yields of the fluorophores were determined before and after the addition of cyanide ion. It is clearly seen that the fluorescence quantum yields significantly increased after the addition of cyanide ion which readily react with the hydrogen-bonded aldehyde group. Assuming that the cyanohydrin products do not allow the ICT process, the quantum yield difference (%ΦFCN-%ΦF) should fairly represent the fluorescence quenching by the ICT process. As shown in **Table 3.2**, **F3** exhibited the highest quantum yield difference implying that **F3** has the highest initial ICT quenching which may be attributed to the fact that **F3** has two quenchable fluorogenic branches. It is also interesting to note that **F2**, despite having a larger ($\%\Phi_F$CN-$\%\Phi_F$) value, has lower fluorescence enhancement than **F1** as a result of higher quantum yield of **F2**. The results confirmed that the sensitivity of the sensor is also depended on the initial quantum yield of fluorophore. Ideally, a highly sensitive fluorescence turn-on cyanide sensor would require a low initial quantum yield with large quenching effect contributed by the ICT process. In the case, such a sensor design was achieved by combining two fluorogenic units with one ICT unit which also acts as the cyanide active site.

Table 3.2 Photophysical properties of **F1-F3** upon the addition of sodium cyanide (1.5 mM) in 10 mM HEPES buffer pH 7.4 mixed with DMSO

Compound	%DMSO	I/I_0	$\%\Phi_F$	$\%\Phi_F^{CN}$	$\%\Phi_F^{CN}$-$\%\Phi_F$
F1	80	62	1.8	28.2	26.4
F2	70	17	3.1	32.5	29.4
F3	90	114	2.6	39.8	37.2

Quinine sulfate in 0.1 M H_2SO_4 (ΦF = 0.54) was the reference.

3.1.3 Fluorescent sensors study of F1, F2 and F3

Since cyanide ion is more commonly found in aqueous media, we next decided to investigate the use of **F3** for cyanide sensing in aqueous micellar system

because of the poor solubility of the fluorophore in pure aqueous buffer. Fluorescence study was performed in HEPES solution pH 7.4 in the presence of various surfactants using the excitation wavelength at 373 nm. As expected for anion sensors, the cationic surfactants (DTAB, CTAB and TTAB) generally gave higher sensitivity than the anionic surfactant (SBS and SDS) and nonionic surfactant (Brij and TWEEN20). However, among eight surfactants tested, the nonionic surfactant Triton X-100 gave the highest sensitivity (**Figure 3.8**). This unique effect of Triton X-100 has been observed before in the sensors based on phenylene-ethynylene that is likely to be attributed to the oligo(ethylene glycol) chain and the aromatic ring in the structure of Triton X-100[44-46]. The oligo(ethylene glycol) chain can bind with sodium cation which in turn concentrate cyanide anion around its micelle and the 30 mM where the system gave the fluorescence enchantment ratio of 18 (**Figure 3.9**).

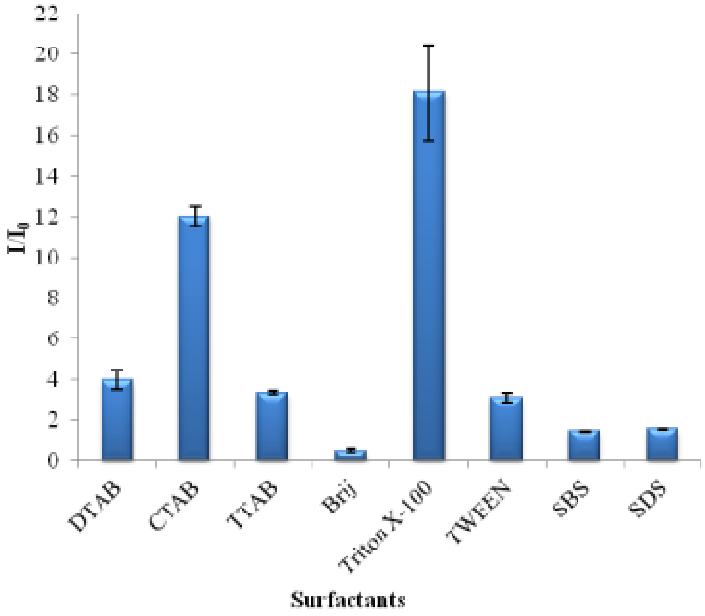

Figure 3.8 Bar chart representing the fluorescence enhancement (I/I_0) of **F3** (5 µM) upon the addition of sodium cyanide (1.5 mM) in HEPES buffer pH 7.4 (10 mM) in the presence of various surfactants (10 mM). The fluorescence intensity at the emission peak of each system was used.

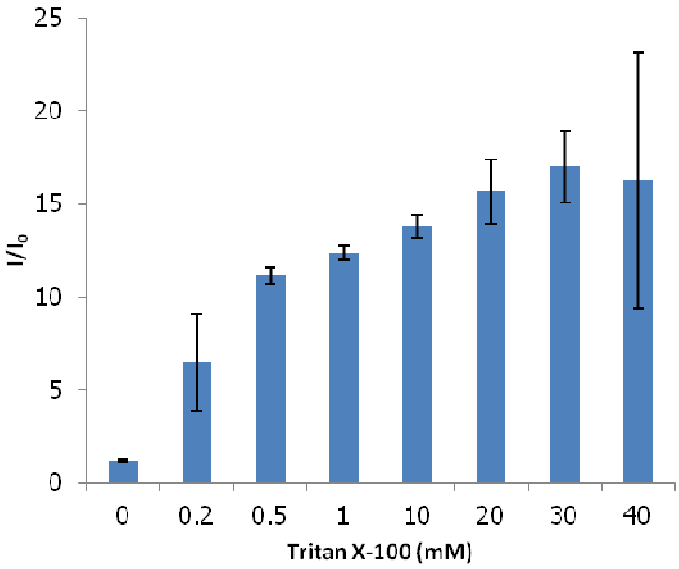

Figure 3.9 Bar chart representing the fluorescence enhancement (I/I_0) of **F3** (5 µM) upon the addition of sodium cyanide (1.5 mM) in HEPES buffer pH 7.4 (10 mM) in the presence of various surfactants (10 mM). The fluorescence intensity at the emission peak of each system was used.

The fluorescence response in relation to cyanide concentration was monitored upon the addition of various equivalents of sodium cyanide in an aqueous solvent (HEPES buffer at pH 7.4, 30 mM Triton X-100). The fluorescence intensity initially increased almost linearly with the cyanide concentration up 1000 equiv (**Figure 3.10**). It is important to mention that the emission spectra were acquired at 5 min for all sensing experiments to ascertain the completion of the reaction although the reaction between cyanide ion and **F3** was complete within 90 sec (**Figure 3.11**). The pH variation also showed only little effect of the pH in the range of 6.0-8.5 on the cyanide sensitivity (**Figure 3.12**).

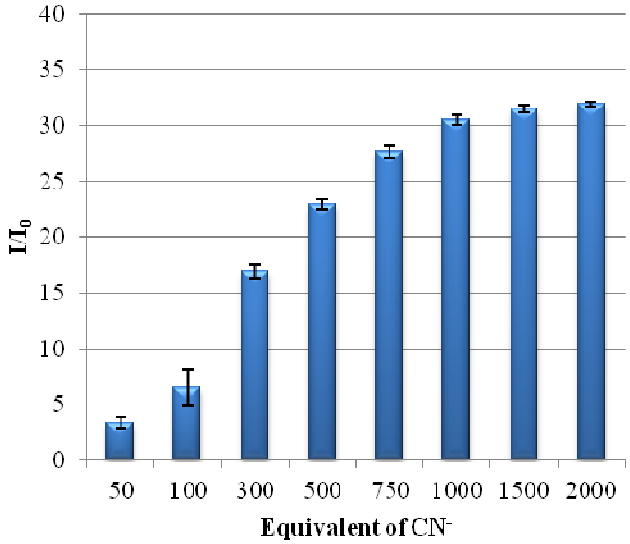

Figure 3.10 The bars represent the fluorescence enhancement ratio (I/I_0) of **F3** (5µM) at various equiv of cyanide in Triton X-100 (30 mM)/HEPES buffer pH 7.4 (10mM).

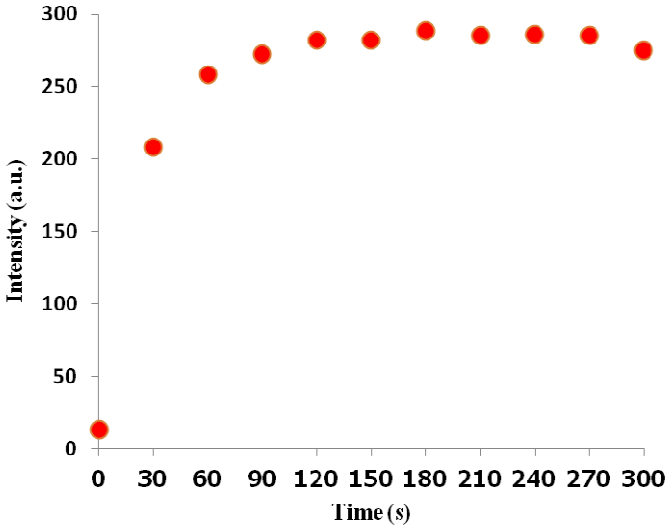

Figure 3.11 Time-dependent changes in the fluorescence intensity of **F3** (5µM) upon addition of cyanide 1000 equiv in Triton X-100 (30 mM)/HEPES buffer pH 7.4 (10mM).

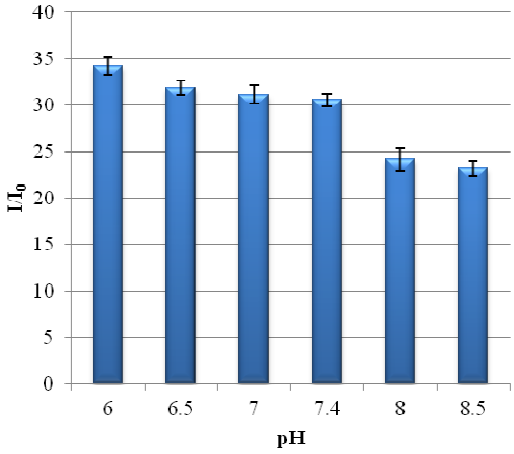

Figure 3.12 Bars represent the fluorescence enhancement ratio (I/I_0) at various pH of HEPES buffer (10mM) in Triton X-100 (30 mM)

In the selectivity and interference tests, F3 exhibited high specificity toward cyanide ion (**Figure 3.13 a**) with very low interference from other anions (**Figure 3.13 b**).

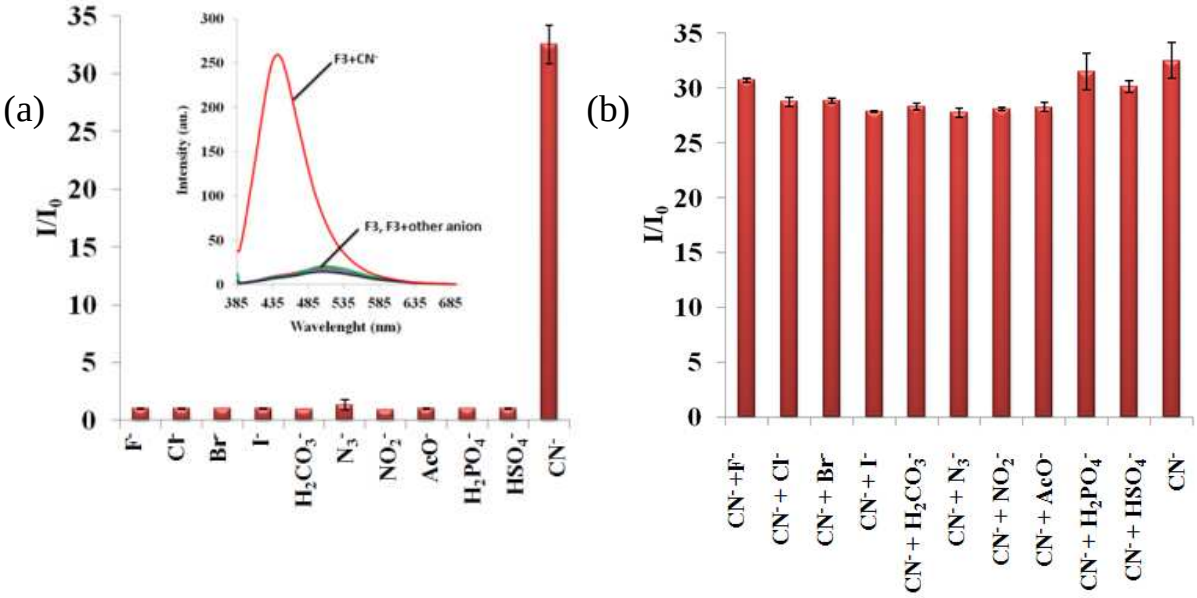

Figure 3.13 (a) Fluorescence enhancement ratio (I/I_0) and fluorescence spectra of **F3** in the presence of various anions. (b) Fluorescence enhancement ratio (I/I_0) of **F3** in the presence of cyanide and another ion. The data were based on the fluorescence intensity at 440 nm acquired from the solution in HEPES buffer pH 7.4 (10mM) containing Triton X-100 (30 mM) with [**F3**] = 5 μM and [anion] = 5.0 mM.

The detection limit at was estimated by a plot of ΔI at 440 nm versus cyanide concentration, which shows a well-behaved linear correlation down to the value of 1.6 μM (**Figure 3.14**). This value is comparable to the WHO guideline of 2.7 μM. (0.07 mg/L) cyanide allowed in drinking water.

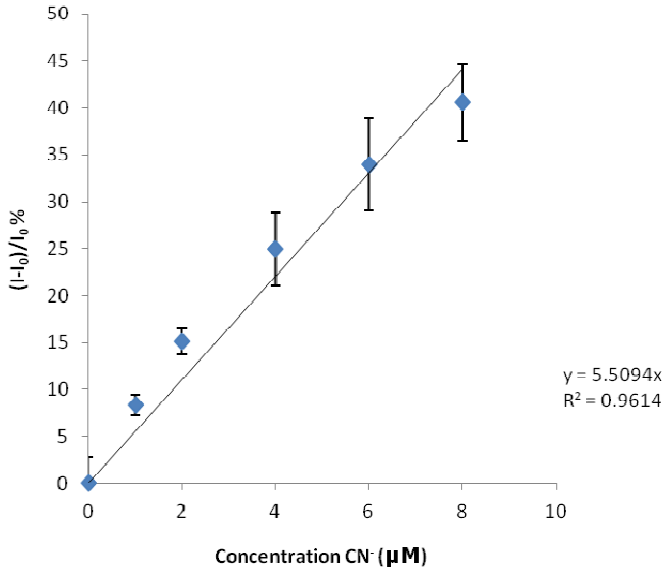

Figure 3.14 A plot of the fluorescence intensity change ((I - I_0)/I_0 x 100) of **F3** vs [CN^-] in Triton X-100 (30 mM)/HEPES buffer pH 7.4 (10mM).

Paper-based solid state sensors have recntly become one of the most convenient and economical sensing platforms [47-51]. We decided to test **F3** as a sensing agent for cyanide detection on paper strips. A series of 1.0 μL of **F3** solutions in EtOH (0.01 mM) was dropped on to a filter paper strip (7 × 11 cm^2) at 0.5 cm above the bottom end of the strip. After air dry, 8 yellow fluorescnt spots, each containing 0.01 nmol of **F3,** appeared. The strip was dropped with a series of 0.5 μL sodium cyanide solutions, containing 5-1000 nmol cyanide ion, at 2 cm vertically above the positions of the fluorophore blots. After drying, the bottom of the strip was dipped into dichloromethane/hexane (1/1, v/v) in a closed chamber and allowed for the solvent to run up to the top. The strip was taken out from the chamber, air dried and visualized under an ordinary 20 W black light lamp. Four strips using 0.5, 1.0, 2.0 and 5.0 nmol of **F3** were tested. The photographic images of the strips showed green

emission spots captured at the cyanide blots. The paper strip with 2.0 nmol of **F3** gave the best visual sensitivity and lowest emission background from the unreacted fluorophore. This paper strip showed the naked eye detection of cyanide down to 5 nmol (**Figure 3.15**). To our knowledge, this is the first fabrication of fluorescence cyanide paper sensor strips which are conveniently and economically prepared from microliter drops of florophore and sensitive enough to visually detect nanomole level of cyanide ion.

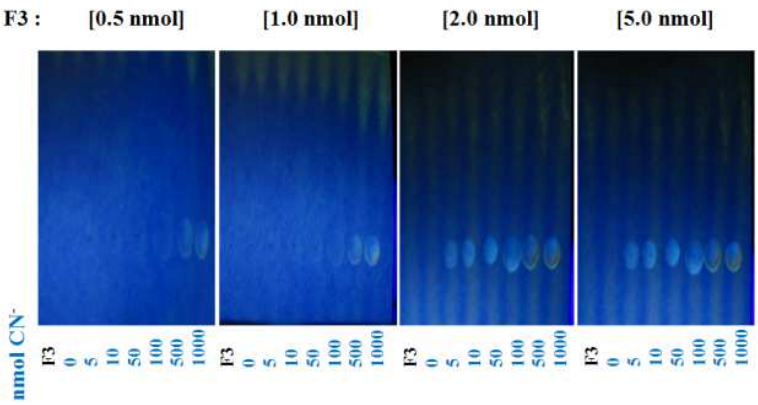

Figure 3.15 Photographic images for paper-based detection of cyanide ion under 20 W black light.

3.2 Cyanide fluorescence sensor from F4

In this contribution, we investigated fluorophores **F4** containing three salicylaldehyde probe conjugated with three phenylene-ethylene fluorogenic units. **F4** was designed in order to compare the CN^- sensitivity of the probe with phenylene-ethylene fluorogenic units containing one sensing unit **(F1-F3)**.

3.2.1 Synthesis and characterization of F4

To enhance the cyanide fluorescence sensing of the fluorophores, 5-*tert*-butylsalicylaldehyde was installed as the peripheral groups of the target molecules. The peripheral building, 5-*tert*-butylsalicylaldehyde was synthesized by Reimer-Tiemann reaction of 5-*tert*-butylphenol with chloroform followed by heating with sodium hydroxide. The iodination of the 5-*tert*-butylsalicylaldehyde using iodine in pyridine and dioxane gave 5-tert-butyl-3-iodosalicylaldehyde. The reactive core, 4, 4′, 4″-triethynylphenylamine, was prepared from triple iodination of triphenylamine using benzyltrimethyl-ammonium iododichloride ($BTMAICl_2$) [52] and proceed with the Sonogashira coupling with ethynyltrimethylsilane followed by desilylation to afford the reactive core. The Sonogashira coupling of the reactive core and 5-*tert*-butyl-3-iodosalicylaldehyde gave **F4** (**Scheme 3.2**).

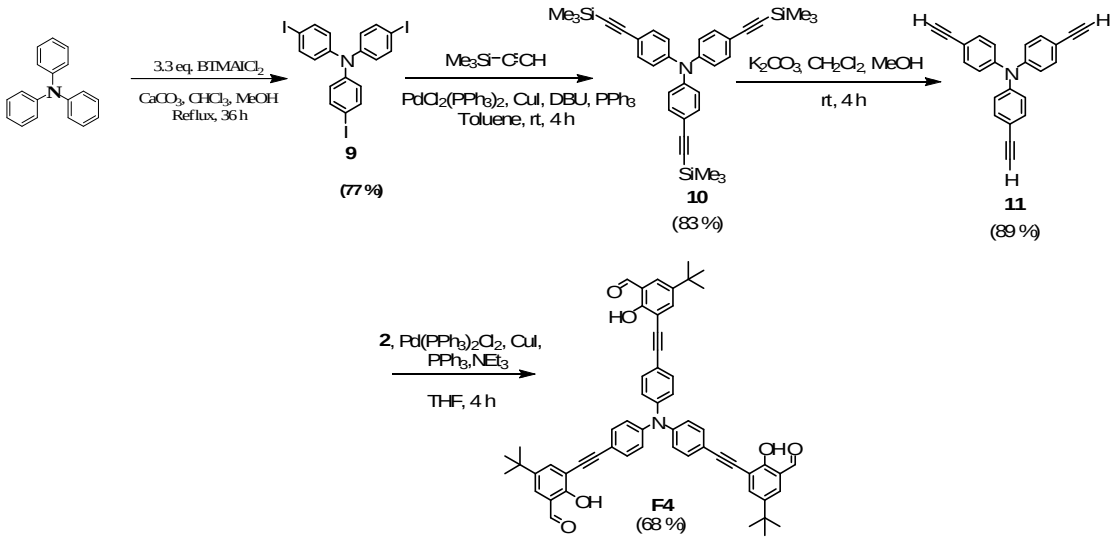

Scheme 3.2 Synthetic route of fluorophore **F4.**

The compound **9** showed signals of aromatic protons as two doublet at 7.5 and 6.8 ppm Then, compound **9** coupling with ethynyltrimethylsilane by using Sonogashira reaction, the trimethylsilane product showed signals of methylsilane protons as a singlet at 0.2 ppm. The desilylation of compound **10** gave compound **11.** The spectrum showed that the singlet signal of trimethylsilane protons at 0.2 ppm totally disappeared upon the desilylation. Upon incorporation of compound **2** to compound **11**, **F4** showed new signals of aldehyde proton as a singlet at 10.4 ppm and one singlet signals of alkyl protons at 1.4 ppm (**Figure 3.16**).

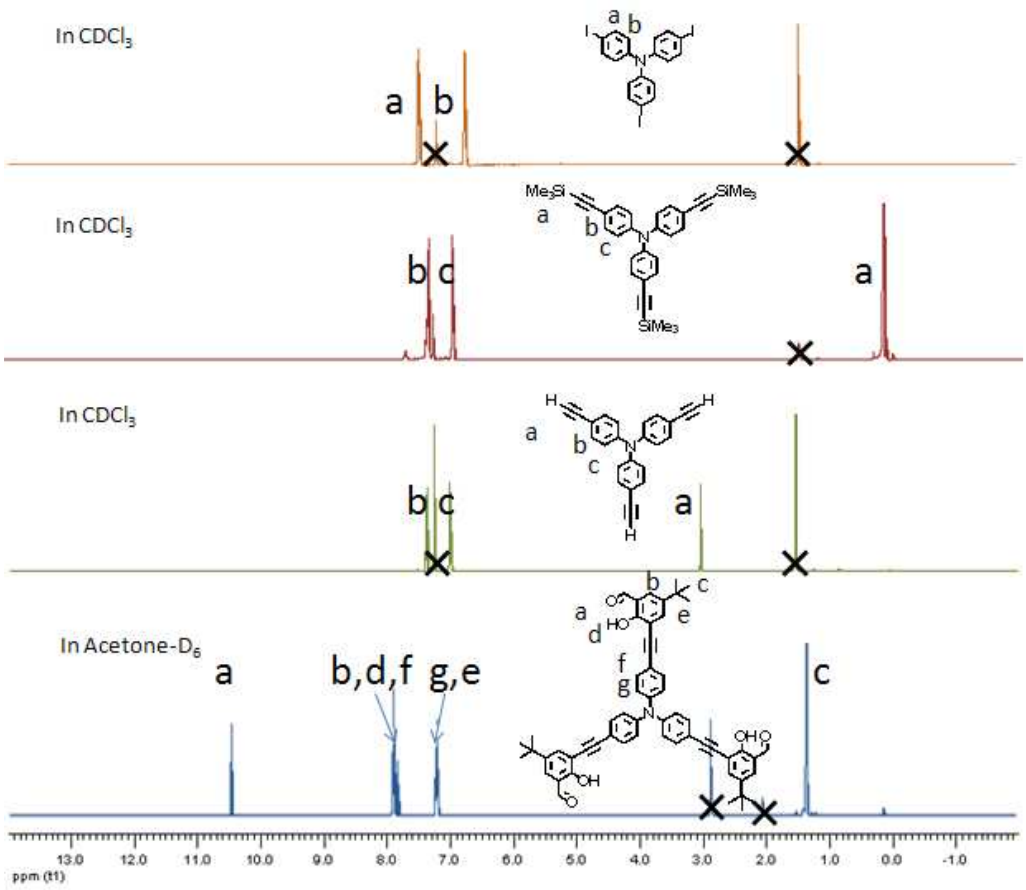

Figure 3.16 ^{1}H NMR spectra of starting material compounds **9, 10, 11 and F4.**

3.2.2 Photophysical property study of F4

In 75% DMSO/10 μM HEPES pH 7.4, **F4** showed emission maximum at 463 nm. The time-dependent fluorescence changes exhibited the increase of the fluorescence intensity upon the addition of sodium cyanide (1.5 mM) that reached the saturation after 5 min (**Figure 3.18**). To ensure completion of the spectral change, the mixing time of 10 min was allowed for all subsequent experiments. A slight blue shift from 397 to 390 nm in the absorption maximum was also observed (**Figure 3.17**) suggesting a small loss of π-conjugation length. These spectral changes as well as their time scale are in good correspondent with the reaction of cyanide adding to the aldehyde group to form cyanohydrin.

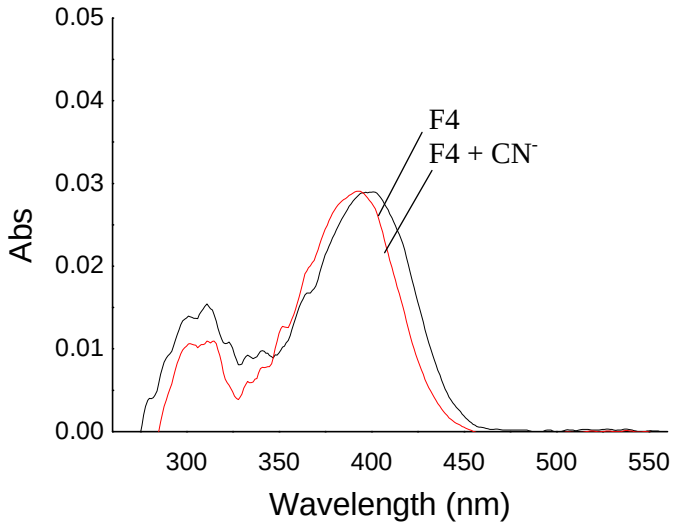

Figure 3.17 Electronic absorption spectra of **F4** in the absence and presence of CN^-. (Medium = 75% DMSO/HEPES buffer pH 7.4; [**F4**] = 1 μM; [CN^-] = 1.5 mM)

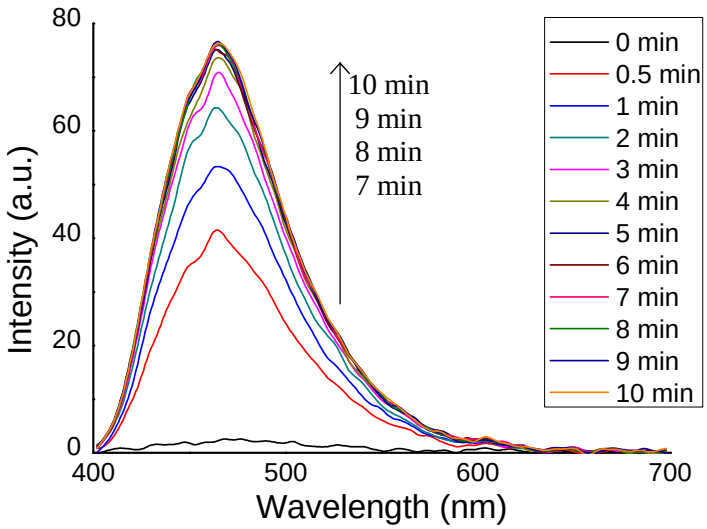

Figure 3.18 Time dependence of the fluorescence spectra of **F4** (λ_{ex} = 397) after the addition of CN^-. (Medium = 75% DMSO/HEPES buffer pH 7.4; [**F4**] = μM; [CN^-] = 1.5 mM)

3.2.3 Fluorescent sensor study of F4

We also tested the pH dependence of the sensitivity of **F4** toward cyanide ion in the pH range of 6.5-8.0. The results revealed that the physiological pH of 7.4 buffered by HEPES gave the highest fluorescence enhancement with fluorescence intensity ratio (I/I_0) greater than 50 (**Figure 3.19**). The relatively neutral pH of the optimum sensing condition confirmed the need of the nearby phenolic proton to assist the addition of cyanide ion to the aldehydic carbonyl carbon as previously proposed in literatures.

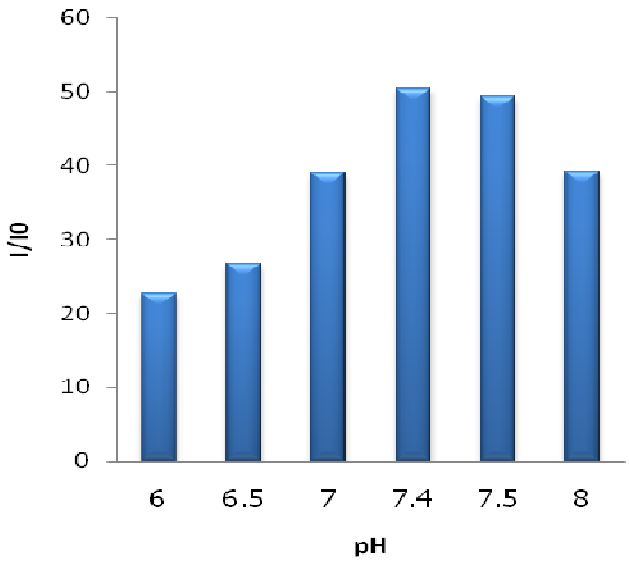

Figure 3.19 pH-dependence of the fluorescence spectra of **F4** (λ_{ex} = 397 nm) after the addition of CN^-. (Medium = 75% DMSO/HEPES buffer; [**F4**] = 1 μM; [CN^-] = 1.5 mM)

To study the selectivity of **F4** for cyanide detection, 11 other anions (N_3^-,NO_2^-, F^-, Cl^-, Br^-, I^-, $H_2PO_4^-$, HSO_4^-, HCO_3^-, AcO^-, NO_3^-) were also tested. **Figure 3.20** clearly shows that only cyanide ion can enhance the fluorescence signal. The results demonstrated very high selectivity of **F4** toward cyanide ion against these ions. The interference test was also conducted by adding cyanide and another anion to the **F4** solution. As shown in **Figure 3.21**, the presence of another anion did not give any significantly different fluorescence response of **F4** compared to cyanide ion in the absence of these interfering anions.

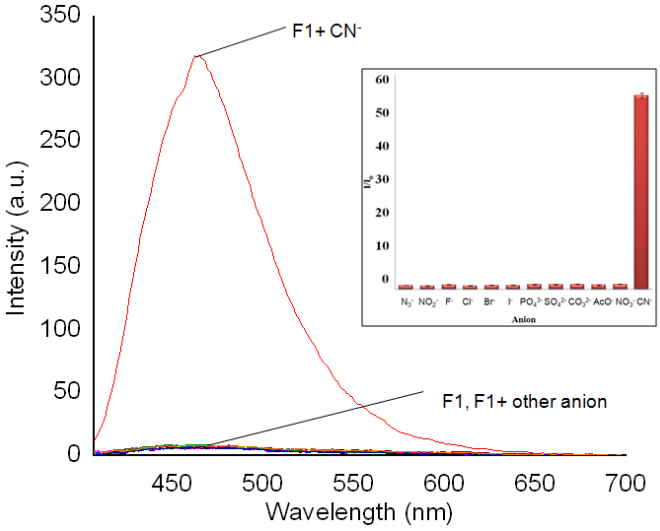

Figure 3.20 Fluorescence spectra of **F4** and **F4** + anion (N_3^-, NO_2^-, F^-, Cl^-, Br^-, I^-, $H_2PO_4^-$, HSO_4^-, HCO_3^-, AcO^-, NO_3^-, CN^-,). Insets show histograms of I/I_0 obtained from the corresponding fluorescence spectra. (λ_{ex} = 397 nm; Medium = 75% DMSO/HEPES buffer pH 7.4; [**F4**] = 1 μM; [anion] = 1.5 mM)

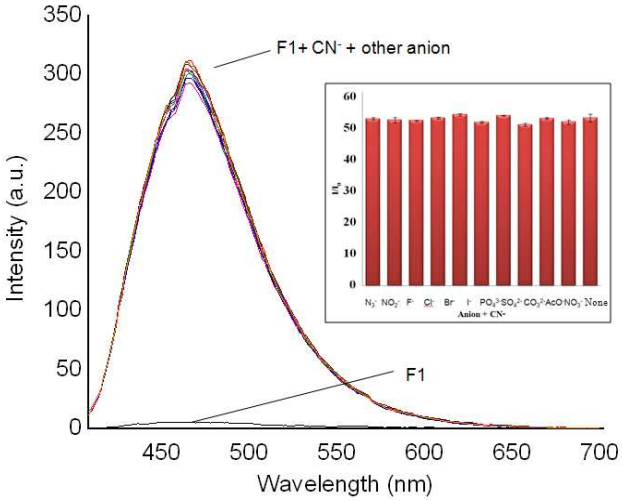

Figure 3.21 Fluorescence spectra of **F4** upon the addition of CN^- in the presence of another anion (N_3^-, NO_2^-, F^-, Cl^-, Br^-, I^-, $H_2PO_4^-$, HSO_4^-, HCO_3^-, AcO^-, NO_3^-, none). Insets show histograms of I/I_0 obtained from the corresponding fluorescence spectra. (λ_{ex} = 397 nm; Medium = 75% DMSO/HEPES buffer pH 7.4; [**F4**] = 1 μM; [anion] = 1.5 mM)

The degree of the fluorescence intensity change ((I - I_0)/I_0 x 100) plotted against the cyanide concentration in the range of 2-10 μM yielded a linear line (**Figure 3.22**). The plot also gave the detection limit (at 3 × noise) of cyanide ion as 1.3 μM or 35 ppb below the concentration limit of 2.7 μM allowed to be present in drinking water by WHO guideline.

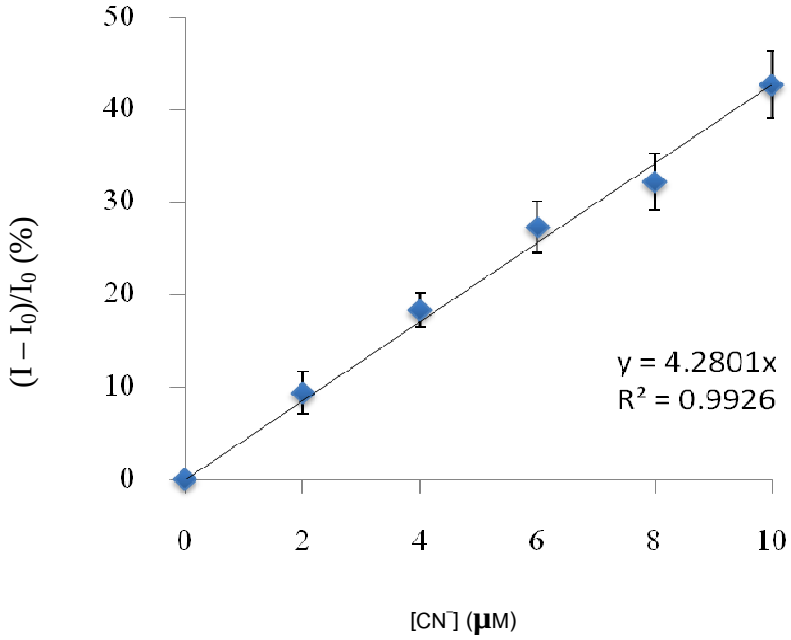

Figure 3.22 A plot of the fluorescence intensity change ((I - I_0)/I_0 x 100) of **F4** vs [CN^-]. (λ_{ex} = 397 nm; λ_{em} = 463 nm; Medium = 75% DMSO/HEPES buffer pH 7.4; [**F0**] = 1 μM;)

We determined the fluorescence quantum efficiency (Φ_F) of **F4** in the presence of cyanide ion 1.5 mM in comparison with **F4** alone and found that the fluorescence quantum efficiency increased from 0.01 to 0.20 upon the addition of cyanide ion. The increase of the quantum efficiency is presumably associated with the change of the internal charge transfer (ICT) process. The addition of cyanide converts the aldehyde group into tetrahedral cyanohydrins which in turn destroys its electron withdrawing ability and thus reduces the ICT process.

CHAPTER IV

CONCLUSION

4.1 Conclusion

Four new fluorophores (**F1-F4**) containing phenylene-ethynylene as fluorogenic center and salicylaldehyde as selective probe for cyanide ion were succesfully synthesized via Sonogashira coupling reaction. All fluorophores showed highly selective fluorescence "turn-on" signal upon the addition of cyanide anion in aqueous media. Among these four fluorophores, **F3** displayed the highest sensitivity toward cyanide detection. The fluorescence quantum yields determined in the absence and presence of cyanide ion revealed that the fluorescence quenching by the ICT process in **F3** is reduced the most by the cyanide addition. The detection limit of **F3** is 1.6 μM (42 ppb) which is below the concentration limited by WHO in drinking water of 2.7 μM. Paper-based solid state sensor for cyanide ion was also fabricated from **F3**. The naked eye detection of cyanide anion down to 5 nmole was achieved by a simple dropping and eluting technique.

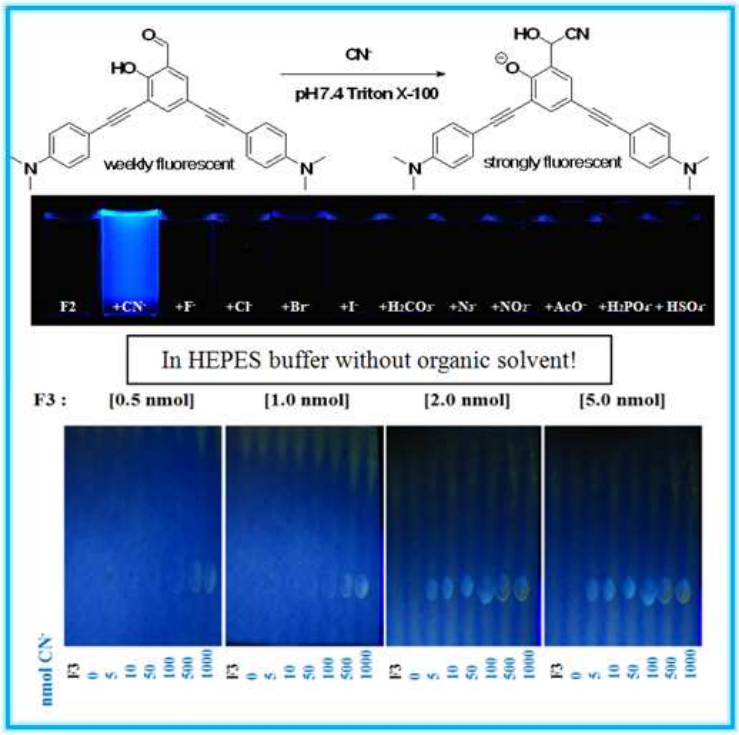

Figure 4.1 Reaction mechanism of receptor **F3** in aqueous media and photographic images for paper-based detection of cyanide ion under 20 W black light.

4.2 Suggestion for future works

This study be continued for the future applications such as analysis of real samples in an industrial or natural water sources. Therefore, we further focus on rapid and simple turn-on paper-based fluorescence sensor due to the decreases of ICT process into a commercial application.

REFERENCES

[1] Bhattacharya, R.; and Flora, S. J. S. *In handbook of toxicology of chemical warfare agents*; Gupta, R. C., Ed.; Academic Press: Boston, 2009; pp 255-270.

[2] Young, C.; Tidwell, L.; and Anderson, C. Cyanide: Social, Industrial, and Economic Aspects; Minerals, Metals, and Materials Society: Warrendale, 2001.

[3] Vetter, J. Plant cyanogenic glycosides. *Toxicon.* 38 (2000): 11–36.

[4] Jones, D. A. Why are so many food plants cyanogenic?. *Phytochemistry.* 47 (1998): 155–162.

[5] Greenfield, R. A.; Brown, B. R.; Hutchins, J. B.; Iandolo, J. J.; Jackson, R.; Slater, L. N.; and Bronze, M. S. Microbiological, biological, and chemical weapons of warfare and terrorism. *Am. J. Med. Sci.* 49 (2002): 326-340.

[6] World Health Organization. Guidelines for drinking-water quality [Online]. 2004. Available From: http://www.who.int/water_sanitation_health/dwq/guidelines/en[2011, Oct 15]

[7] Skoog, D. A.; Holler, F. J.; and Crouch, S. R. Analytical Chemistry, 4th; Saunders College Publishing, PA, 1982.

[8] Lakowicz, J. R. Principles of fluorescence spectroscopy; 3rd ed.; John Wiley & Sons, Inc, Kluwer, 2006.

[9] Xu, Z.; Xiao, Y.; Qian, X.; Cui, J. ; and Cui, D. Colorimetric and ratiometric fluorescent chemosensor with a large red-shift in emission: Cu(II)-only sensing by deprotonation of secondary amines as receptor conjugated to naphthalimide fluorophore. *Org. Lett*. 7 (2005): 889-892.

[10] Chung, S. K.; Tseng, Y. R.; Chen, C. Y.; and Sun, S. S. A selective colorimetric Hg2+ probe featuring a styryl dithiaazacrown containing platinum(II) terpyridine complex through modulation of the relative strength of ICT and MLCT. *Inorg. Chem.* 50 (2011): 2711-2713.

[11] Chattopadhyay, N.; Serpa, C.; Pereira, M. M.; Melo, S.; Arnaut, L. G.; and Formosinho, S. Intramolecular charge transfer of p-

(dimethylamino)benzethyne: A case of nonfluorescent ICT State. *J. Phys. Chem. A.* 105 (2001); 10025-10030.

[12] Zachariasse, K. A.; Druzhinin, S. I.; Bosch, W.; and Machinek, R. Intramolecular charge transfer with the planarized 4-aminobenzonitrile 1-*tert*-butyl-6-cyano-1,2,3,4-tetrahydroquinoline(NTC6). *J. Am. Chem. Soc.* 126 (2004); 1705-1715.

[13] Yoshihara, Y.; Druzhinin, S. I.; and Zachariasse, K. A. Fast intramolecular charge transfer with a planar rigidized electron donor/acceptor molecule. *J. Am. Chem. Soc.* 126 (2004); 8535-8539.

[14] Chakraborty, A.; Kar, S.; Nath, D. A.; and Guchhait, N. Photoinduced intramolecular charge-transfer reactions in 4-amino-3-methyl benzoic acid methyl ester: A fluorescence study in condensed phase and jet-cooled molecular beams. *J. Chem. Sci*. 119 (2007); 195-204.

[15] Druzhinin, S. I.; Mayer, P.; Stalke, D.; Bülow, R.; Noltemeyer, M.; and Zachariasse, K. A. Intramolecular charge transfer with 1-tert-butyl-6-cyano-1,2,3,4-tetrahydroquinoline (NTC6) and other aminobenzonitriles. A comparison of experimental vapor phase spectra and crystal structures with calculations. *J. Am.Chem. Soc*. 132 (2010); 7730-7744.

[16] Galievsky, V. A.; Druzhinin, S. I.; Demeter, A.; Mayer, P.; Kovalenko, S. A.;Senyushkina, T. A.; and Zachariasse, K. A. Ultrafast intramolecular charge transfer with N-(4-cyanophenyl)carbazole. Evidence for a LE precursor and dual LE + ICT fluorescence. *J. Phys. Chem. A.* 114 (2010); 12622-12638.

[17] Samori, S.; Tojo, Sachiko.; Fujitsuka, M.; Spitler, E. L.; Haley, M. M.; and Majima, T. Donor-Acceptor-Substituted Tetrakis(phenylethynyl)benzenes as Emissive Molecules during Pulse Radiolysis in Benzene. *J. Org. Chem.* 72 (2007): 2785-2793.

[18] Spitler, E. L.; Monson J. M.; and Haley, M. M. Structure-Property Relationships of Fluorinated Donor/Acceptor Tetrakis(phenylethynyl)benzenes and Bis(dehydrobenzoannuleno)benzenes. *J. Org. Chem.* 73 (2008): 2211-2223.

[19] Galievsky, V.A.; and Zachariassey, K.A. Intramolecular charge transfer with N,N-dialkyl-4-(trifuoromethyl) anilines and 4-(dimethylamino)benzonitrile in polar solvents. Investigation of the excitation wavelength dependence of the reaction pathway. *Acta Phys Pol*. 112 (2007); 39-56.

[20] Caballero, A. Highly selective chromogenic and redox or fluorescent sensors of Hg^{2+} in aqueous environment based on 1, 4-disubstituted azines. *J. Am. Chem. Soc.* 127 (2005): 15666–15667.

[21] Tang, Y. L. Direct visualization of glucose phosphorylation with a cationic polythiophene. *Adv. Mater*. 20 (2008): 703-705.

[22] McQuade, D. T.; Pullen, A. E.; and Swager, T. M. Conjugated polymer-based chemical sensors. *Chem. Rev*. 100 (2000): 2537-2574.

[23] Thomas, S. W.; Joly, G. D.; and Swager, T. M. Chemical sensors based on amplifying fluorescent conjugated polymers. *Chem. Rev.* 107 (2007): 1339-1386.

[24] Service, R. F. Getting a charge out of plastics. *Science.* 290 (2000): 425-427.

[25] Perepichka, I. F.; Perepichka, D. F.; Meng, H.; and Wudl, F. Light-emitting polythiophenes. *Adv. Mater*. 17 (2005): 2281-2305.

[26] Patil, A. O.; Heeger, A. J.; and Wudl, F. Optical properties of conducting polymers. *Chem. Rev.* 88 (1988): 183-200.

[27] Scherf, U.; and List, E. J. W. Semiconducting polyfluorenes towards reliable structure property relationships. *Adv. Mater*. 14 (2002): 477-487.

[28] Kraft, A.; Grimsdale, A. C.; and Holmes, A. B. Electroluminescent Conjugated polymers seeing polymers in a new light. *Angew. Chem. Int. Ed.* 37 (1998): 402-428.

[29] Bunz, U. H. F. Poly(aryleneethynylene)s: syntheses, properties, structures, and applications. *Chem. Rev.* 100 (2000): 1605-1644.

[30] Niamnont, N.; Siripornnoppakhun, W.; Rashatasakhon, P.; and Sukwattanasinitt, M. A polyanionic dendritic fluorophore for selective detection of Hg^{2+} in triton X-100 aqueous media. *Org. Lett.* 13 (2009): 2768-2771.

[31] Niamnont, N.; Mungkarndee, R.; Techakriengkrai, I.; Rashatasakhon, P.; and Sukwattanasinitt, M. Protein discrimination by fluorescent sensor array constituted of variously charged dendritic phenylene–ethynylene fluorophores. *Biosens. Bioelectron.* 26 (2010): 863-867.

[32] Lee, K.S.; Kim, S.J.; Kim, J.H.; Shin, I.; and Hong, J.I. Fluorescent chemodosimeter for selective detection of cyanide in water. *Org. Lett*., 10 (2008): 49–51.

[33] Jo, J.; and Lee, D. Turn-on fluorescence detection of cyanide in water: activation of latent fluorophores through remote hydrogen bonds that mimic peptide ß-turn motif. *J. Am. Chem. Soc.* 131 (2009): 16283–16291.

[34] Khatua, S.; Samanta, D.; Bats, J. W.; and Schmittel, M. Rapid and highly sensitive dual-channel detection of cyanide by bis-heteroleptic ruthenium(ii) complexes. dx.doi.org/10.1021/ic2022853

[35] Badugu, R.; Lakowicz, J.R.; and Geddes, C.D. Enhanced fluorescence cyanide detection at physiologically lethal levels: reduced ICT-based signal transduction. *J. Am. Chem. Soc.* 127 (2005): 3635-3641.

[36] Jamkratoke, M.; Ruangpornvisuti, V.; Tumcharern, G.; Tuntulani, T.; and Tomapatanaget, B**.** A-D-A sensors based on naphthoimidazoledione and boronic acid as turn-on cyanide probes in water. *J. Org. Chem.* 74 (2009): 3919–3922.

[37] Yang, Y. K.; and Tae, J. Acridinium Salt Based Fluorescent and Colorimetric Chemosensor for the Detection of Cyanide in Water. *Org. Lett.* 25, (2006): 5721-5723.

[38] Kim, H. J.; Ko, K. C.; Lee J. H.; Lee, J. Y; and Kim J. S. KCN sensor: unique chromogenic and ‘turn-on’ fluorescent chemodosimeter: rapid response and high selectivity. *Chem. Commun.* 47 (2011): 2886–2888.

[39] Shiraishi, Y.; Sumiya, S.; and Hirai, T. Highly sensitive cyanide anion detection with a coumarin–spiropyran conjugate as a fluorescent receptor. *Chem. Commun*. 47 (2011): 4953–4955.

[40] Fang, J. K.; An, D. L.; Wakamatsu, K.; Ishikawa, T.; Iwanaga, T.; Toyota, S.; Akita, S.; Matsuo, D.; Orita, A.; and Otera, J. Synthesis and

spectroscopic study of phenylene–(poly)ethynylenes substituted by amino or amino/cyano groups at terminal(s): electronic effect of cyano group on charge-transfer excitation of acetylenic π-systems. *Tetrahedron.* 66 (2010): 5479-5485.

[41] Du, H.; Fuh, R. A.; Li, J.; Corkan, A.; and Lindsey, J. S. Photochem CAD: A computer-aided design and research tool in photochemistry. Photochem Photobiol. 68 (1998): 141-142.

[42] Fery-Forgues, S.; and Lavabe, D. Are fluorescence quantum yields so tricky to measure? a demonstration using familiar stationery products. J. Chem. Educ. 76 (1999): 1260-1264.

[43] Zangmeister, C. D.; Robey, S. W.; Zee R. D.; Kushmerick, J. G.; Naciri J.; Yao, Y.; Tour, J. M.; Varughese, B.; and Xu, B. Reutt-Robey, J. E. Fermi level alignment in self-assembled molecular layers: the effect of coupling chemistry. *J. Phys. Chem. B*, 110 (2006): 17138-17144.

[44] Wosnick, J. H.; Mello, C. M.; and Swager, T. M. synthesis and application of poly(phenylene ethynylene)s for bioconjugation: a conjugated polymer-based fluorogenic probe for proteases. *J. Am. Chem. Soc.* 127 (2005); 3400-3405.

[45] Tan, C.; Xie, Y.; He, X.; Wang, K.; and Jiang, Y. hyper-efficient quenching of a conjugated polyelectrolyte by dye-doped silica nanoparticles: better quenching in the nonaggregated state. *Langmuir*. 26 (2010): 1528–1532.

[46] Sirilaksanapong, S. ; Sukwattanasinitt, M.; and Rashatasakhon, P. 1,3,5-Triphenylbenzene fluorophore as a selective Cu^{2+} sensor in aqueous media. *Chem. Commun.* 48 (2012): 293-295.

[47] Martinez, A. W.; Phillips, S. T.; Carrilho, E; Thomas, S. W.; Sindi, H.; and Whitesides, G. M. Simple Telemedicine for Developing Regions:Camera Phones and Paper-Based Microfluidic Devices for Real-Time, Off-Site Diagnosis. *Anal. Chem.* 80 (2008); 3699–3707.

[48] Ellerbee, A. K.; Phillips, S. T.; Siegel, A. C.; Mirica, K. A.; Martinez, A. W.; Striehl, P.; Jain, N.; Prentiss, M.; and Whitesides, G. M. Quantifying colorimetric assays in paper-based microfluidic devices by measuring the transmission of light through. *Anal. Chem.* 81 (2009): 8447–8452.

[49] Martinez, A. W.; Phillips, S. T.; and Whitesides, G. M. Diagnostics for the developing world: microfluidic paper-based analytical devices. *Anal. Chem.* 82 (2010): 3–10.

[50] Schilling, K. M.; Lepore, A. L.; Kurian, J. A.; and Martinez, A. W. Fully enclosed microfluidic paper-based analytical devices. *Anal. Chem.* 84 (2012): 1579−1585.

[51] Martinez, A. W.; Phillips, S. T.; Butte, M. J.; and Whitesides, G. M. Patterned paper as a platform for inexpensive, low-volume, portable bioassays. *Angew. Chem. Int. Ed.* 46 (2007): 1318 –1320.

[52] Kajigaeshi, S.; Kakinami, T.; Moriwaki, M.; Fujisaki, S.; Maeno, K.; and Okamoto, T. α-Chlorination of aromatic acetyl derivatives with benzyltrimethylammonium dichloroiodate. *Synthesis.* 1988: 545–546.

APPENDIX

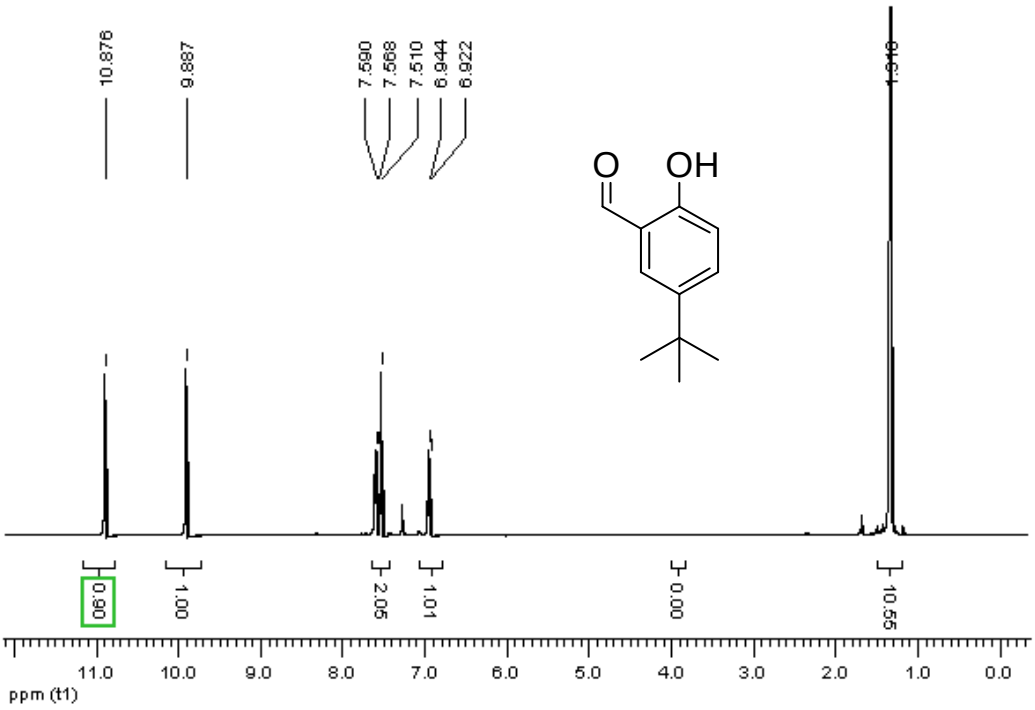

Figure A.1 ^{1}H NMR spectrum of 5-*tert*-butyl-2-hydroxybenzaldehyde in $CDCl_3$**.**

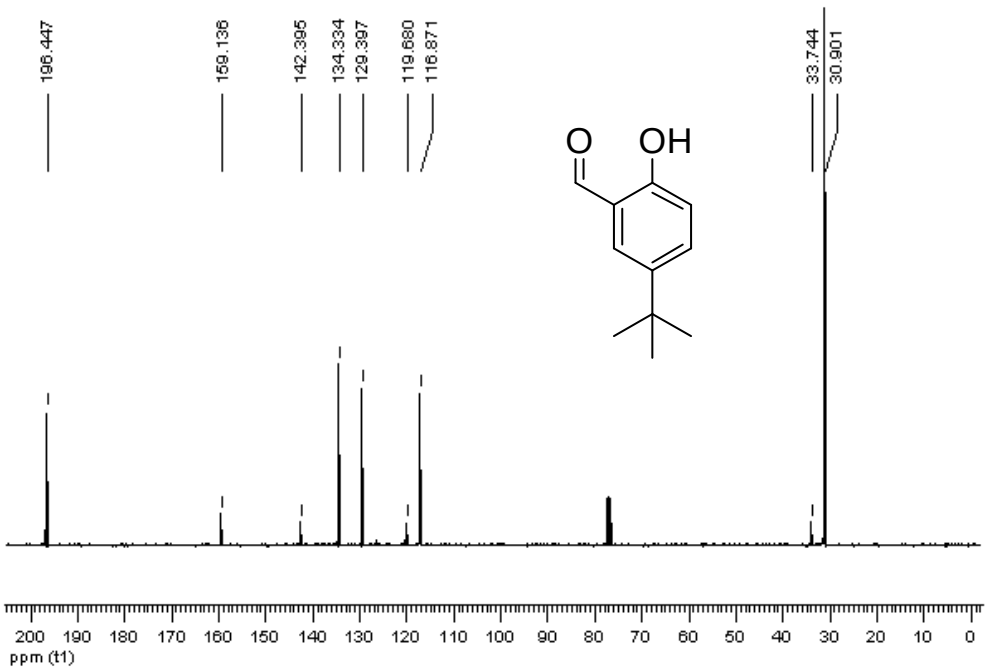

Figure A.2 ^{13}C NMR spectrum of 5-*tert*-butyl-2-hydroxybenzaldehyde in $CDCl_3$**.**

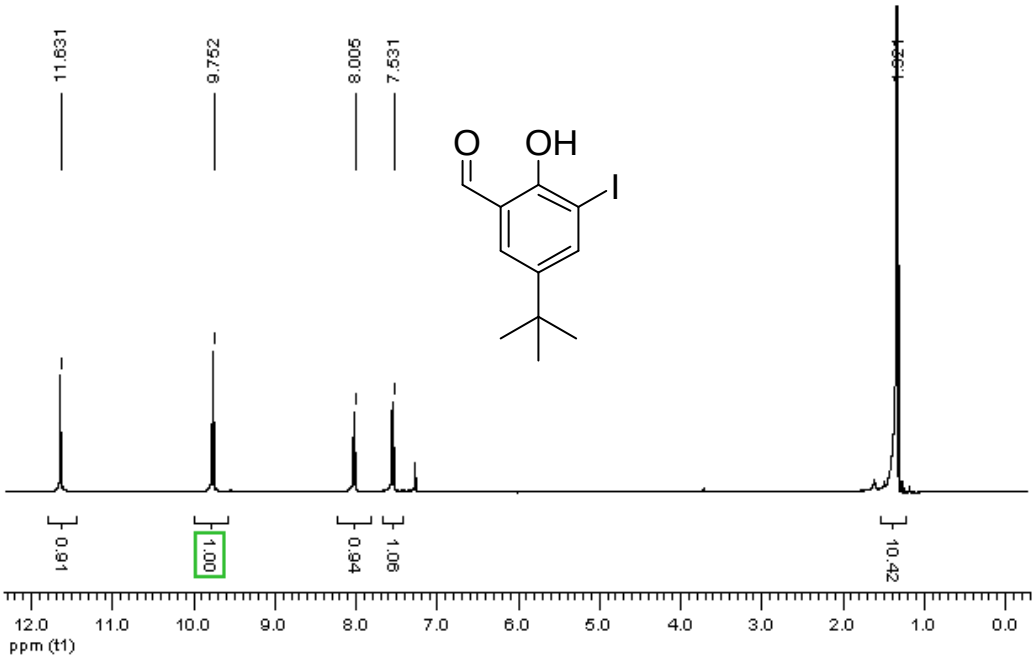

Figure A.3 ^{1}H NMR spectrum of 5-*tert*-butyl-2-hydroxy-3-iodobenzaldehyde in $CDCl_3$**.**

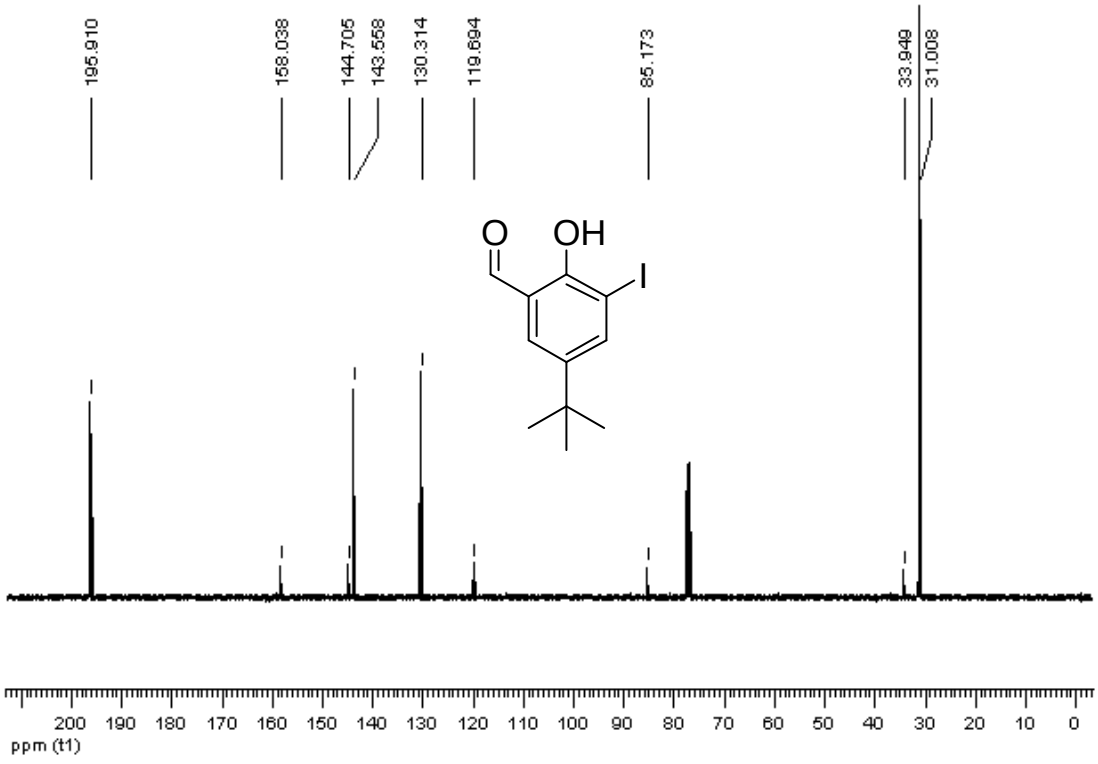

Figure A.4 ^{13}C NMR spectrum of 5-*tert*-butyl-2-hydroxy-3-iodobenzaldehyde in $CDCl_3$**.**

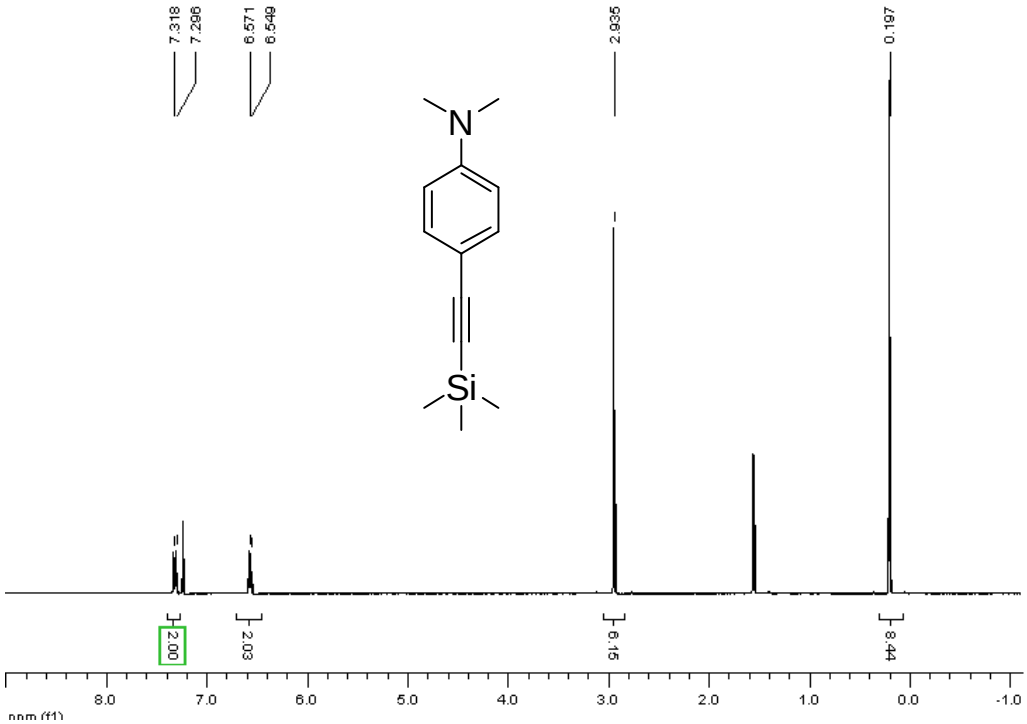

Figure A.5 ^{1}H NMR spectrum of *N*,*N*-dimethyl-4-((trimethylsilyl)ethynyl)aniline in $CDCl_3$**.**

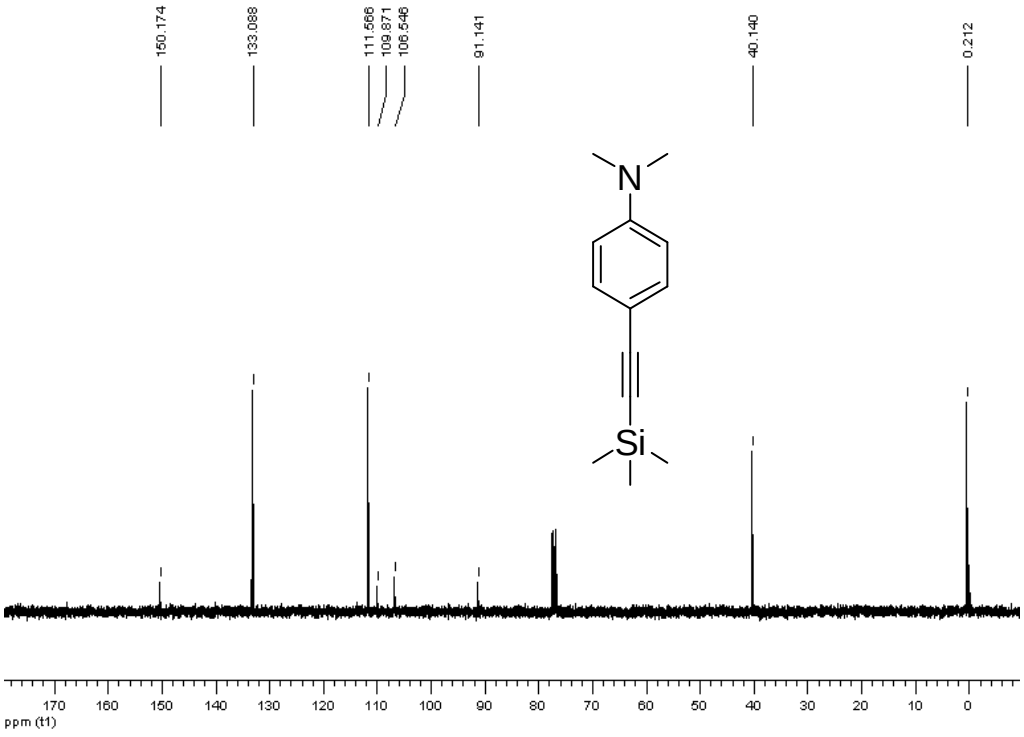

Figure A.6 ^{13}C NMR spectrum of *N*,*N*-dimethyl-4-((trimethylsilyl)ethynyl)aniline in $CDCl_3$**.**

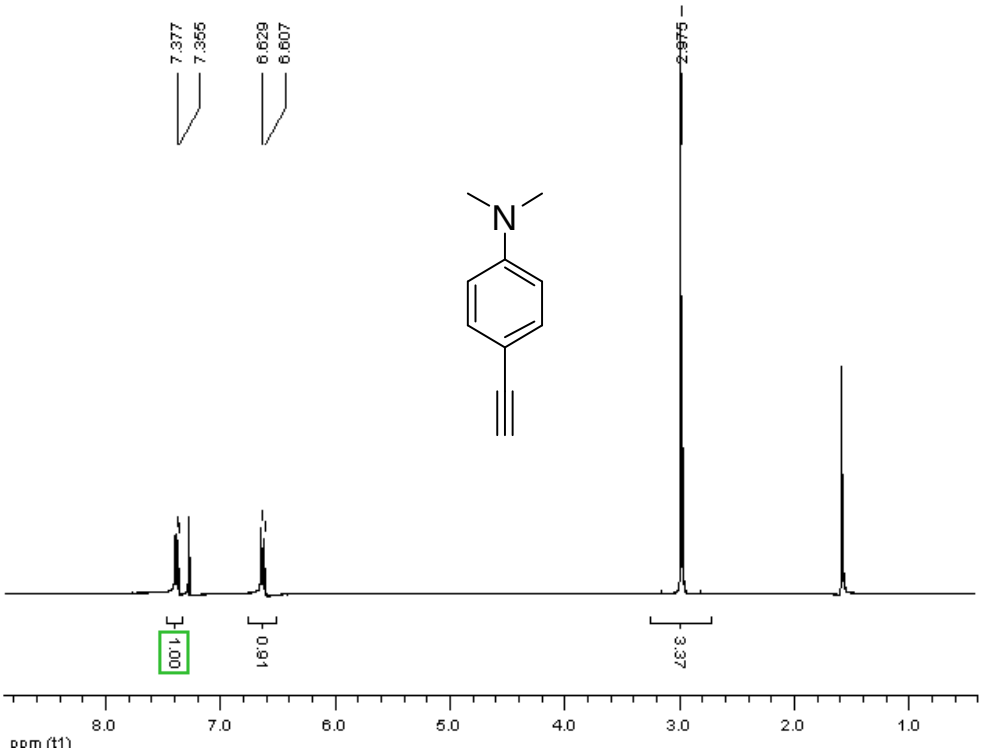

Figure A.7 ^{1}H NMR spectrum of 4-ethynyl-*N*, *N*-dimethylaniline in $CDCl_3$.

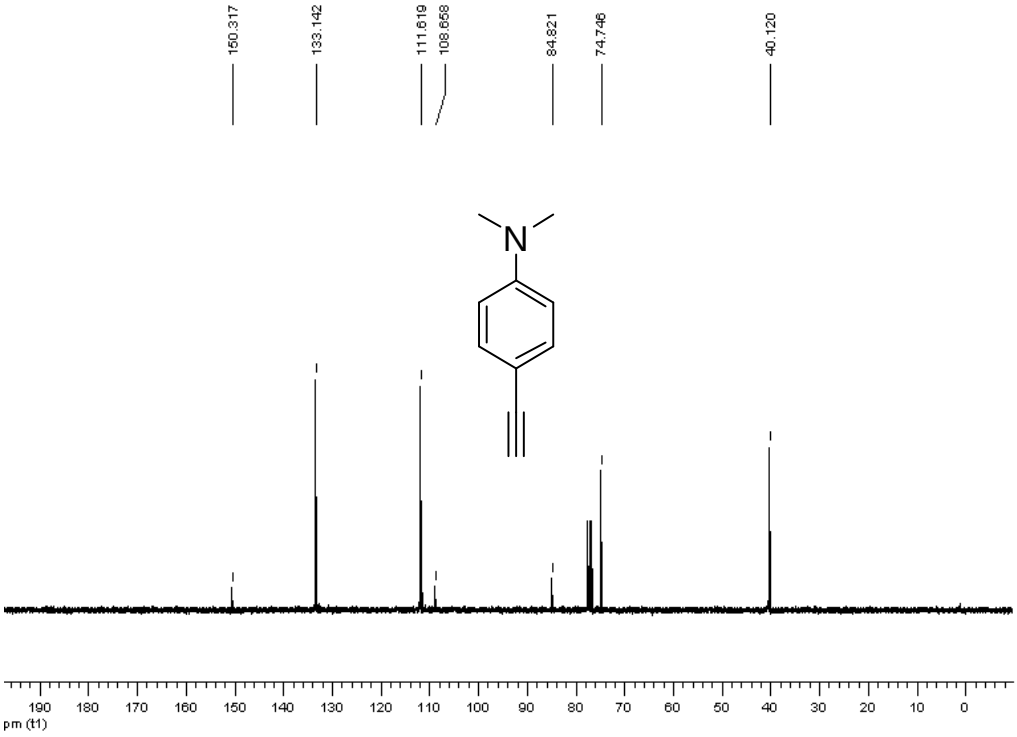

Figure A.8 ^{1}C NMR spectrum of 4-ethynyl-*N*, *N*-dimethylaniline in $CDCl_3$.

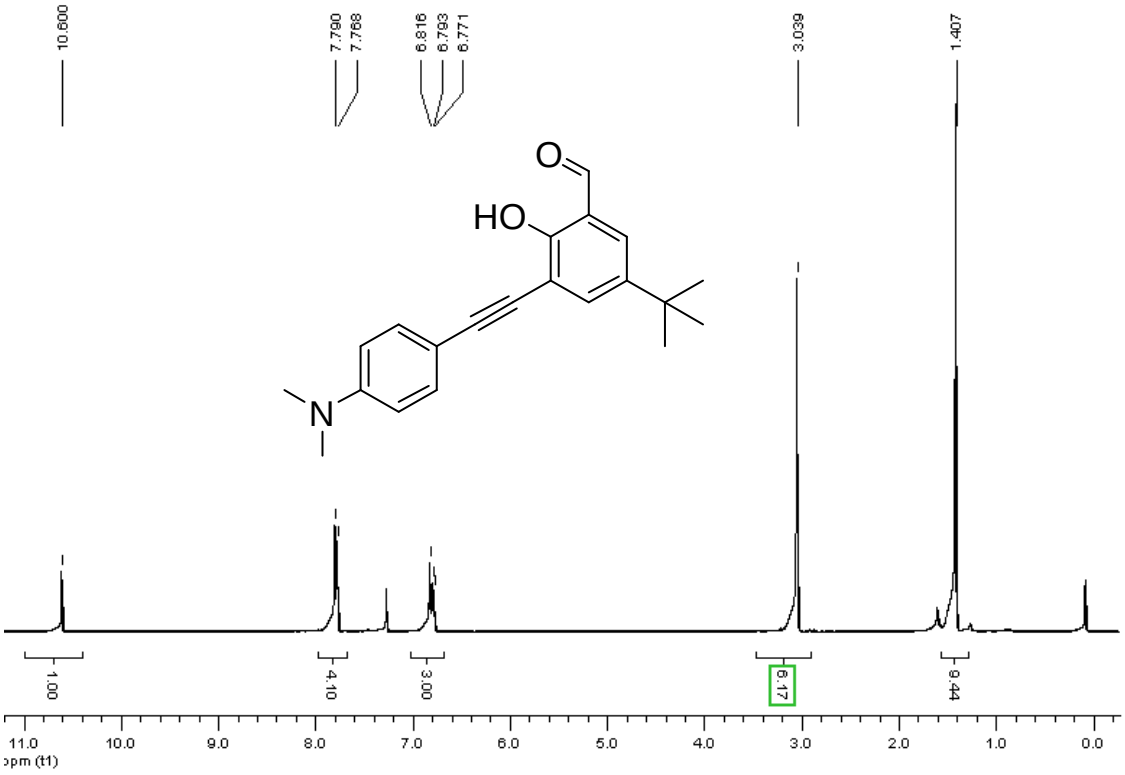

Figure A.9 ^{1}H NMR spectrum of **F1** in $CDCl_3$.

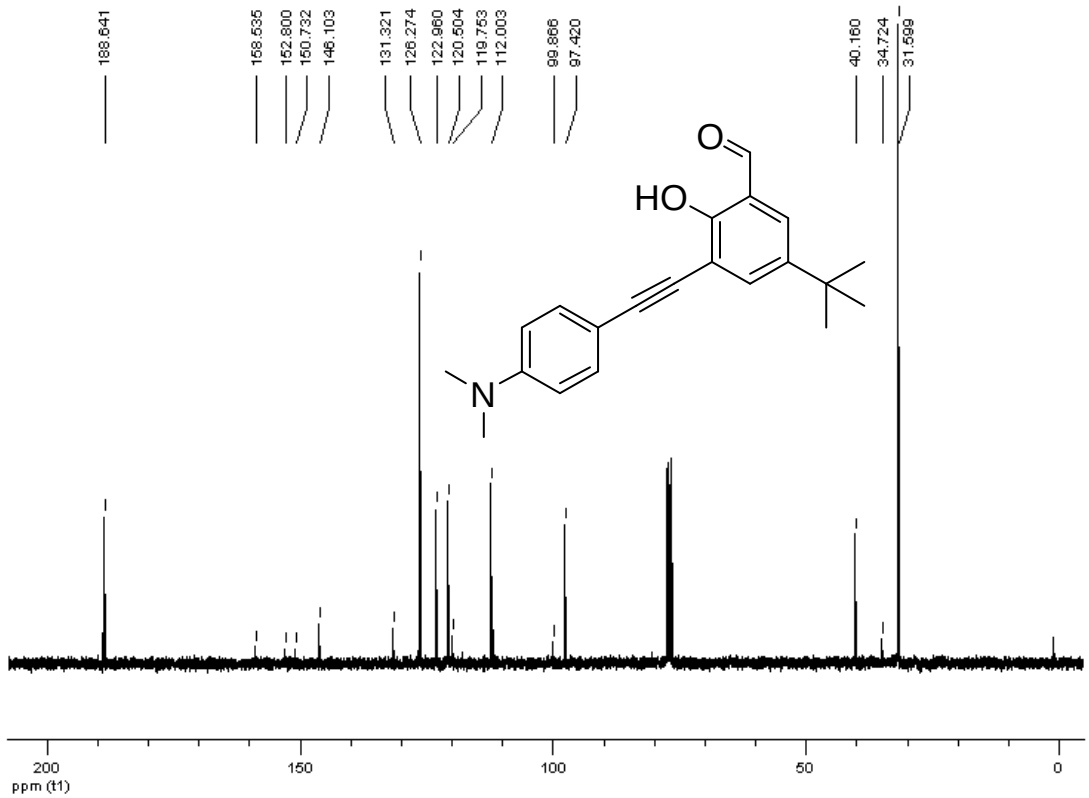

Figure A.10 ^{13}C NMR spectrum of **F1** in $CDCl_3$.

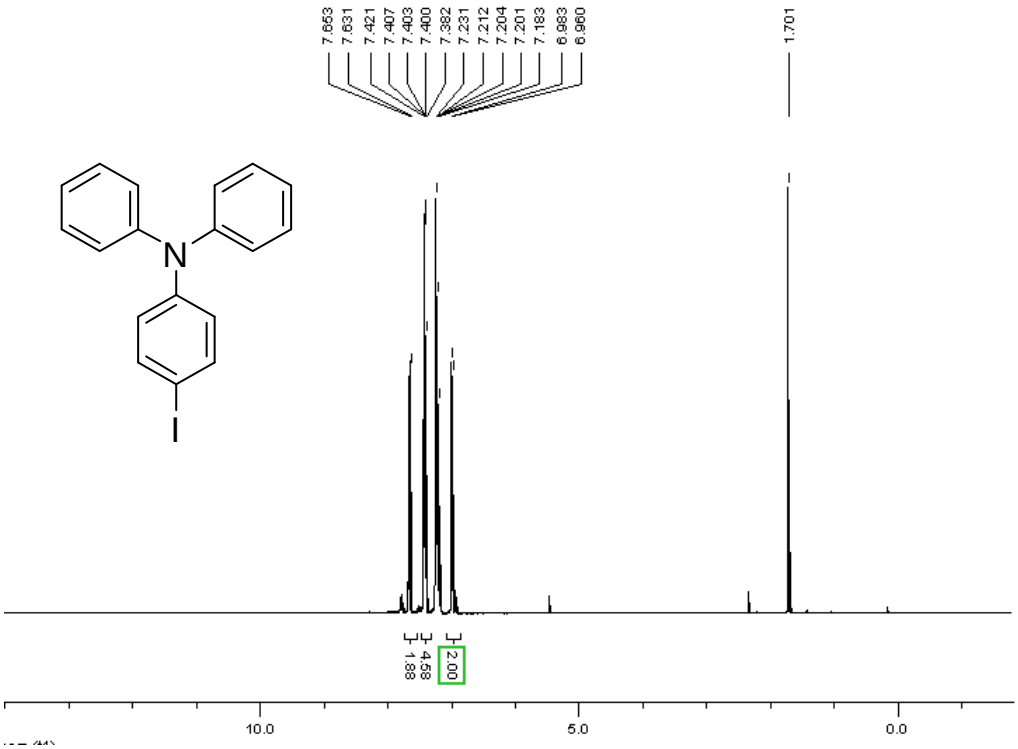

Figure A.11 ^{1}H NMR spectrum of 4-iodo-*N*,*N*-diphenylaniline in $CDCl_3$.

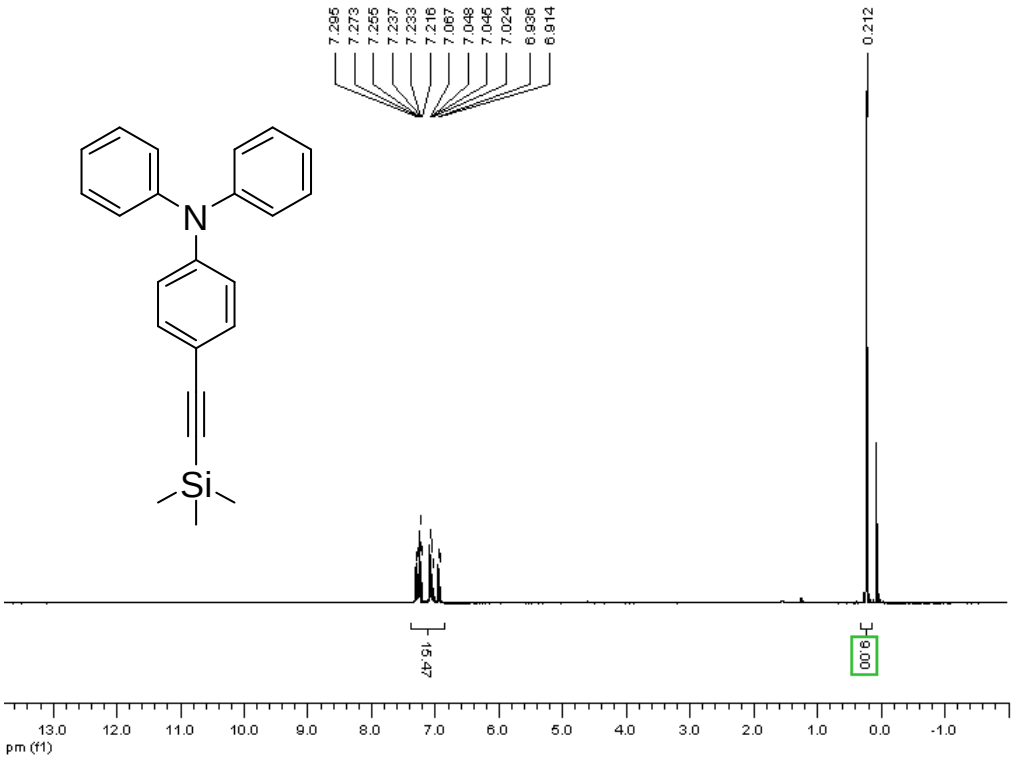

Figure A.12 ^{1}H NMR spectrum of 4-(trimethylsilyl)ethynyl-*N*,*N*-diphenylaniline in $CDCl_3$.

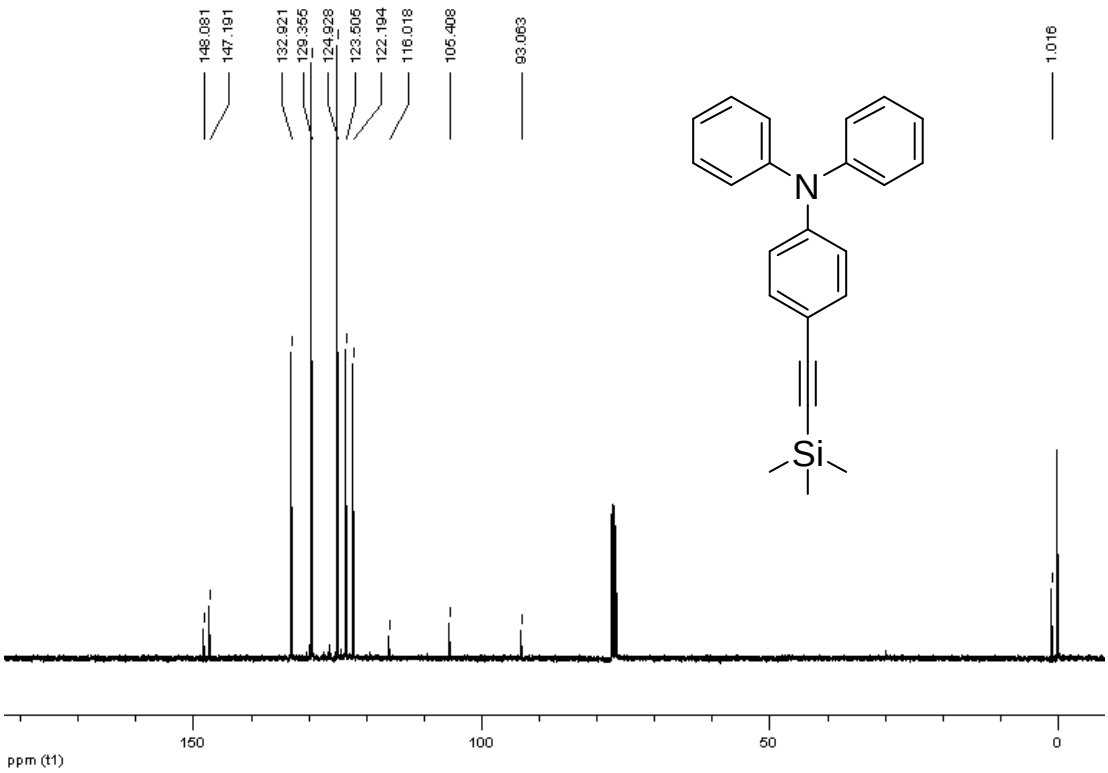

Figure A.13 ^{13}C NMR spectrum of 4-(trimethylsilyl)ethynyl-*N*,*N*-diphenylaniline in $CDCl_3$.

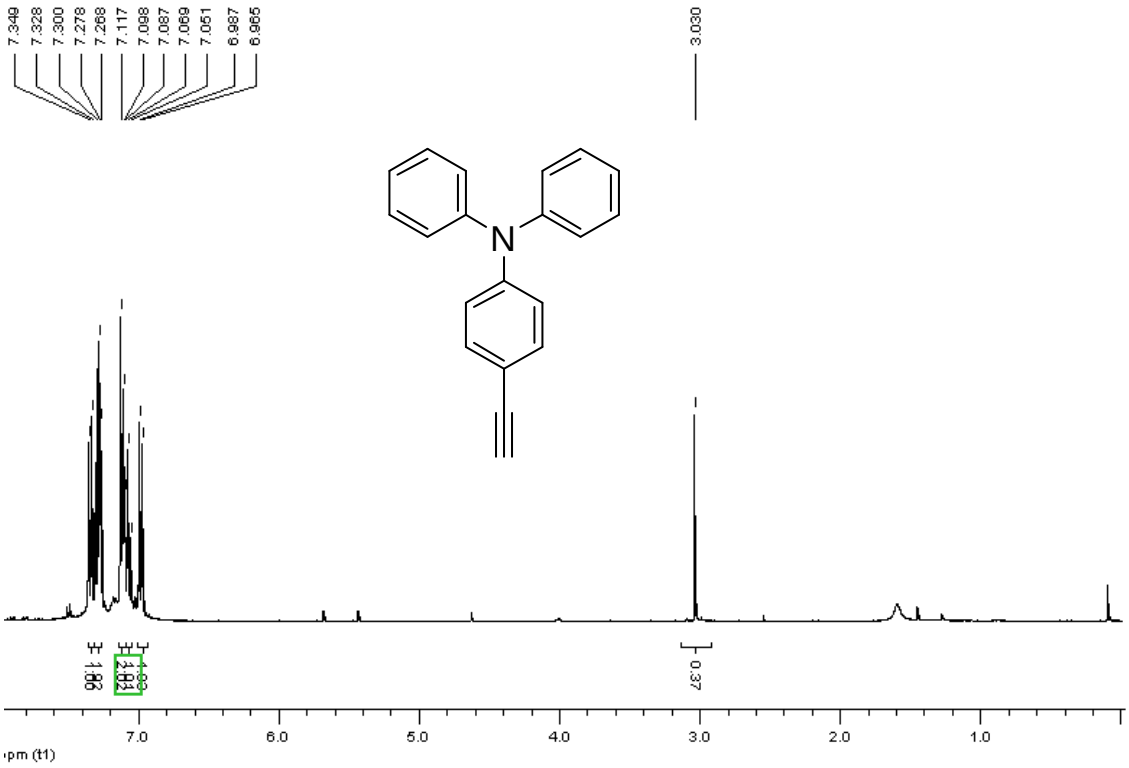

Figure A.14 ^{1}H NMR spectrum of 4-ethynyl-*N*,*N*-diphenylaniline in $CDCl_3$.

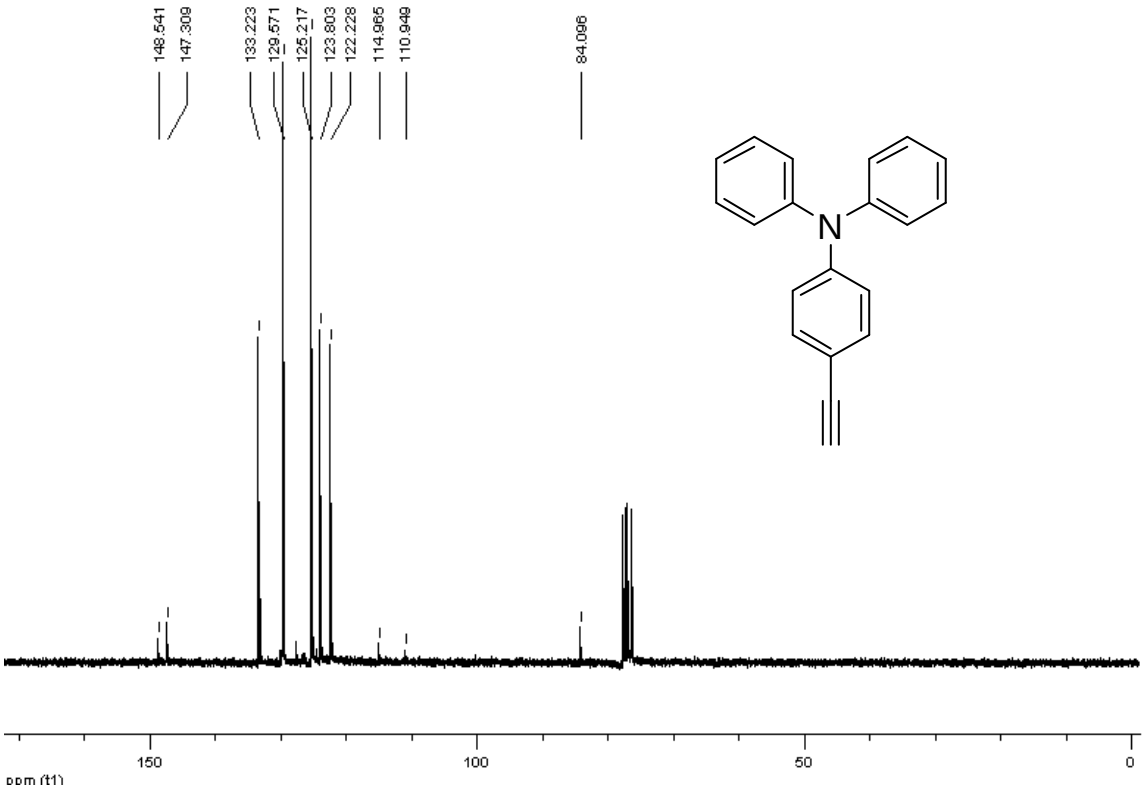

Figure A.15 ^{13}C NMR spectrum of 4-ethynyl-*N*,*N*-diphenylaniline in $CDCl_3$.

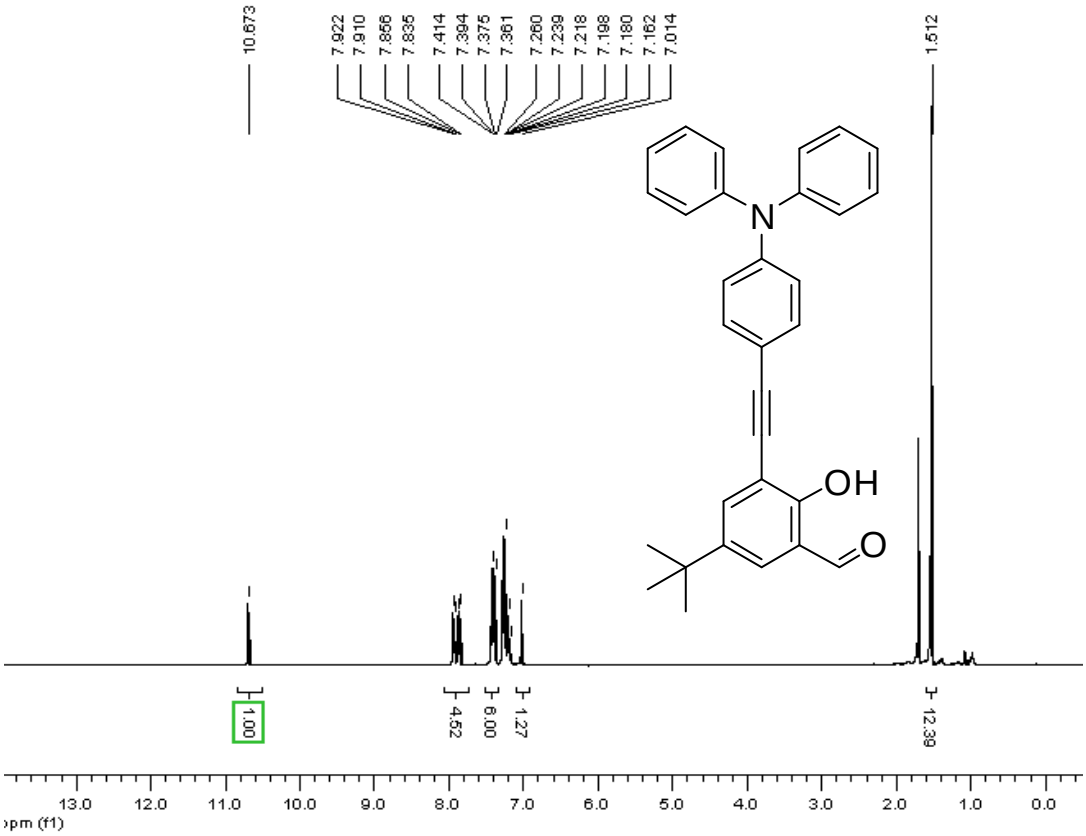

Figure A.16 ^{1}H NMR spectrum of **F2** in $CDCl_3$.

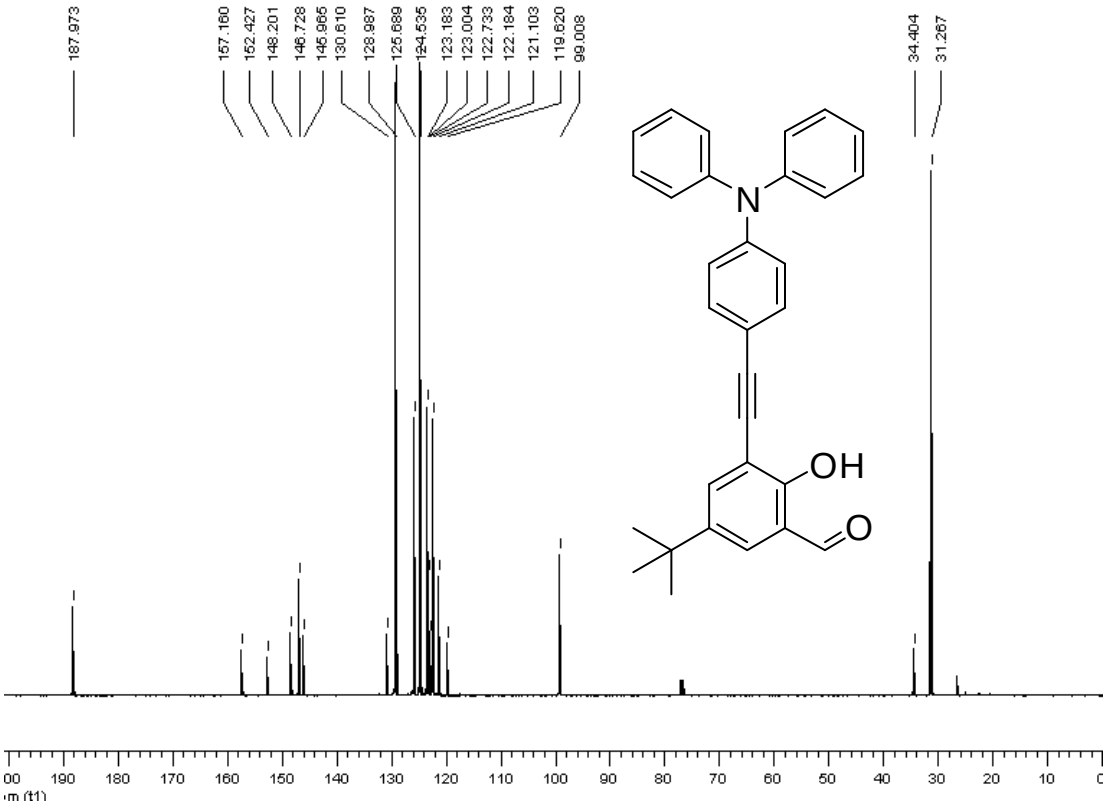

Figure A.17 ^{13}C NMR spectrum of **F2** in $CDCl_3$.

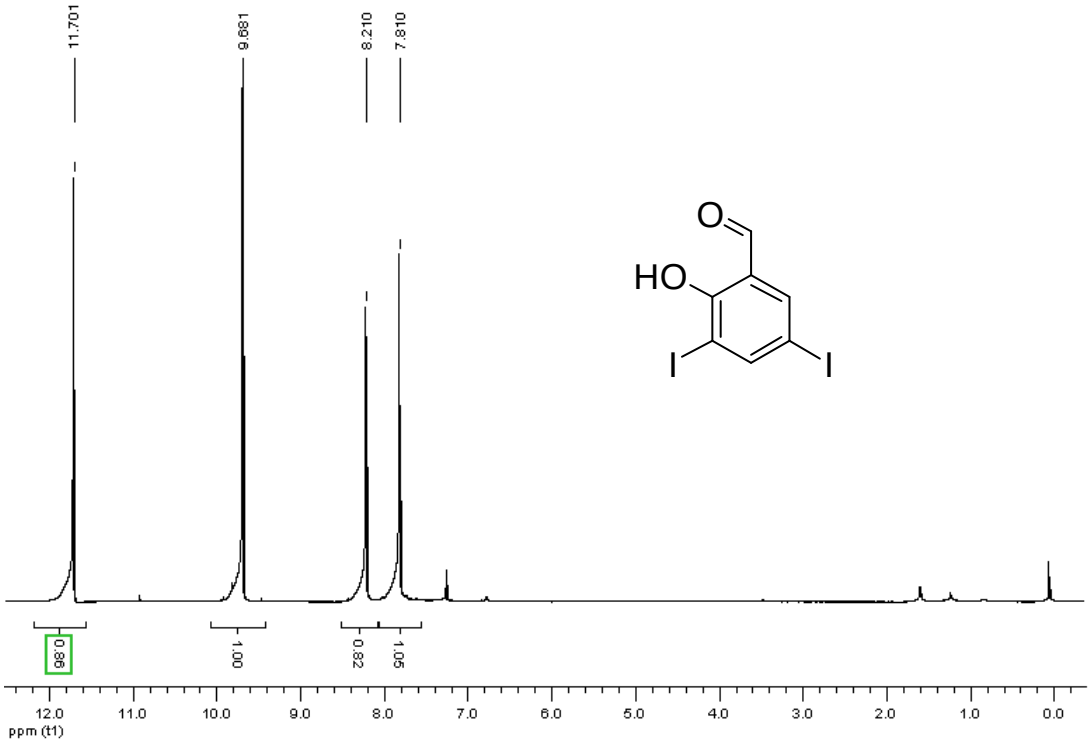

Figure A.18 ^{1}H NMR spectrum of 2-hydroxy-3,5-diiodobenzaldehyde in $CDCl_3$.

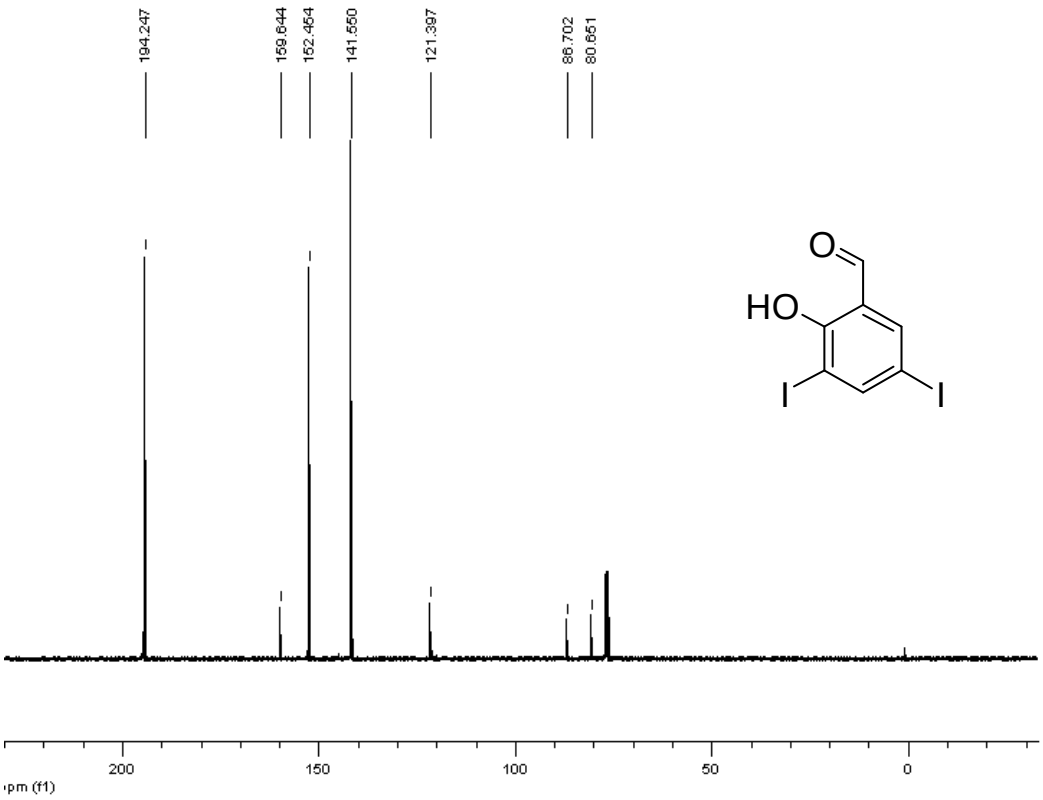

Figure A.19 ^{13}C NMR spectrum of 2-hydroxy-3,5-diiodobenzaldehyde in $CDCl_3$.

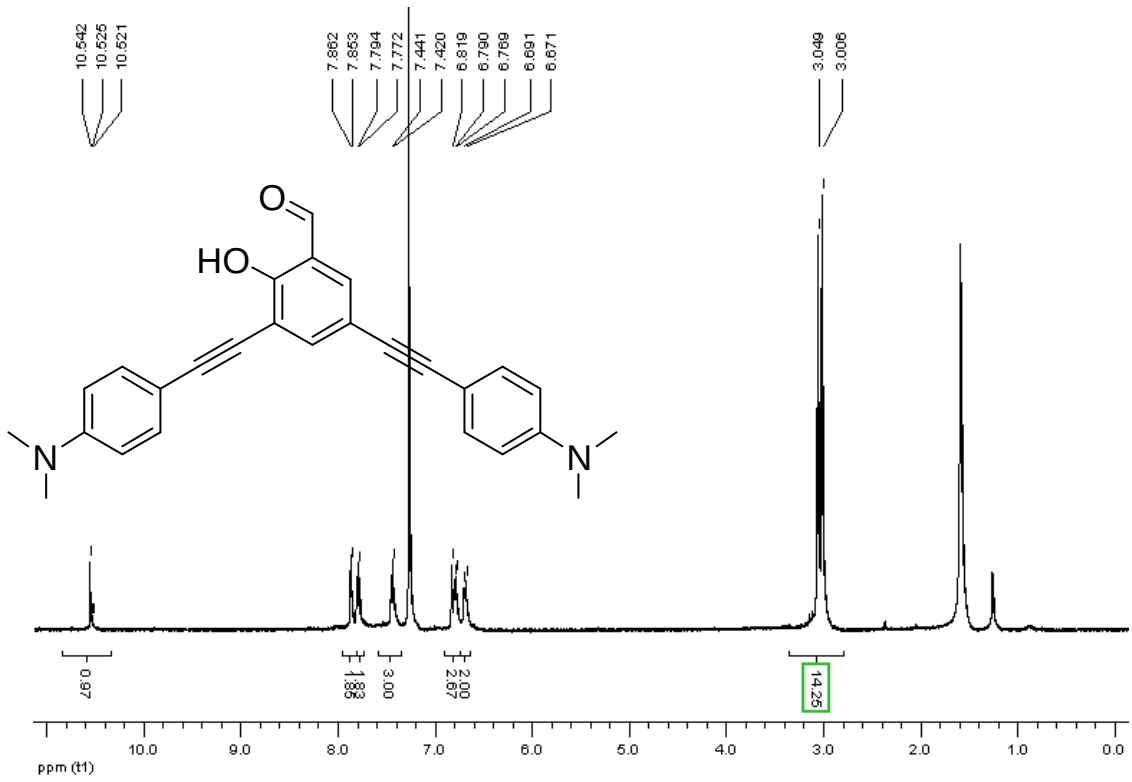

Figure A.20 ^{1}H NMR spectrum of **F3** in $CDCl_3$.

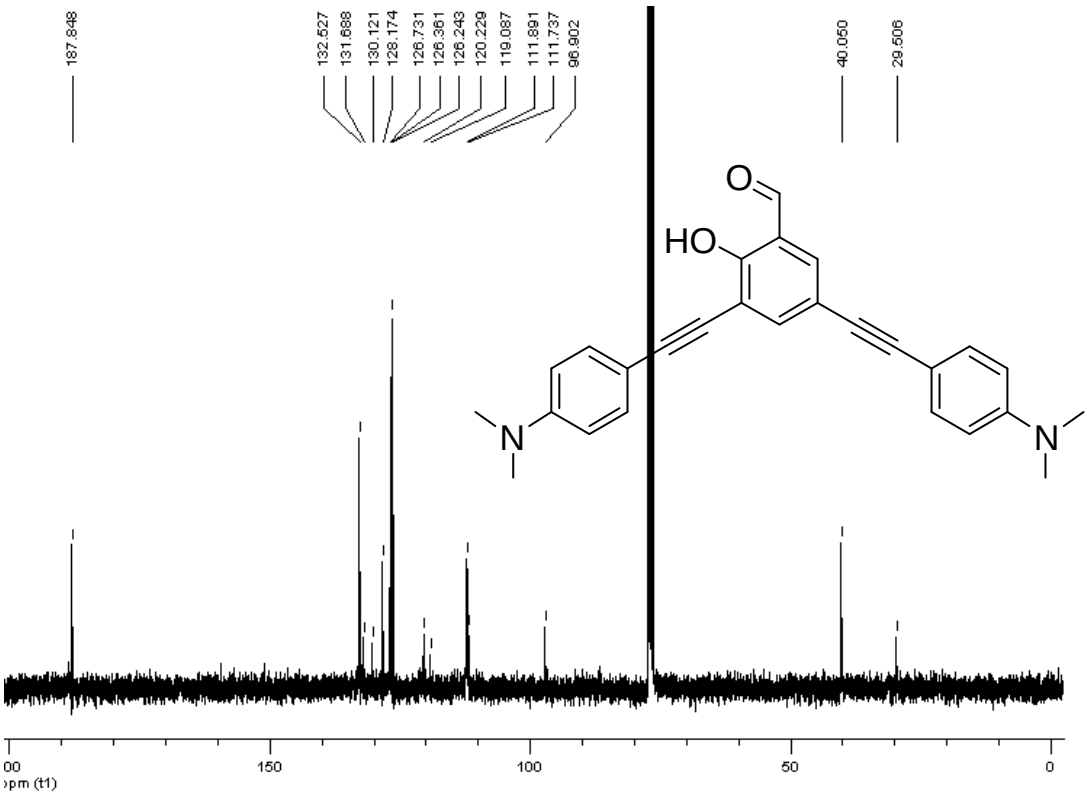

Figure A.21 ^{13}C NMR spectrum of **F3** in $CDCl_3$.

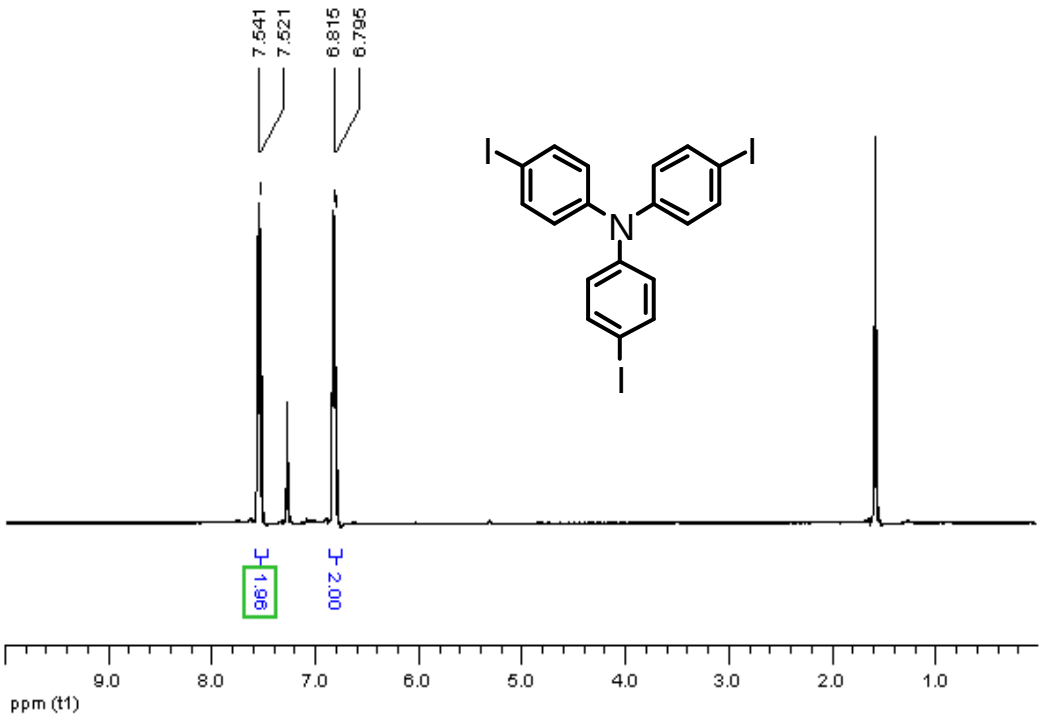

Figure A.22 ^{1}H NMR spectrum of triiodotriphenylamine in $CDCl_3$.

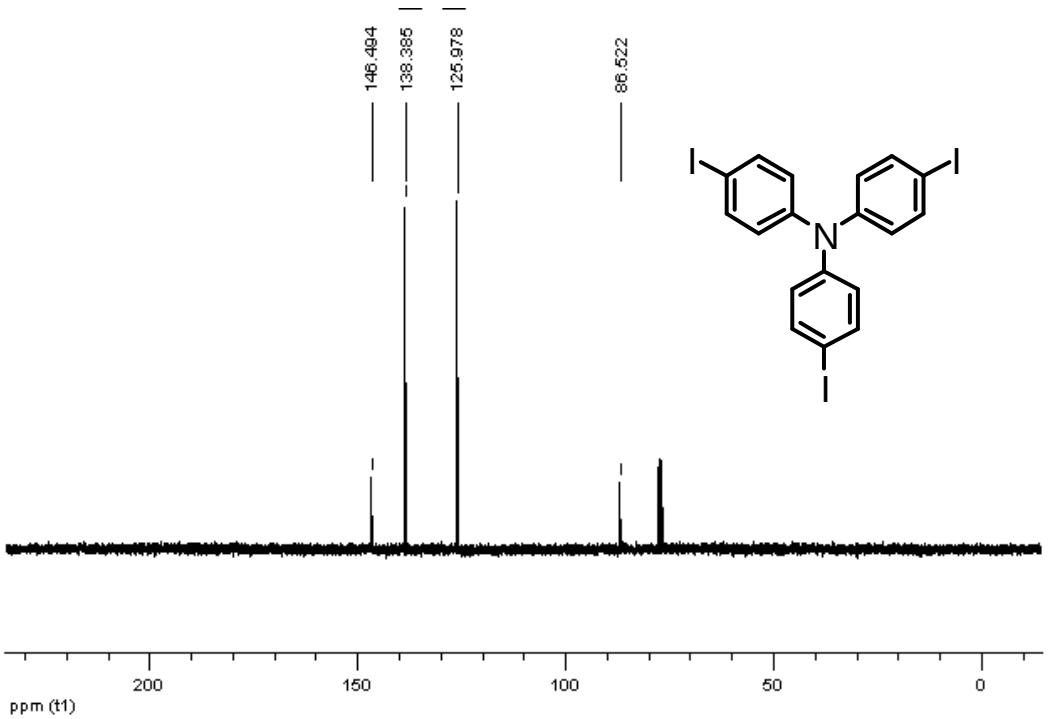

Figure A.23 ^{13}C NMR spectrum of triiodotriphenylamine in $CDCl_3$.

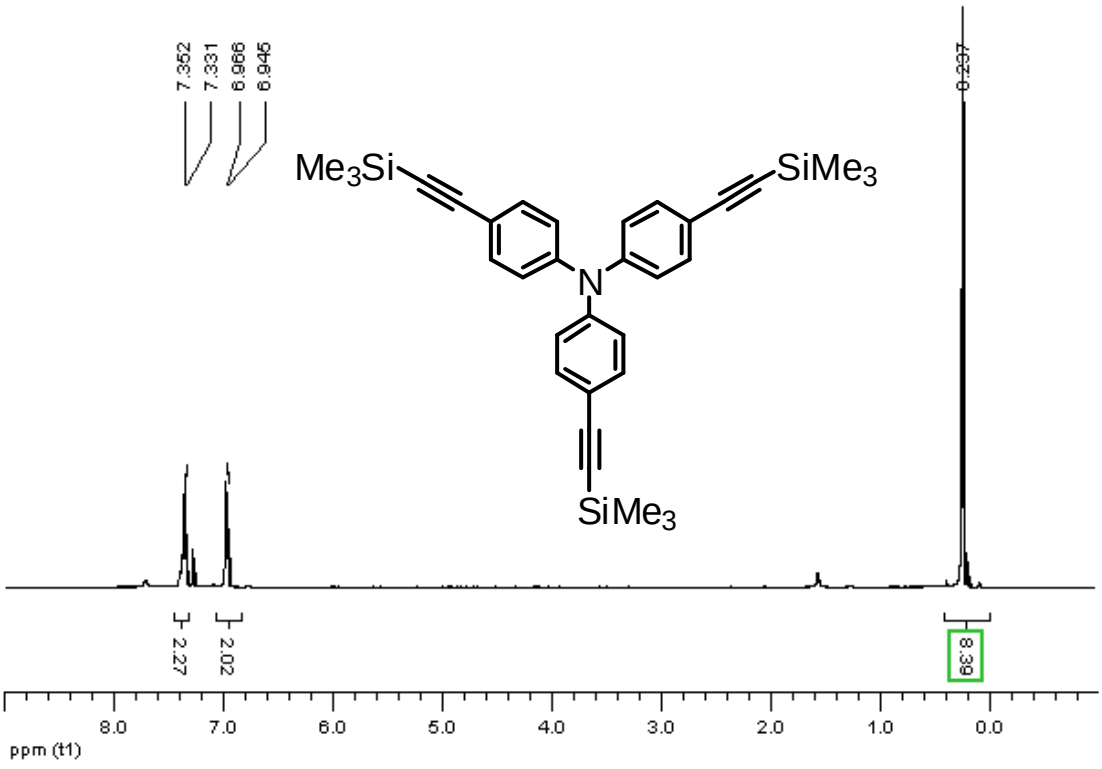

Figure A.24 ^{1}H NMR spectrum of 4, 4', 4''-trimethylsilylethynylphenylamine in $CDCl_3$.

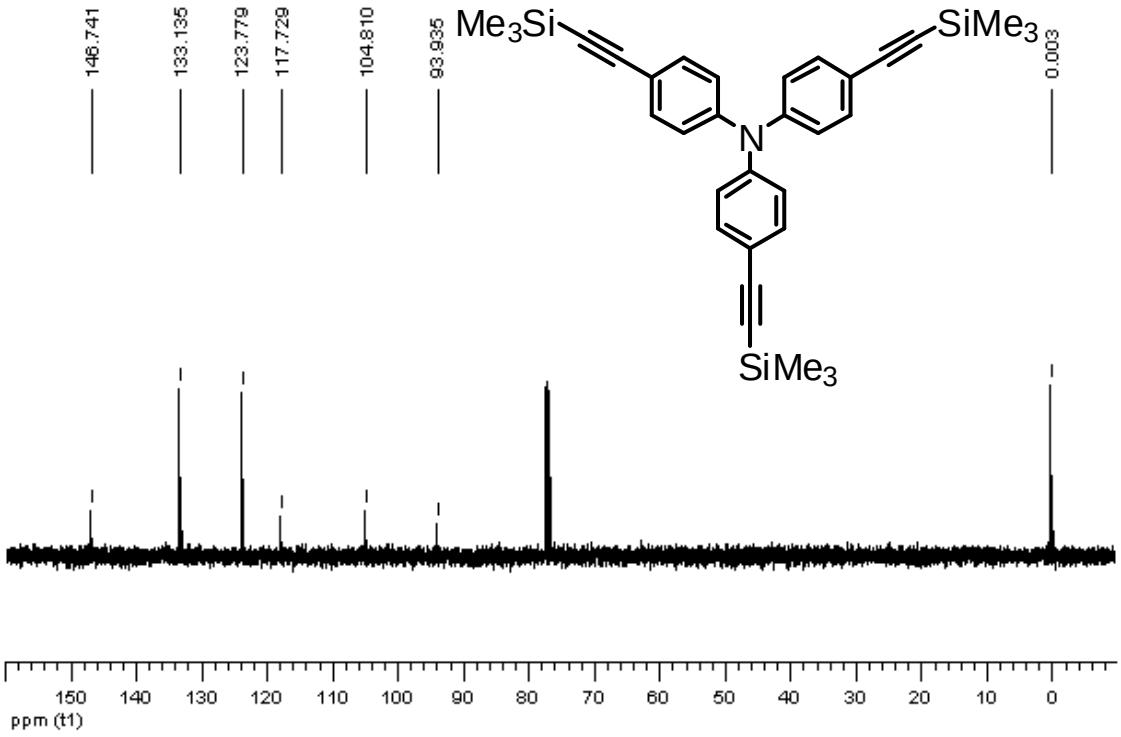

Figure A.25 ^{13}C NMR spectrum of 4, 4', 4''-trimethylsilylethynylphenylamine in $CDCl_3$.

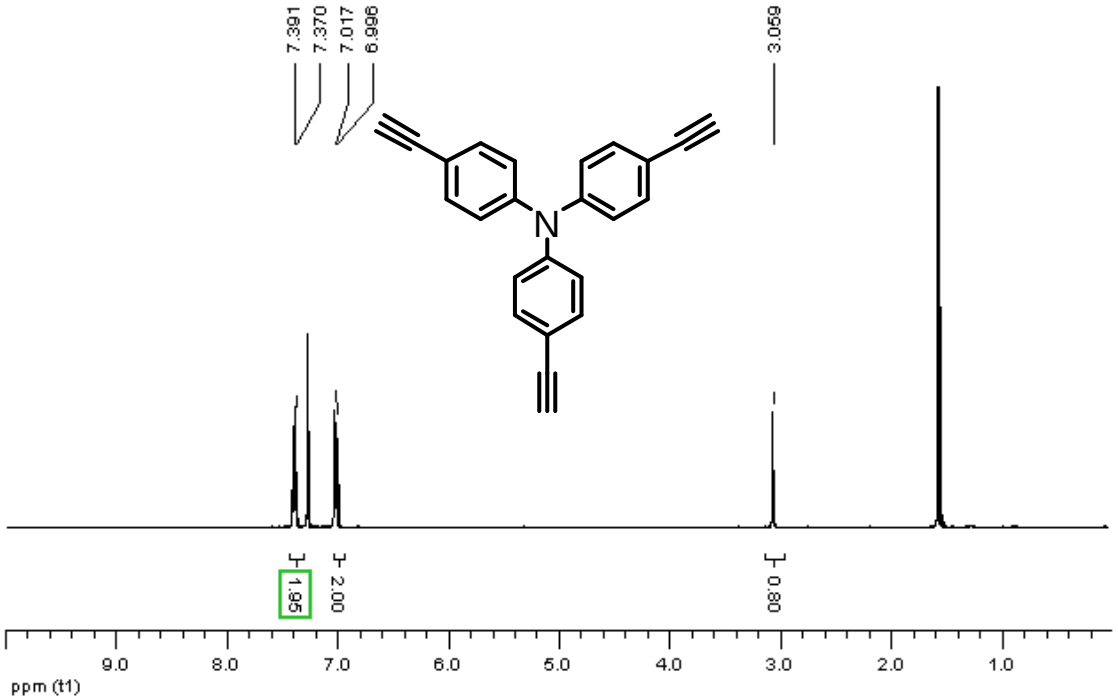

Figure A.26 ^{1}H NMR spectrum of 4, 4', 4''-triethynylphenylamine in $CDCl_3$.

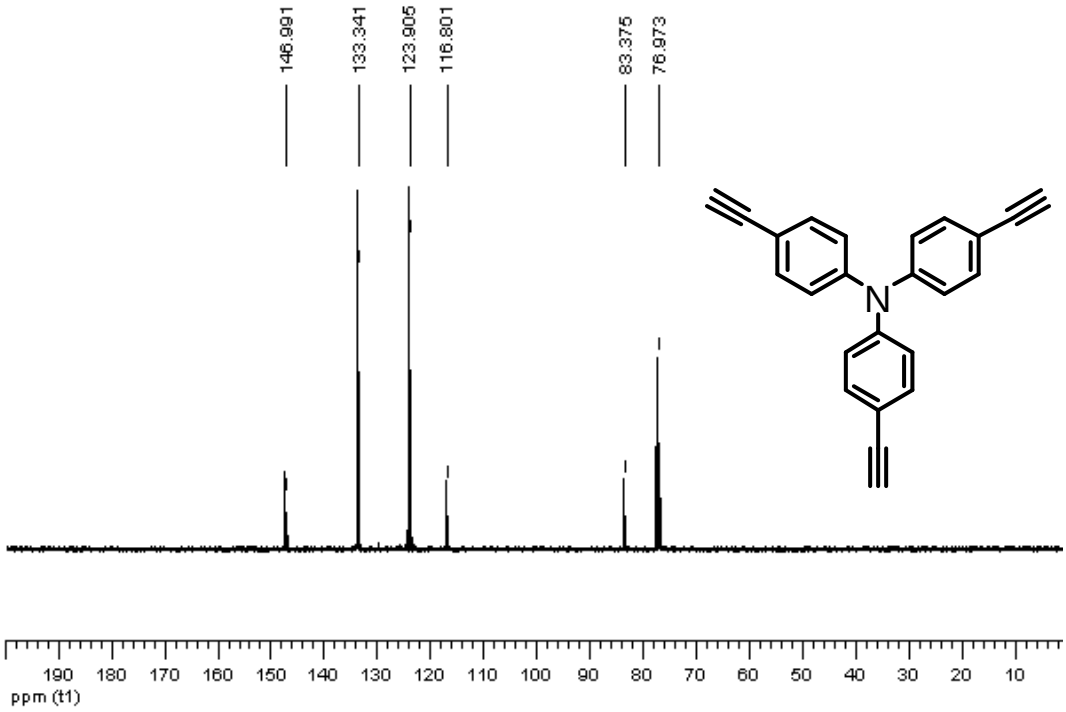

Figure A.27 ^{13}C NMR spectrum of 4, 4', 4''-triethynylphenylamine in $CDCl_3$.

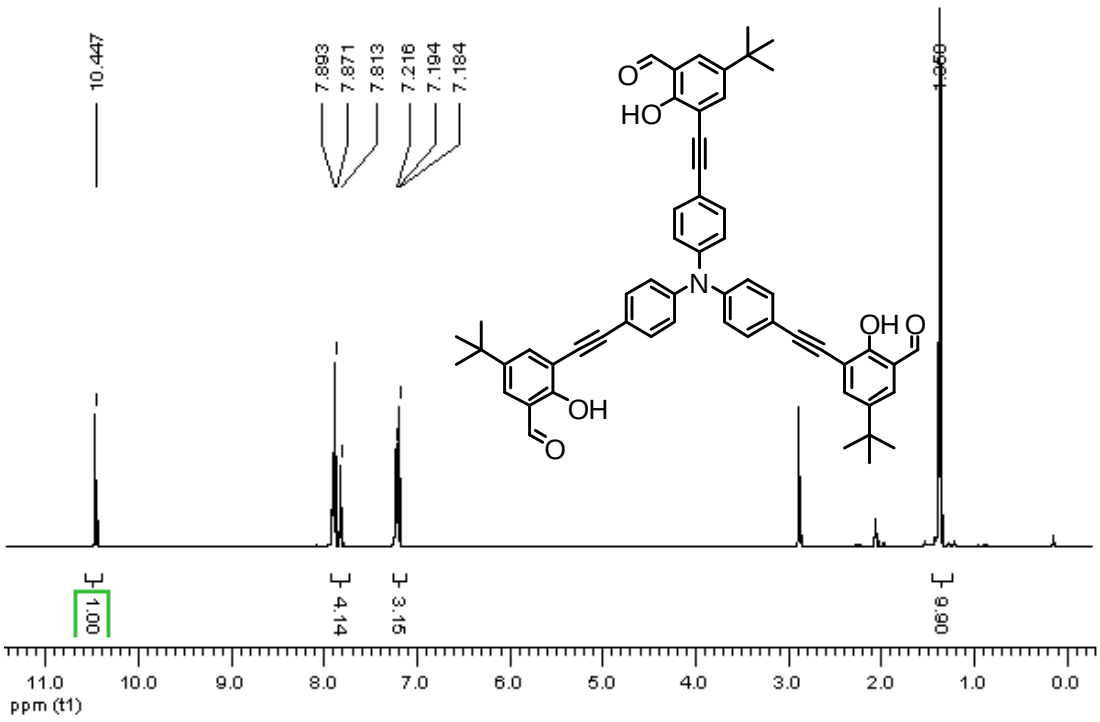

Figure A.28 ^{1}H NMR spectrum of **F4** in acetone D_6.

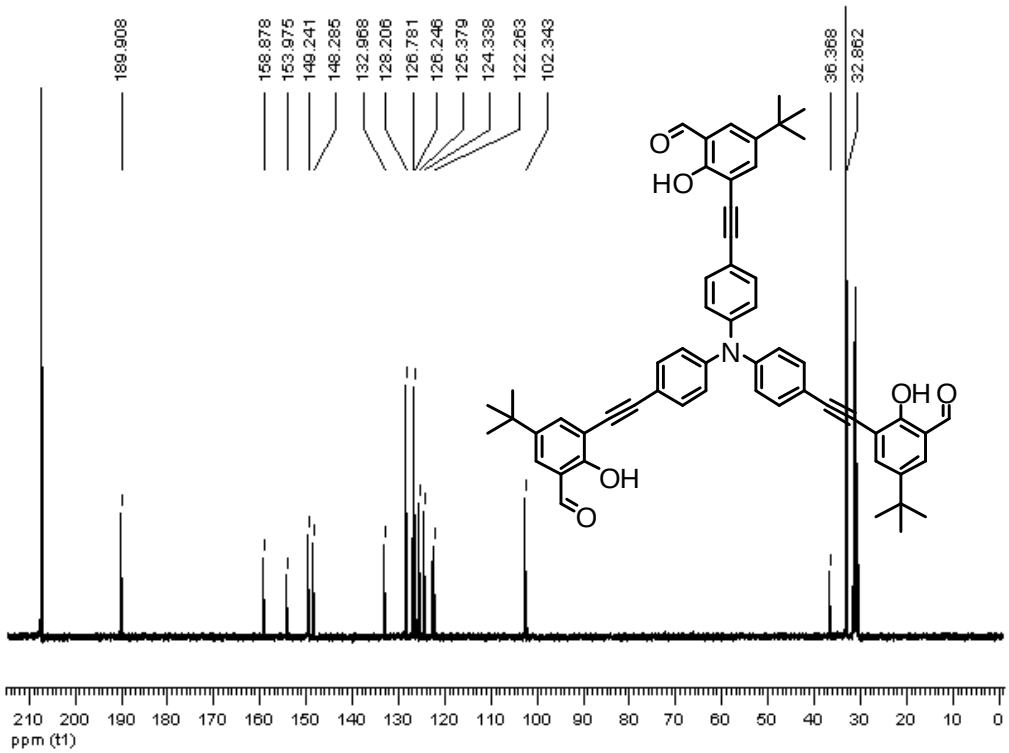

Figure A.29 ^{13}C NMR spectrum of **F4** in acetone D_6.

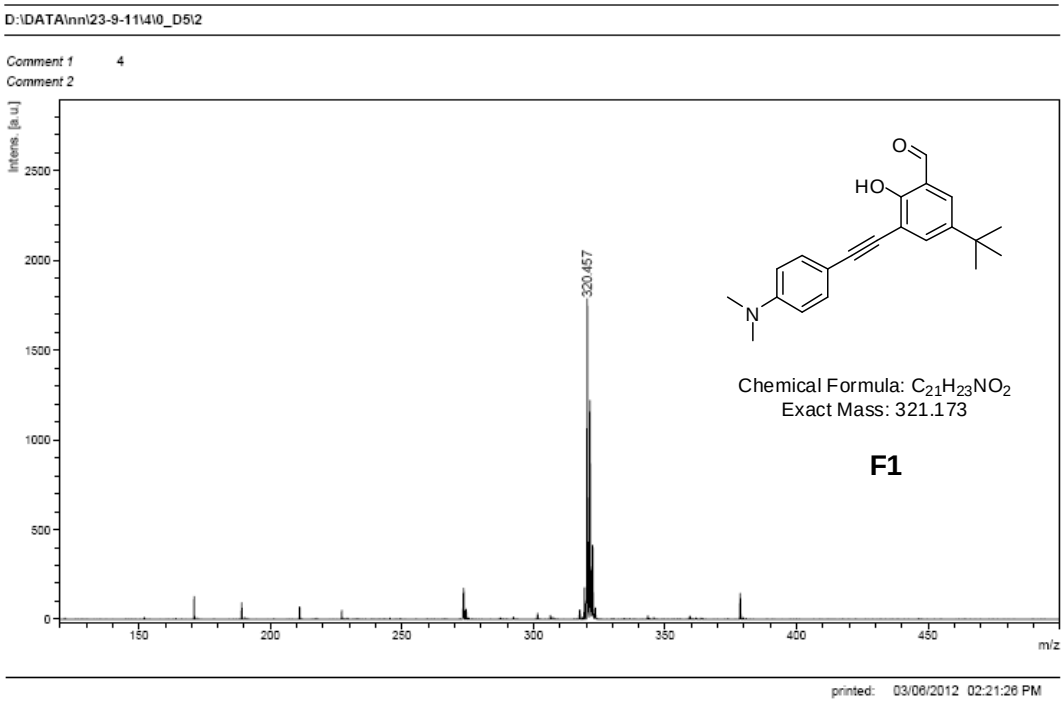

Figure A.30 MALDI-TOF-MS of **F1**.

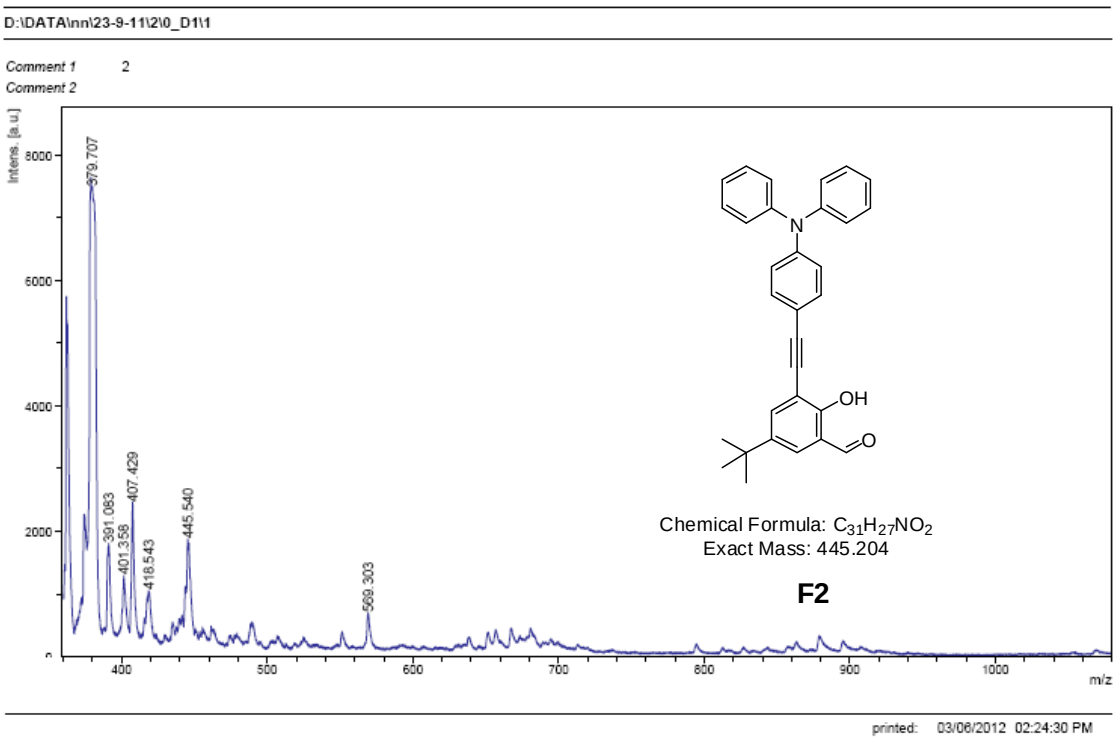

Figure A.31 MALDI-TOF-MS of **F2**.

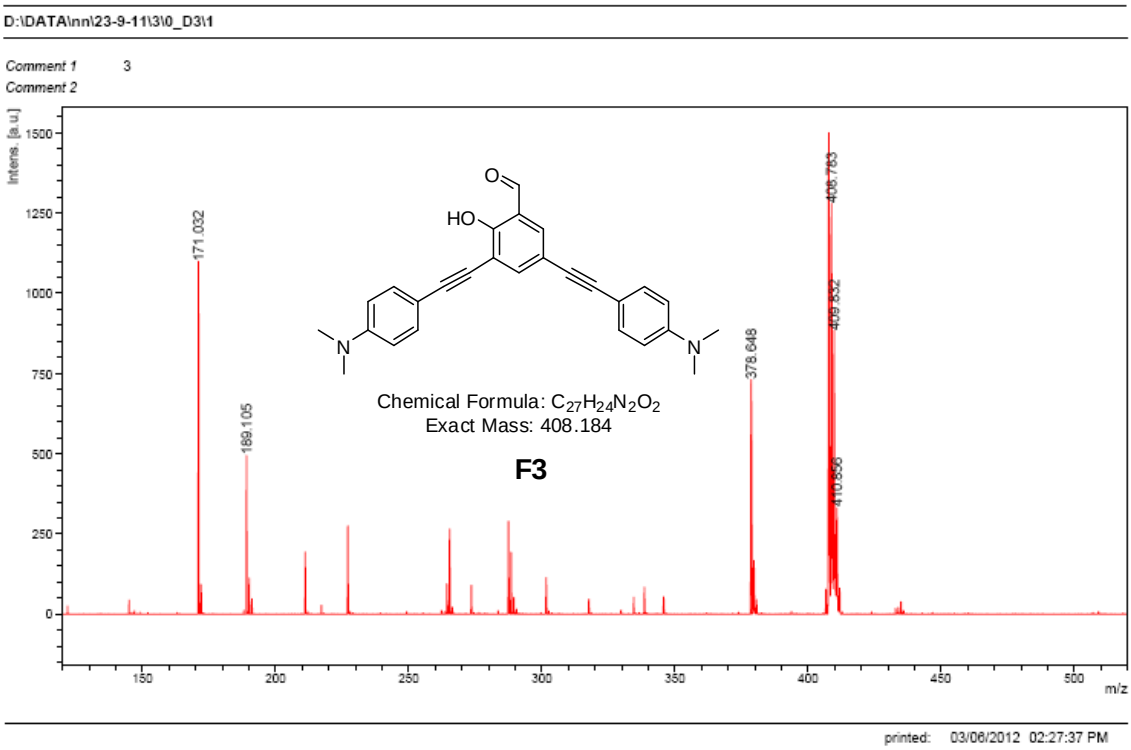

Figure A.32 MALDI-TOF-MS of **F3**.

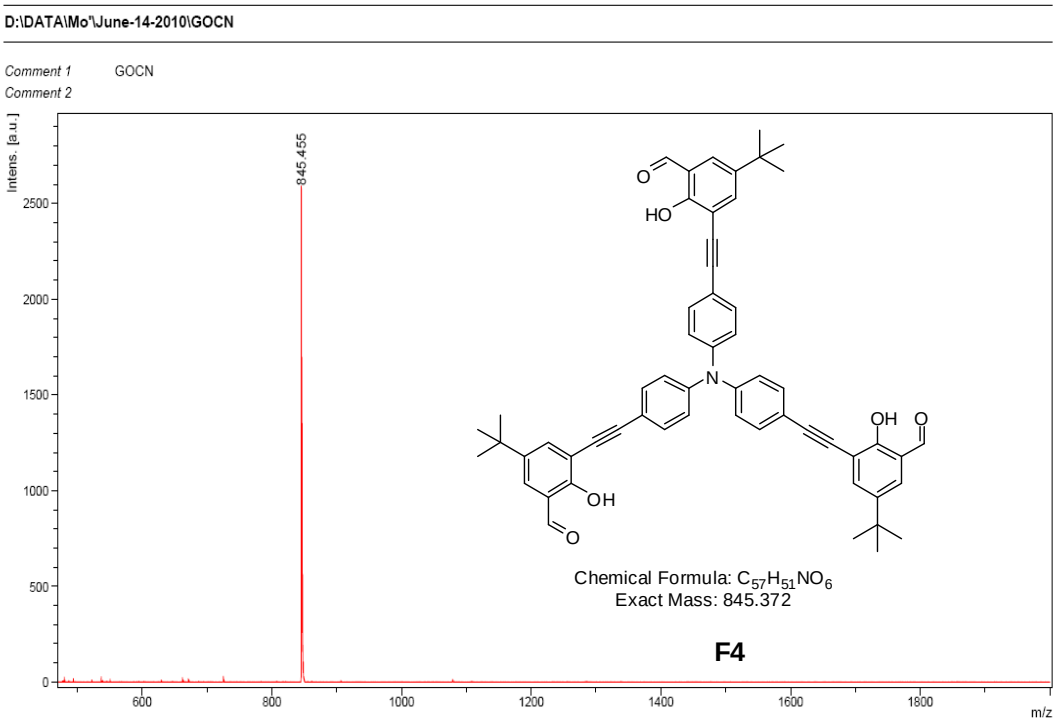

Figure A.33 MALDI-TOF-MS of **F4**.

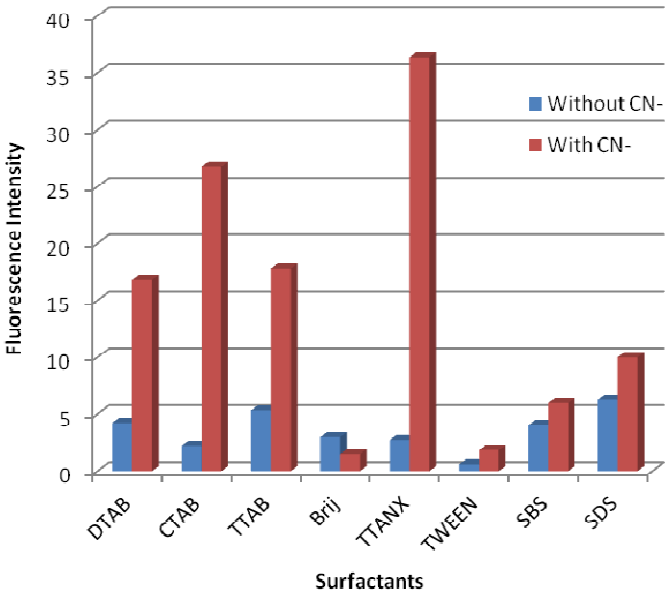

Figure A.34 Bar chart representing the fluorescence intensity of **F3** (5 µM) upon the addition of sodium cyanide (1.5 mM) in HEPES buffer pH 7.4 (10 mM) in the presence of various surfactants (10 mM). The fluorescence intensity at the emission peak of each system was used.

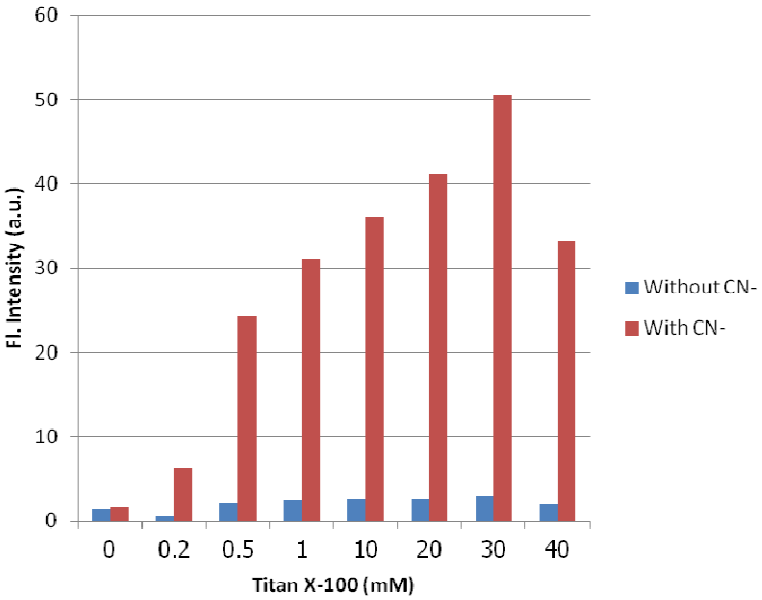

Figure A.35 The bars chart shown the fluorescence intensities before and after addition of cyanide (1.5 mM) to various concentration of Triton X-100 in 10mM HEPES buffer pH 7.4.

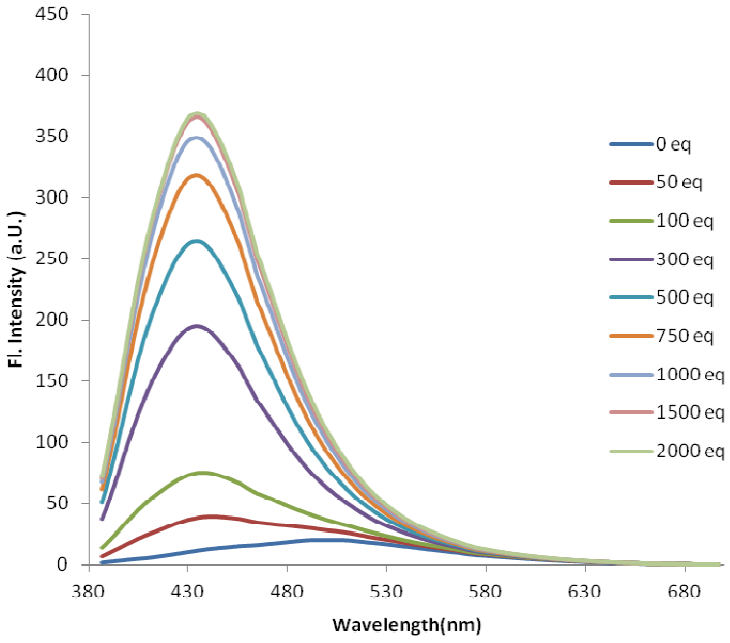

Figure A.36 Fluorescence intensity of **F3** (5µM) at various equiv of cyanide in Triton X-100 (30 mM)/HEPES buffer pH 7.4 (10mM).

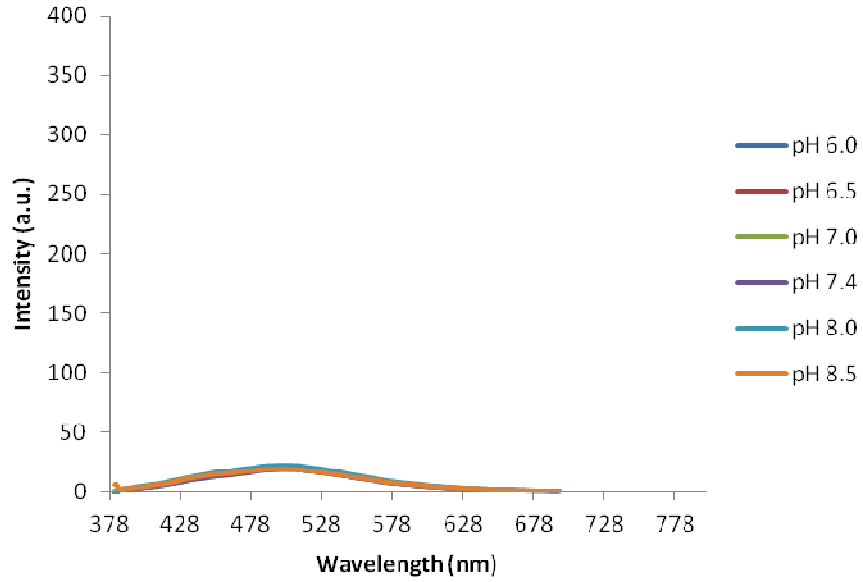

Figure A.37 Fluorescence intensityof **F3** at various pH of HEPES buffer (10mM) in Triton X-100 (30 mM).

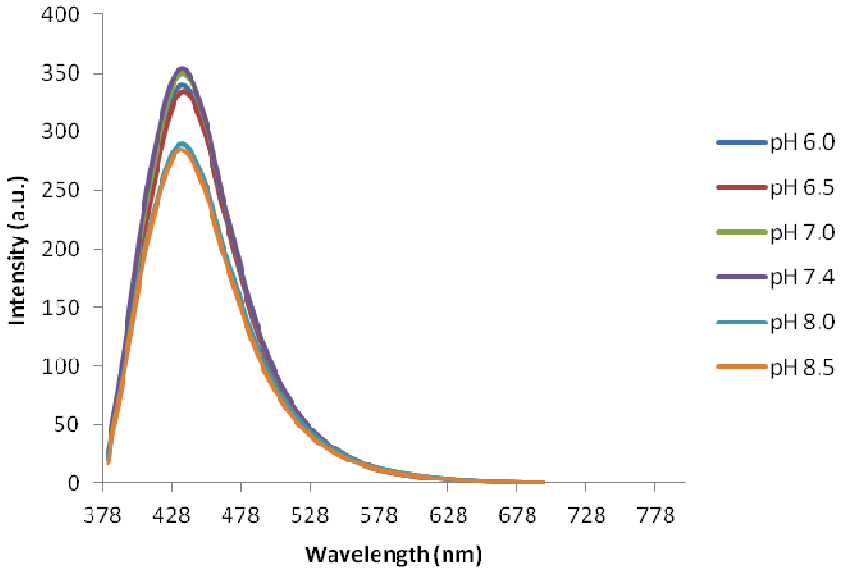

Figure A.38 Fluorescence intensityof **F3** at various pH of HEPES buffer (10mM) in Triton X-100 (30 mM) after addition of cyanide (5 mM).

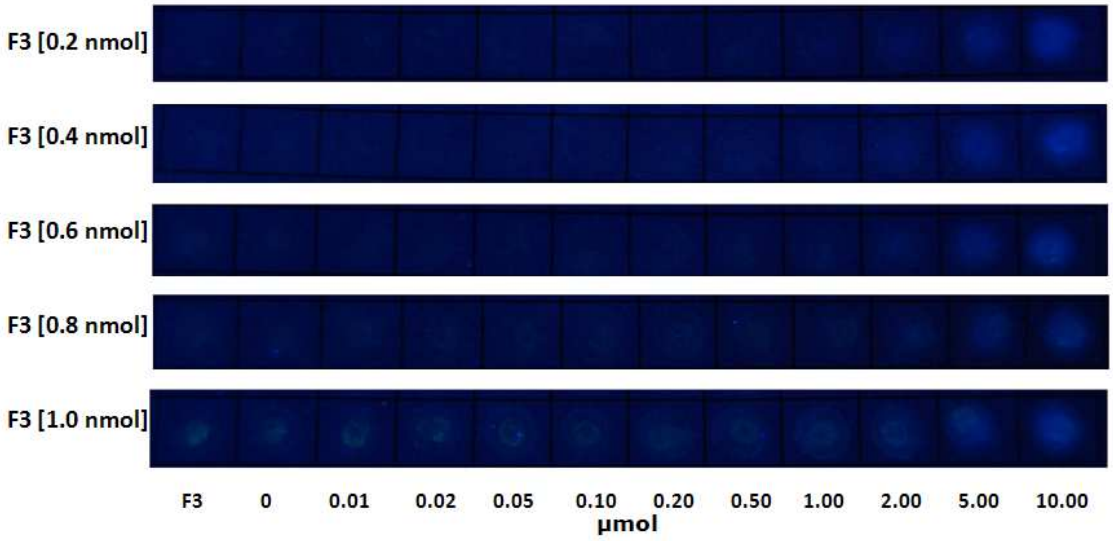

Figure A.39 Photographic images for paper-based detection of cyanide ion under 20 W black light (Dropping cyanide on the **F3** spot).

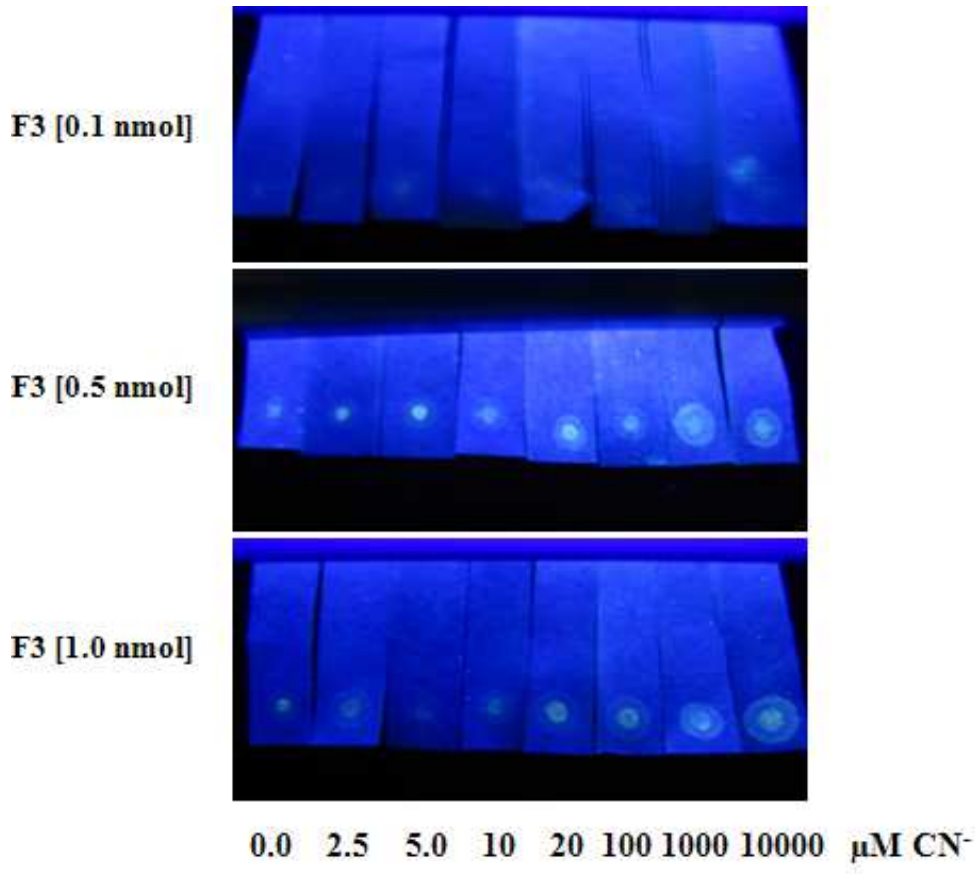

Figure A.40 Photographic images for paper-based detection of cyanide ion under 20 W black light (Fluorescnt spots was dipped on cyanide solution).

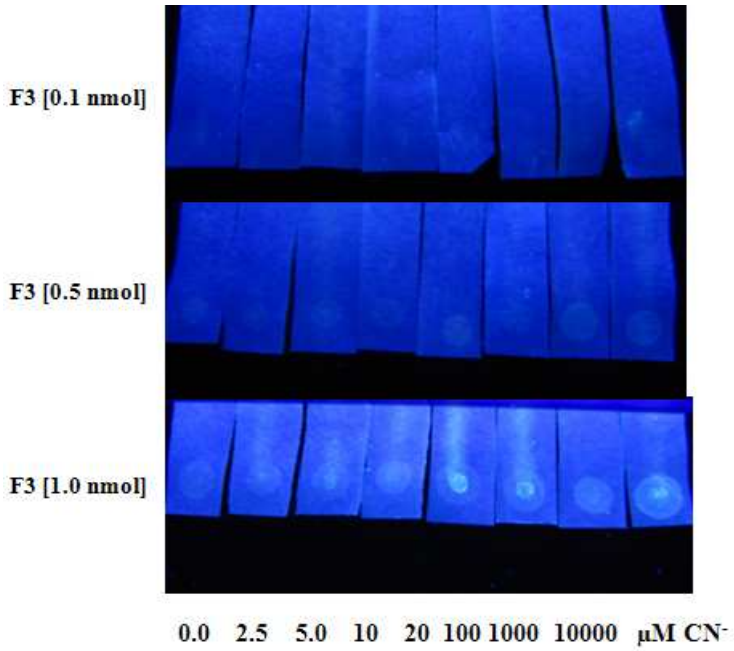

Figure A.41 Photographic images for paper-based detection of cyanide ion under 20 W black light (Fluorescnt spots was dipped on cyanide solution and allowed for the solvent to run up to the top).

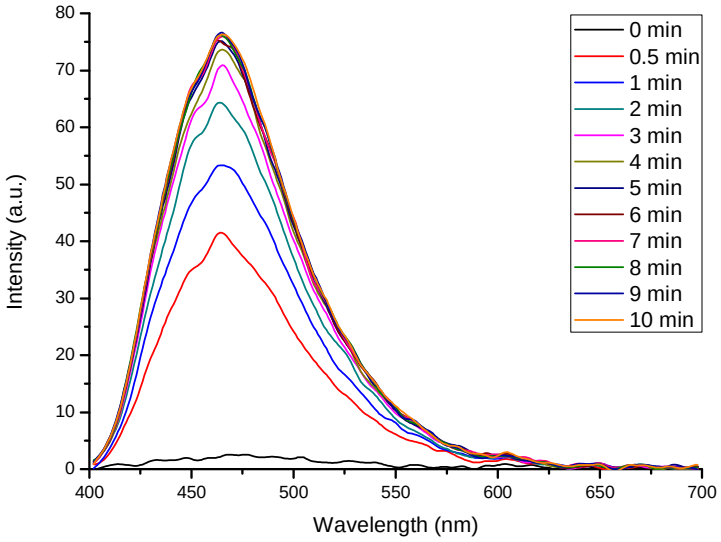

Figure A.42 Fluorescence spectra of **F4** (1.0 μM) (black line) and after (color-coded) time addition of NaCN 1,500 eq at 75% DMSO/HEPES pH = 7.4, 10 mM. (λex= 390 nm)

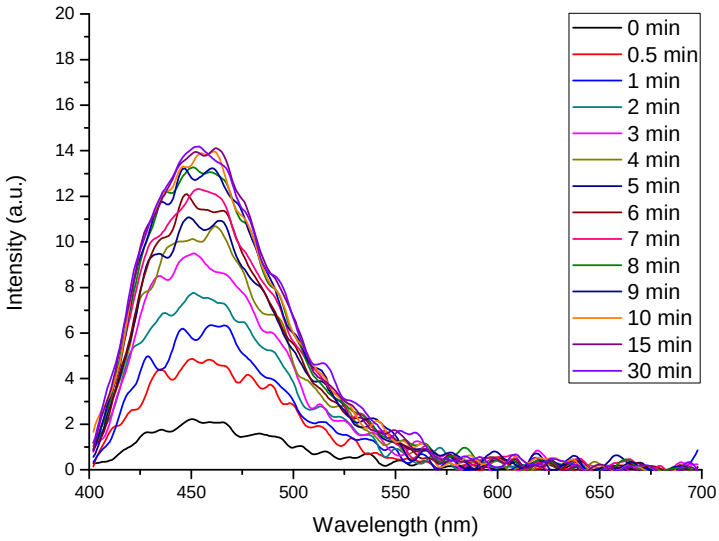

Figure A.43 Fluorescence spectra of **F4** (1.0 µM) (black line) and after (color-coded) time addition of NaCN 1,500 eq at 60% EtOH/HEPES pH = 7.4, 10 mM. (λex= 390 nm)

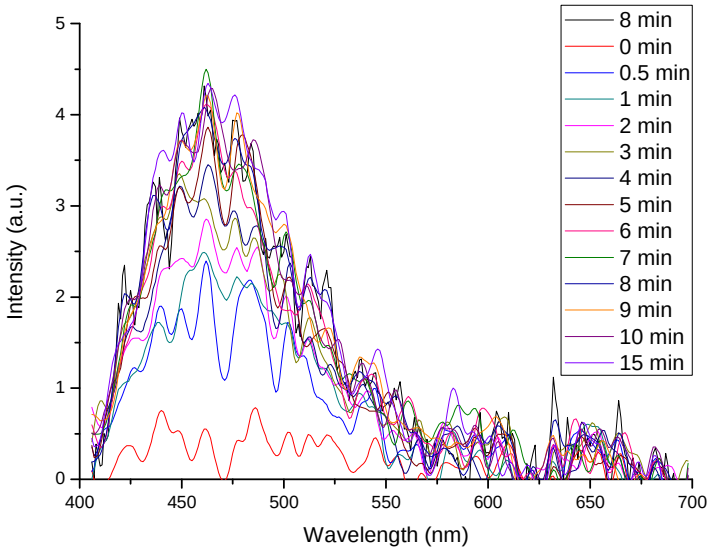

Figure A.44 Fluorescence spectra of **F4** (1.0 µM) (black line) and after (color-coded) time addition of NaCN 1,500 eq and 50% CH_3CN/HEPES pH = 7.4, 10 mM. (λex= 395 nm)

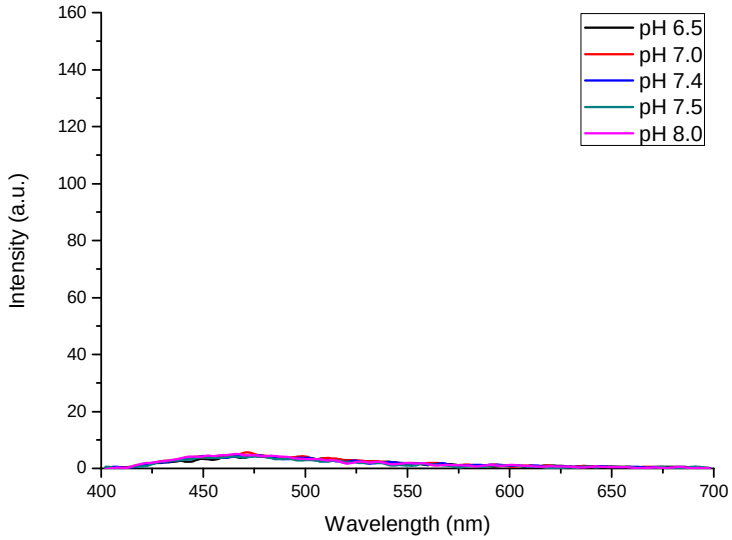

Figure A.45 Emission spectra of **F4** (1.0 μM) in 75 % DMSO/HEPES 10 mM (λex= 390 nm) at various pH values (6.5-8.0)

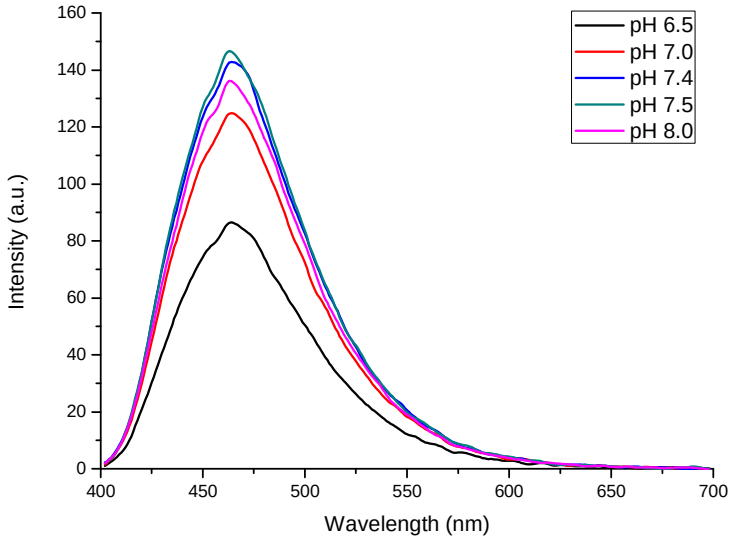

Figure A.46 Emission spectra of **F4** (1.0 μM) in 75 % DMSO/HEPES 10 mM (λex= 390 nm) at various pH values (6.5-8.0). Fluorescence enhancement after addition of NaCN (1.5 mM)

VITAE

Mr. Akachai Khumsri was born on October 29th, 1987 in Trang, Thailand. He graduated with high school degree from Samakkeesuksa School, Huai Yot, Trang. He graduated with Bachelor Degree of Science, majoring in Chemistry from Chulalongkorn University in 2009. In 2009, he has been a graduate student in organic chemistry and become a member of Organic Synthesis Research Unit under supervision of Assoc. Prof. Dr. Mongkol Sukwattanasinitt and he further received a Master Degree in Department of Chemistry from Chulalongkorn University. During the course of study, she received the scholarship from the ADB under the Petroleum & Petrochemical Technology Consortium and 100th anniversary of Chulalongkorn University Fund and from the Thailand Graduate Institute of Science and Technology (TGIST) of National Science and Technology Development Agency.

His present address is 57 Moo. 9 Nawong, Huai Yot, Trang, Thailand 92210.